Eskom	Report	Nuclear Engineering

Title: **Containment Re-Analysis for Long-Term Operation**

Document Identifier:	**331-691**
Alternative Reference Number:	**ERJ-1074**
Area of Applicability:	**Nuclear Engineering**
Functional Area:	**Engineering**
Revision:	**4**
Total Pages:	**147**
Next Review Date:	**August 2026**
Disclosure Classification:	**CONTROLLED DISCLOSURE**

Compiled by	Functional Responsibility	Authorised by
N Behardien	**TD Moila Pr Eng**	**N Ryland**
Civil Engineer	**Responsible Engineer (Civils)**	**Design Engineering Manager**
Date: 2025-07-09	Date: 2025-07-09	Date: 2025-07-09

Nuclear Additional Classification Information

Business Level:	**4**
Working Document:	**3**
Importance Classification:	**NSA**
NNR Approval:	**No**
Safety Committee Approval:	**No**
ALARA Review:	**No**
Functional Control Area:	**Engineering**

Executive Summary

Eskom has embarked on a project to extend the operating life of the Koeberg Nuclear Power Station (Koeberg). Koeberg requested an IAEA Safety Aspects of Long-Term Operation (SALTO) support mission to ensure a safe and structured approach. As part of this process, the containment buildings were subjected to an ageing management assessment to ensure that the required design margins would be maintained throughout long-term operation (LTO). These reinforced concrete containment buildings are post-tensioned and have a leak-tight steel liner.

The containment building design is similar to that of the Électricité de France (EDF) 900 MW series fleet. Their ageing mechanisms are well known and understood. The structure's post-tensioning cables ensure that the concrete remains in compression even under severe loads. Over time, the cable tension reduces, and even though the design is over conservative and makes provision for some reduction in tension, international codes and standards require an analysis of the factors that may reduce the tension and determine the extent to which adequate design margins remain. To this extent, Eskom analysed the containment structures (referred to as the 're-analysis' or time-limited ageing analysis, TLAA) to determine if a sufficient design margin remains for continued safe operation for 20 years.

The specific design criterion investigated is the requirement that all the concrete sections of the containment structures shall remain in compression during a Loss of Coolant Accident (LOCA), referred to as the 'compressive requirement'. The analysis method is similar to that used for the original analysis to demonstrate safe operation for 40 years, but now uses actual data measured over the 40-year period of operation. The strain gauge data used is scrutinized and extrapolated for the additional 20-year life extension. The re-analysis using the extrapolated data concluded that the containment structures comply with the compressive design requirement at 60 years and are suitable for LTO.

While the analysis concluded that the containment structures met the international requirements for continued safe operation for an additional 20 years, further testing and analysis were done to provide confidence in the results and to the NNR. The 2015 ILRT strain data provided empirical evidence of the structural response under full pressure conditions. The data was used to cross-validate the results of the initial analysis, and the outcome confirmed that the assumptions made were conservative and that the compressive requirement is met for 60 years.

Furthermore, several concrete samples were taken from both containment structures and tested to determine the important material properties. The test results confirmed that the concrete remains well within design expectations, even exceeding the conservative assumptions and the two containment structures have comparable behaviour in terms of their stiffness. The increased design margin is shown in the figure below.

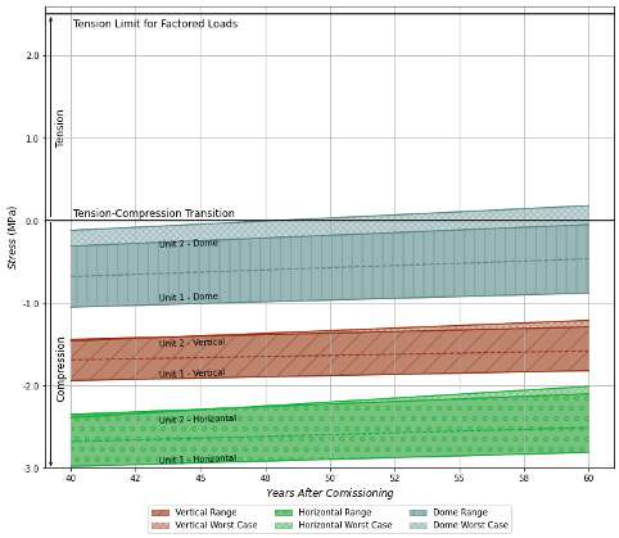

TLAA Results with initial assumptions

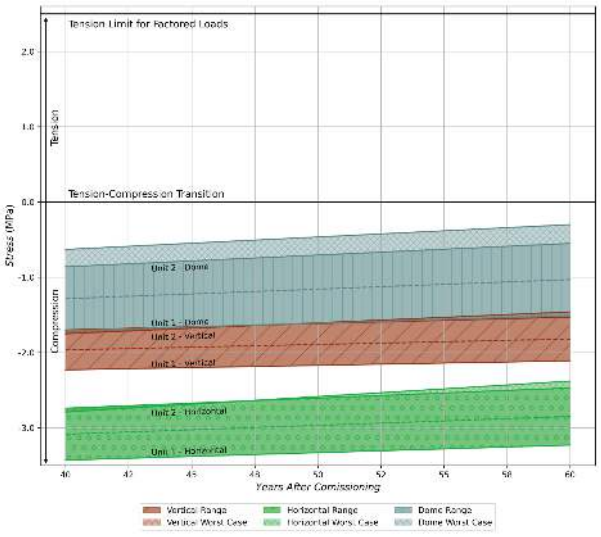

TLAA Results with In-situ material properties

A comparison with the EDF fleet of containment buildings showed that the Koeberg and the EDF fleet behave consistently over time and there are no concerns about the integrity of the Koeberg containment buildings.

The analysis demonstrated that the containment buildings are safe to continue operating for an additional 20 years. Ongoing monitoring, testing, inspection and maintenance will ensure that the containment buildings remain in good condition and any deterioration is detected timeously. Refurbishment of existing containment online monitoring instrumentation was completed, and this will aid in the monitoring and inspection of the containment structures.

The ongoing concrete repairs will address the spalling in the short to medium term, while the ICCP will address this in the medium to long term. Additional modern instrumentation, such as externally mounted vibrating wire strain gauges and optical fibre, is currently being installed on the containment buildings to enhance the monitoring capability.

In conclusion, the containment structures remain structurally sound, with confidence in their design and safety for the additional 20 years of operation.

Content

Figures

Tables

1. Introduction

During the design of the Koeberg's containment structures, assumptions were made to predict the future behaviour of the structures' useful life. At the time, these assumptions were used to predict the future structural mechanics of the structures over the foreseeable lifetime.

The design of the containment structures was performed in accordance with the Containment Structural Design Rules [27] and estimates for structural mechanics prediction models were used per the codes and standards deemed applicable during the design. This included the prediction of the change in the concrete creep, concrete shrinkage and the loss of the tension force in the tendons over time, which are material properties that affect the behaviour of the structures over time. The preliminary design report was compiled in 1976, while the containment structures were commissioned in 1984 and 1985 for Unit 1 and Unit 2 respectively.

The two reinforced concrete and post-tensioned containment structures house the respective reactors of Koeberg and are referred to as the reactor buildings or the containment structures (HRX). The structures were fitted with several online monitoring instrumentation sets which collectively form the EAU system. The system's monitoring equipment includes:

- Invar wires,
- Pendulums,
- Strain gauges,
- Thermocouples, and
- Dynamometers.

The monitoring equipment measures various parameters throughout the lifetime of the structures, specifically during:

- Commissioning,
- During Integrated Leak Rate Testing (ILRTs) which occurs 10-yearly, and
- Normal operation through in-service testing and monitoring.

These devices are used to monitor the structural behaviour of the containment structures and can also be used to validate the assumptions made during the design of the containment structures.

Koeberg was initially licenced for 40 years operational period. Koeberg Unit 1 successfully acquired a licence for long-term operation (LTO) to operate for an additional 20 years until 21 July 2044, while Unit 2 licence will expire on 9 November 2025. .

For LTO, Koeberg commissioned a Safety Aspects of Long-Term Operation (SALTO) ageing management assessment project which aimed to revalidate, amongst others, the containment structures for LTO. The assessment sought to validate the containment for 60 years of operation.

The TLAA for LTO considered the original design, the monitoring results as well as predictions of the structural mechanics of the containment structures for the LTO period, to determine whether the structures are suitable for operation for the full 20-year period of LTO. Furthermore, cross revalidation was conducted using strain data obtained from 3rd ILRT (2015) to further refine and increase confidence in the initial TLAA calculations. Results from material testing of in-situ concrete were used to further strengthen and support the original TLAA assumptions and calculations.

2. Supporting Clauses

2.1 Scope

The containment structures (inclusive of the steel liner) are the ultimate safety barrier to prevent the escape of radioactive substances in the event of a 'Loss of Coolant Accident' (LOCA).

The scope of this report is multi-fold and aims to achieve the following:

(1) Provide an overview of the containment structures and their structural design (Chapter 3).

(2) Provide a summary of relevant design assumptions and predictions utilised in the original design of the containment structures (Chapter 3.3).

(3) Provide a holistic overview of the on-line monitoring equipment (EAU System) installed on the containment structures and the original assumptions relating to the design (Chapter 4).

(4) Address certain comments by the National Nuclear Regulator (NNR) contained in [25] (throughout the report).

(5) Perform a review of the available EAU results for both the 1HRX and 2HRX structures (Chapters 5, 6).

- Re-perform the containment tendon prestress TLAA 301 (Chapter 7).
    - Perform cross-revalidation of TLAA 301 using 2015 ILRT data (Chapter 8).
    - Perform refinement of the TLAA 301 calculations using in-situ concrete properties (chapter 9).

(6) Analyse shortcomings that exist with respect to the online monitoring equipment and results.

(7) Provide recommendations for the anticipated modifications to the on-line monitoring equipment.

2.2 Purpose

The report demonstrates that the containment structures are safe for the period of LTO (60 years of operation) and includes:

- An evaluation of the online monitoring equipment data, instrument calibration and comparison of data between Unit 1 and Unit 2 and the EDF fleet's strain data.
- The results of TLAA 301 based on the methodology applied in reference [16].
- The cross-validation of TLAA 301 using strain data from the previous ILRTs, and results of testing done on containment concrete samples.

The additional cross-validation using the data measured during the ILRTs and the results of testing done on containment concrete samples serve to demonstrate, through independent analysis and verified and validated data inputs, that the containment buildings are safe for 60 years of operation with adequate safety margins that envelope specified accident conditions.

2.3 Applicability

This document is applicable to the Koeberg Nuclear Power Station.

2.4 Effective Date

This document is effective once authorised.

2.5 Normative/Informative References

Parties using this document shall apply the most recent edition of the documents listed in the following paragraphs.

2.5.1 Normative

[1] 240-128949939: Koeberg SALTO Scoping and Ageing Management Evaluation Bulk Work Technical Requirement Specification, TRS, Attachment 21, Eskom, 2017

[2] ASME Section XI, Subsection IWL: Requirements for Class CC Concrete Components of Light-Water Cooled Plants

[3] KAU-030: Basis and Scope for Licence Binding Civil Surveillances at Koeberg Nuclear Power Station

[4] Koeberg Safety Analysis Report: II-1.9 CIVIL WORKS – BUILDINGS

[5] L1124-GN-LIS-010, Rev.5: L1124 SALTO Project, Comprehensive List of Koeberg TLAAs, SALTO Consortium LESEDI-Framatome, 2020

[6] RCC-CW: Rules for Design and Construction of PWR Nuclear Civil Works

[7] SSG-48: IAEA Safety Standards – Ageing Management and Development of a Programme for Long Term Operation of Nuclear Power Plants, IAEA, 2018.

[8] US NRC RG 1.90: Inservice Inspection of Prestressed Concrete Containment Structures with Grouted Tendons

[9] Wienand, B. Post-Assessment of Pre-stressed containment structures by Evaluation of Monitored Long-Term Deformation Results, 2013.

2.5.2 Informative

[10] 240-128799825: Dome Repairs for 1/2 HRX, 2017

[11] 331-623: Engineering Position on Containment Structures for Long-term Operation, 2022

[12] Broomfield, J.P. Corrosion of Steel in Concrete-Understanding, Investigation and Repair, 2nd ed.; Taylor and Francis: London, UK, 200

[13] Brownfield, A.H., et. al. Control of Shrinkage of Concrete. SEAOC Committee, 1965

[14] CE 18360: Justification for acceptance criteria for Topographical survey, 2022

[15] Cement & Concrete Institute. Fulton's concrete technology. ISBN 978-0-9584779-1-8, 2009

[16] D02-ARV-01-183-095 Rev. C: SALTO Koeberg - TLAA 301 Containment Reanalysis, 2021

[17] FHWA-HRT-14-039: An FHWA Special Study: Post-Tensioning Tendon Grout Chloride Thresholds

[18] Hubler, M.H., et al. Comprehensive Database for Concrete Creep and Shrinkage: Analysis and Recommendations for Testing and Recording. ACI Material Journal, 2015

[19] JN411-NSE-ESKB-R-5830, Rev3: Containment Buildings, Surface Defects - Numerical Analysis Report

[20] JN426-NSE-ESKB-4988: Deterioration of the Cover Concrete of Containment Buildings

[21] JN465-NSEESKB-R-5704: Long Term Repair Strategies for the Containment Buildings - Expert Panel Report

[22] JN843-NSE-ESKB-L-8468: Aseismic Vault - Level Deformation Survey, 2021

[23] JN848-NSE-ESKB-L-8443: 1HRX online monitoring results for Q1

[24] JN848-NSE-ESKB-L-8524: 2HRX online monitoring results for Q2

[25] k29021N - Koeberg Nuclear Power Station: Environmentally Assisted Fatigue (EAF) Analysis Methodology and Submission of the List of Analysed and Reanalysed Time Limited Ageing Analyses (TLAAs) for the Period of Long-Term Operation

[26] KBA00A1C01009: Containment Structural Design Rules

[27] KBA0906D00104: Containment: Summary of Final Results of Stress Analysis

[28] KBA09A1C01017: Technical Specification for Strain Gauges

[29] KBA09A1C01019: Technical Specification for Thermocouples

[30] KBA09A1C02004: Technical Specification for Steel Used in Prestressed Concrete

[31] KBA09A1C02086: Technical Specification Load Cells

[32] KBA09A1C03008: Containment Instrumentation

[33] KBA09A1C03025: Containment U1: Report on Load Cell Cables In-Service Relaxation Tests

[34] KBA1201A70019: Technical Specification of the Pendulums

[35] KBA1201A70020: Technical Specification of the Invar Wires

[36] L1124-GN-RPT-019 Rev. 3: Validity of KNPS Containment Civil TLAA 301 SALTO TLAA Assessment Report.

[37] JN913-NSE-ESKB-L-A080: Evaluation of Koeberg Nuclear Power Station (KNPS) Concrete Containment Unit Properties Based on Drilled Cores

[38] JN922-NSE-ESKB-L-A106: Results of Poisson's Ratio Testing at University of Pretoria

[39] TR-NPP-24-001 Rev 1: Safety Evaluation Report-Koeberg Long Term Operation

2.6 Definitions

Time Limited Ageing Analysis: is a design basis evaluation created to justify equipment useability for a specific period or limit. This study uses analysis methods and techniques to establish safe envelops or extent of useability. It is viewed as fundamental documented evaluations used as inputs or assumptions in plant operation and plant management.

Validated: Refers to specific Structures, Systems, and Components (SSCs) that have been subjected to Time-Limited Ageing Analysis (TLAA) and have been demonstrated, through technical evaluation, to retain adequate design safety margins beyond their original design life, thereby supporting continued operation for a defined extended period. The extended period defined in this report is 20 years.

2.7 Abbreviations

Abbreviation	Description
EAU	On-line monitoring equipment of the HRX Structures
EPRI	Energy and Power Research Institute
HRX	Containment structures, also referred to as the reactor buildings
IGALL	International Generic Ageing Lessons Learned
ILRT	Integrated Leak Rate Test
KNPS	Koeberg Nuclear Power Station
LOCA	Loss of Coolant Accident
LTO	Long Term Operation
NIL	Nuclear Installation Licence
NNR	National Nuclear Regulator
SALTO	Safety Aspects of Long-Term Operation
SIT	Structural Integrity Test
TLAA	Time-Limited Ageing Analysis
GUTS	Guaranteed Ultimate Tensile Strength
SSE	Safe Shutdown Earthquake

2.8 Symbols

Symbol	Description
A_{Cable}	Cross-Sectional Area of a single post-tensioned cable
bar	Stress measurement, $1\ bar = 100\ kPa$
$\Delta\cdot$	Delta – Notation for a change in value
ε	Strain
F	Force
h	Hecto – Metric Prefix denoting a factor of one hundred (100)
$\cdot_i$	Notation for 'Initial'
k	Kilo – Metric Prefix denoting a factor of one thousand (1,000)
$kdaN$	Kilo-deka-Newtons
$m\cdot$	Milli – Metric Prefix denoting a factor of one thousandth (0,001)
m	Metre – Metric Unit of Length
N	Newton – Metric Unit for Force
Pa	Pascal – Metric Unit for Stress
σ	Stress
$\cdot_T$	Notation for 'Tension'
$\cdot_{t=x}$	Notation for 'Time' where x is a numerical value either in hours or years
V	Volt – Unit of electric potential

2.9 Roles and Responsibilities

Design Engineering is responsible for the TLAAs of the Koeberg Nuclear Power Station.

2.10 Process for Monitoring

N/A

2.11 Related/Supporting Documents

N/A

3. Background and Description of the Component

3.1 Design of Koeberg Containment Structures

The containment structures provide support and protection to the primary system and some auxiliary equipment and components. It provides shielding to protect personnel and the environment from ionizing radiation. It also acts as the third barrier by preventing the release of radioactive substances into the environment in the unlikely event of a nuclear accident.

The buildings are located on the nuclear island with other safety-related structures, including the Nuclear Auxiliary Building (NAB), Electrical Buildings (HLX), Fuel Buildings (HKA) and the ASG Tank Rooms (see Figure 1 and Figure 2).

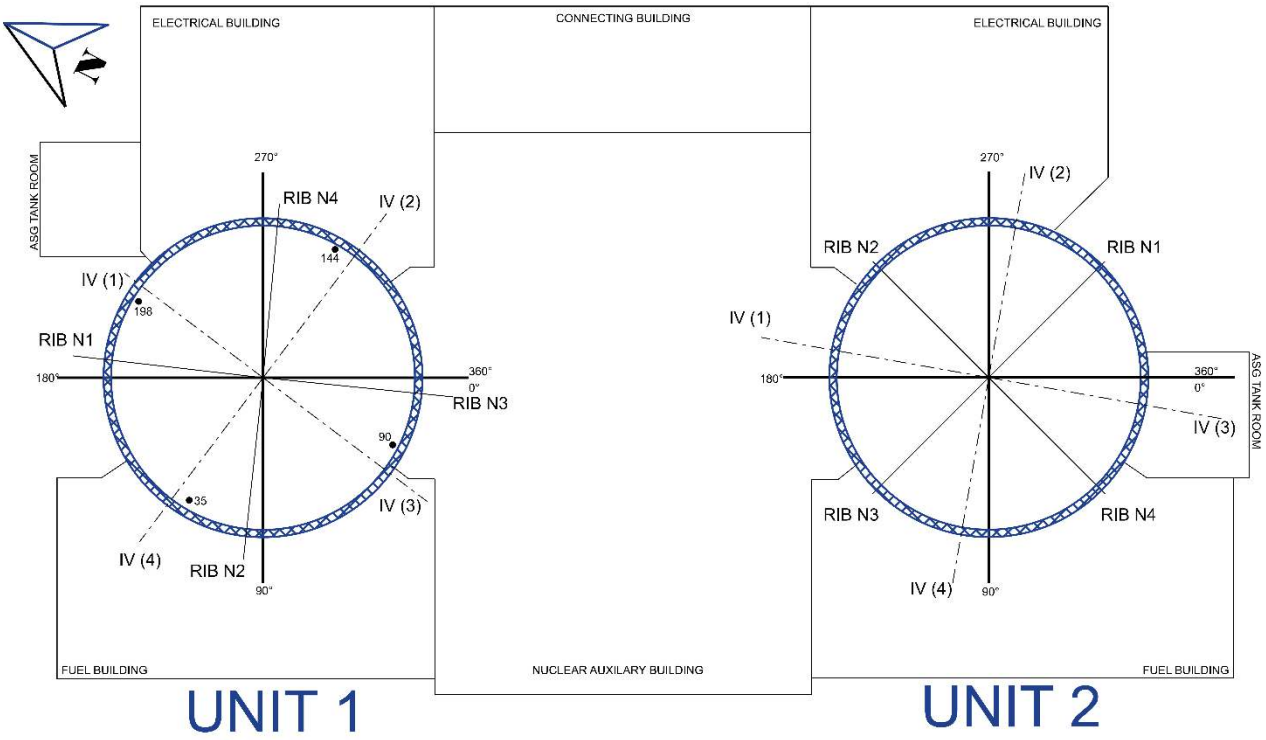

Figure 1: Plan view of the Nuclear Island

The structures were designed to house the nuclear reactors and associated plant equipment. The design requirements are to withstand conventional structural loads, a 'Safe Shutdown Earthquake' (SSE) and a Loss of Coolant Accident (LOCA) which will induce an internal pressure on the structures of 400 kPa.

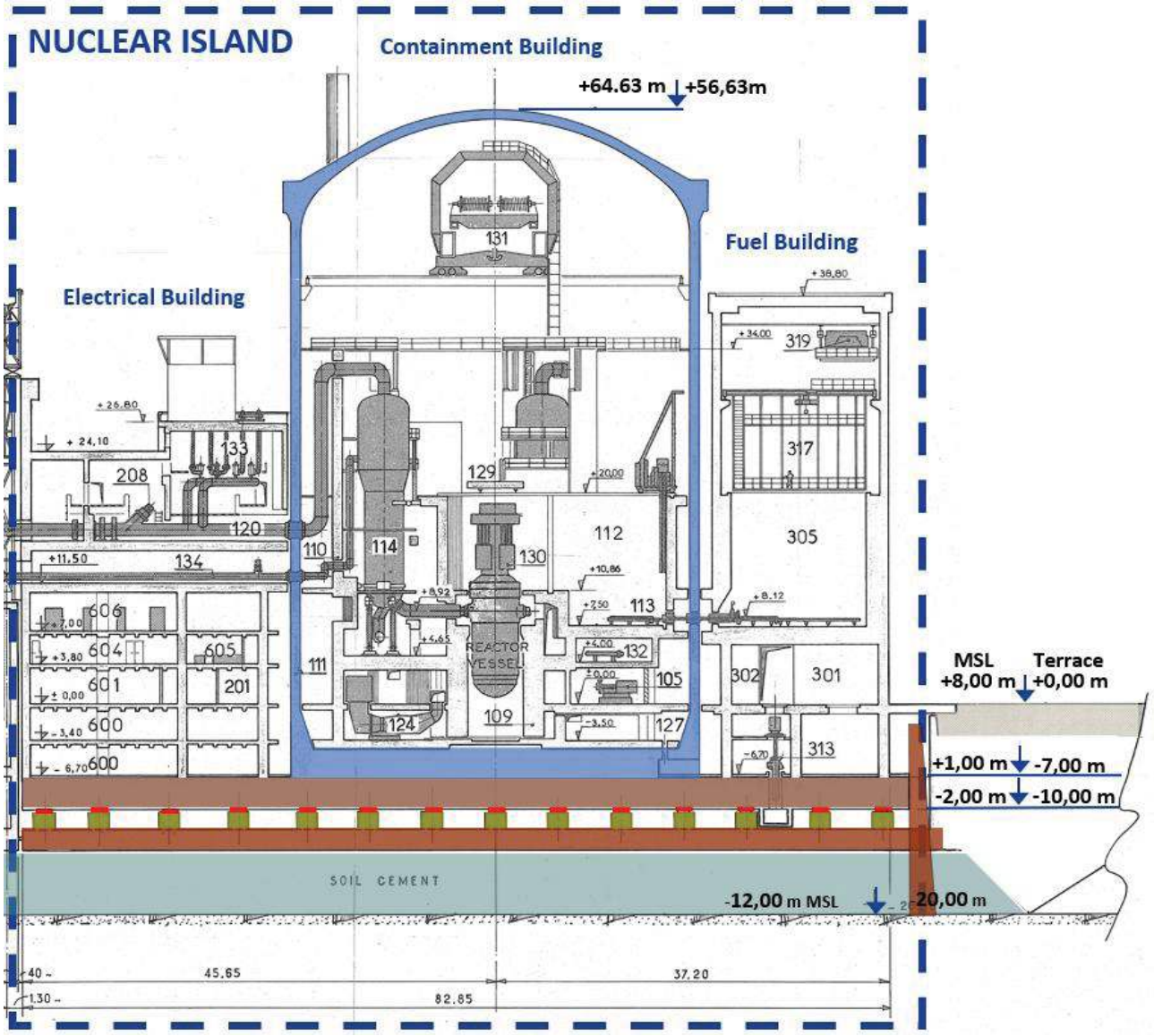

Figure 2: Section of a Containment Structure

The containment structures comprise of different sections and components, and the following terms are defined and illustrated in Figure 3:

Cylindrical Wall:	The walls of the containment structures
Dome:	Torispherical roof of the containment structures
Gusset:	A thickened area connecting the cylindrical wall to the Upper Raft
Ring Beam:	A thickened area of the containment structures for the connection of the dome and the cylindrical wall
Upper Raft:	A concrete raft forming the foundation of the containment structures.

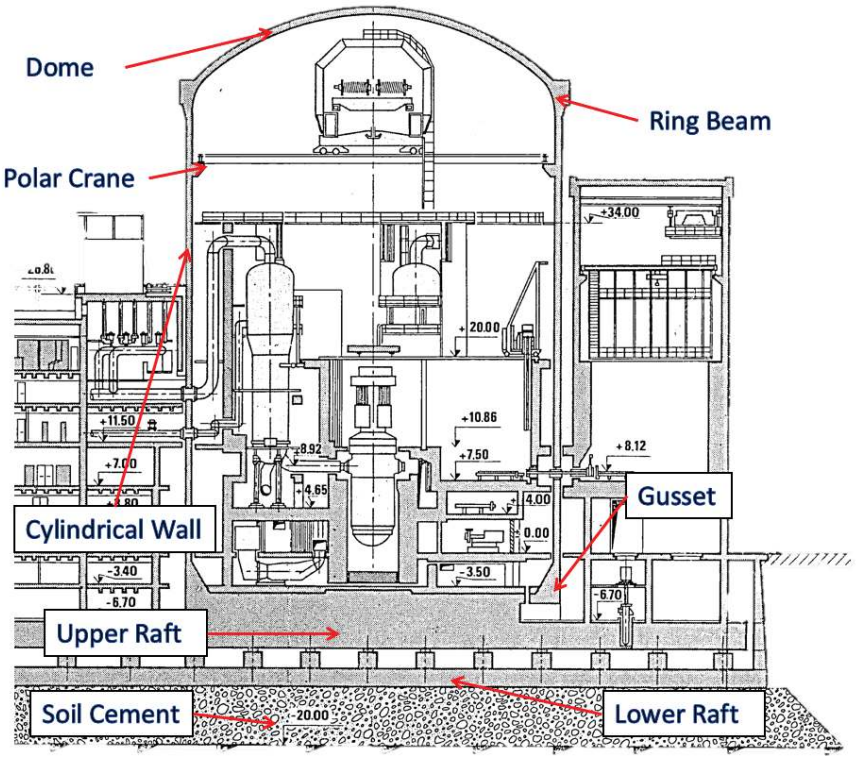

Figure 3: Overview of Containment

The design of the containment structures was based on the design of 900 MW series French containments and the French Power Station, Tricastin, as the Koeberg reference station.

The containment structures are fitted with a 6mm steel liner. The leak resistance of the containment is entirely dependent on the steel liner and under no circumstances can the concrete shell be considered to contribute in part or in whole to the leak resistance of the structure [26].

3.2 Post-tensioned Tendons

Koeberg's containment buildings are post-tensioned* concrete structures. The post-tensioning is provided through cable tendons. Embedded post-tensioned tendons are high tensile strength steel wires that are grouped together to form a group of cables and are enclosed in a protective steel duct that is placed inside concrete and then tightened (tensioned) after the concrete has hardened. These cables introduce additional compressive resistance to the concrete which helps counteract tensile forces that may cause cracking.The tendons can be divided into three groups with distinctly different orientations, namely:

- Vertical tendons in the cylindrical part of Containment. The vertical post-tensioning of the cylinder is made up of 216 steel wire cables which are rectilinear along the cylinder wall.
- Horizontal tendons placed around the circumference of the cylindrical part of containment. The horizontal post-tensioning of the cylinder is made up of 255 three-quarter turn hoops whose anchorage is embedded in four vertical ribs.

* Several technical documents refer to the KNPS tensioning cables as 'prestressed' or 'prestressing' cables. This is technically not correct and all tensioning cables were post-tensioned.

- Dome tendons placed in a special configuration across the dome. Post-tensioning of the dome is done by 162 cables grouped into three families having 60º angles between them.

The layout of the tendons of the containment structures are illustrated in Figure 4 while the three families of the dome tendons are provided in Figure 5.

Redacted - NNR Act 47, Section 51; PAIA 38(b)

Figure 4: Layout of Containment Tendons and Reinforcement

Redacted - NNR Act 47, Section 51; PAIA 38(b)

Figure 5: Three Families of Dome Tendons

The tendons each consist of 19 cables and each cable consists of 7 steel wire strands of 5 mm each. The tendons are encased in ducts that were grouted during the construction activities of Koeberg. An illustration of the cross-section of a tendon and all its associated components is given in Figure 6.

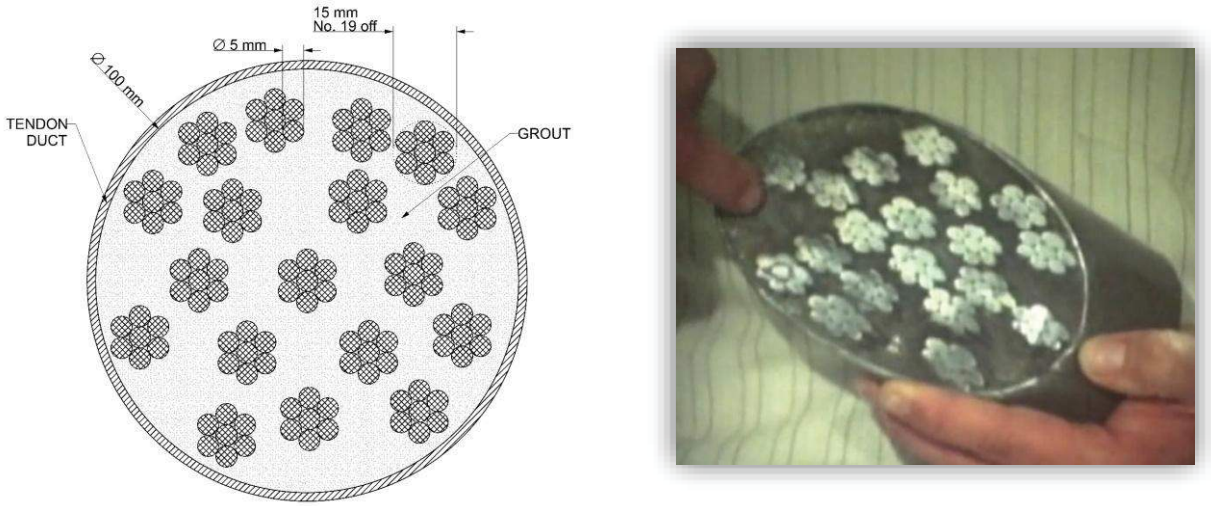

Figure 6: Tendon Cross Section Schematic (L) and Photo (R)

3.3 Design Requirements and Original Assumptions

The design and analysis of the containment structures considered different 'Classifications' of load cases [4], [26]. These classifications, and an extract of their design requirements, are provided below:

3.3.1 Normal Operating Loads

The loads applicable to this load case are (Load Case 2):

- dead loads,
- prestress,
- temperature,
- operating pressure,
- ordinary climatic loads, and
- parasitic bending due to liner tolerances.

The following requirements apply:

a) the membrane stresses in any current wall section (average stress in the concrete section only, excluding the liner) remain compressive.

b) the allowable compressive stress in any current section is only exceeded where the cause of the excess stress is a transient temperature gradient and provided the total stress remains lower than 55 % of the 28-day cylinder strength.

c) concrete tensile stresses in any current section are only admitted where the cause of such stresses is a transient temperature gradient and provided the entire tensile force is taken by bonded reinforcing steel working at a maximum of 2/3 of yield stress.

d) in special zones, in the vicinity of penetrations and anchorages, the allowable concrete compressive stress is 60% of 28-day cylinder strength.

3.3.2 Exceptional Operating Loads

The loads applicable to this load case are:

- Load Case 3: Pressure Test + Ordinary Climatic Loads, and
- Load Case 4: Ordinary Earthquake.
- Load Case 5: Loss of Coolant Accident (LOCA),

The following requirements apply:

a) the membrane stress is compressive in all current sections along the entire section.

b) the allowable compressive stress in any current section is only exceeded where the cause of the excess stress is a transient temperature gradient and provided the total stress remains lower than 55% of the 28-day cylinder strength.

c) concrete tensile stresses in any current section are only admitted where the cause of such stresses is a transient temperature gradient and provided the entire tensile force is taken by bonded reinforcing steel working at maximum 2/3 yield stress.

3.3.3 Factored Loads (Ultimate Limit State Check)

The loads applicable to this load case are:

- Load Case 6: exceptional climatic loads,
- Load Case 7: exceptional earthquake,
- Load Case 8: rupture of steam pipe,
- Load Case 9: missile load,
- Load Case 10: simultaneous occurrence of LOCA and exceptional earthquake, and
- Load Case 11: 1.5 times the design pressure.

The following requirements apply:

a) The concrete stresses are limited to:

Maximum compression: 0.8 of 28-day cylinder strength

Maximum tension: 0.8 of comparable tensile strength

NOTE 1: All steels (prestressing cables, reinforcement bars and the liner[†]) are allowed to resist forces.

NOTE 2: For this report, the Exceptional Operating Loads' worst-case accident (LOCA) is considered. This case is considered the most conservative as the compressive requirement is not a requirement for the Ultimate Limit State conditions, Redacted - NNR Act 47, Section 51; PAIA 38(b)

NOTE 3: Further to NOTE 2, the Koeberg Safety Analysis Report (SAR) [4] Section II-1.9.2.4.8 "The LOCA is considered as the Containment Reference Accident".

Another consideration is 'liner thrust'. In LOCA conditions the liner heats up quickly whereas the concrete remains cool longer in most of the wall section. The liner cannot extend because it is confined by the concrete wall. Therefore, the liner gets compression stresses which are counterbalanced by tensile stresses in concrete, rebars and tendons. This effect is called liner thrust. However, the effect is time-delayed to the maximum LOCA air pressure peak. As the maximum air pressure in Structural Integrity Test (SIT) is higher, the test is decisive for the liner.

3.3.4 Post-tensioning of Tendons

During the design of the containment structures, the tendons' initial tensioning was calculated, and the cables were subsequently tensioned as part of the construction activities.

Several units of measurement can be used when referring to the tensioning in the tendons. It is also worth noting that post tensioned tendons' stresses are generally expressed as a fraction of its Guaranteed Ultimate Tension Stress (GUTS), usually 75-85% of GUTS. Table 1 provides the different measurements that may be used when referring to the cable tension, as well as the design limits of these measurements.

[†] Only in case of the two localised load cases (rupture of steam pipe and missile load) for the Ultimate Limit State condition (§ 3.3.3)

Table 1: Tendon Post-Tension Design Limits for Vertical Tendons

Property	Original Design Unit	Modern Unit	Conversion	Failure Limit	Tensioning Goal	Minimum per Original Analysis
Stress	h bar	MPa	h bar = 10 MPa	1,814 MPa	1,487 MPa	1,274 MPa
Force	k da N	kN	1 k da N = 10 kN	4,790 kN	3,928 kN	3,365 kN
Ratio to Ultimate Stress	GUTS (%)	GUTS (%)	-	100%	82%	70.23 %

Redacted - NNR Act 47, Section 51; PAIA 38(b)

Apart from the requirements mentioned in § 3.3, the design and analysis of post-tensioned concrete structures is a complex topic, and several aspects influence the performance of the post-tensioning. The two major considerations which impact the design of the post-tensioning are:

- Loss of Post-Tensioning and
- Durability (refer to §11).

3.3.5 Loss of Post-Tensioning

There are several factors that will influence the tension force applied to the cables, after the initial tensioning [27]. These factors are:

1. Friction Losses,
2. Anchorage Slip or Wedge Loss,
3. Elastic Deformation of the Concrete,
4. Concrete Shrinkage and Creep, and
5. Steel Relaxation.

Of the factors that reduce the force in the tensioned cables, 2 factors are time-dependent, i.e., steel relaxation of the cables and shrinkage and creep of the concrete. The remainder of the factors referred to above are not time dependent.

Although shrinkage and creep are two distinct properties of concrete, it is not possible to separate the measured strain, i.e., shrinkage strain and creep strain, from one another. Therefore, 'shrinkage and creep strain' are referred to as a single source of strain in general terms, although, as defined below, they are different.

‡ Values presented as per the original design documents

3.3.5.1 Shrinkage

Concrete experiences volume changes in both the fresh and hardened states throughout its existence. Measured shrinkage of concrete under drying conditions includes an autogenous component and a drying component. The autogenous shrinkage develops early (immediately after setting) due to internal consumption of water in hydration reactions, and the rate then reduces rapidly. In normal-strength concrete which experiences little autogenous shrinkage, the total measured shrinkage is usually taken to be the drying shrinkage. Strictly, drying shrinkage is the additional shrinkage caused by moisture loss from the concrete [15].

Shrinkage of concrete has an asymptotic form, where most of the shrinkage occurs at the initial setting time of the concrete, and the change in shrinkage reduces with time. Efforts in the past to estimate the asymptotic limit for shrinkage have proven difficult and complex, with little data available which can be used for prediction model calibration. Ninety six percent (96%) of all laboratory data to estimate the asymptotic limit do not exceed 6 years in duration [18] for example.

Shrinkage occurs quickly initially and thereafter occurs more slowly. One reference [18] [10] for example estimates that:

- 14 – 34% of shrinkage occurred in 2 weeks,
- 20 – 50% of shrinkage occurred in 4 weeks,
- 40 – 80% of shrinkage occurred in 3 months, and
- 66 – 85% of shrinkage occurred in 1 year.

Shrinkage is however influenced by several intrinsic factors. Intrinsic factors which have a significant effect include the water/cement (wc) ratio of concrete mix, degree of hydration, age of paste, cement extenders, temperature, moisture content and aggregate properties. Extrinsic factors include humidity and temperature, rate and time of drying, and member size and geometry. In general terms, Shrinkage (of which drying shrinkage is the main component) is mainly dependent on environmental factors.

Shrinkage is not recoverable and cannot be reversed.

Post-tensioning occurs sometime after the fresh concrete has set and has been subjected to initial shrinkage. Therefore, only the residual shrinkage, i.e., the shrinkage that occurs after the tendons have been tensioned, will influence the post-tensioning force.

3.3.5.2 Creep

Creep is defined as the time-dependent increase in strain of a solid body under constant or controlled stress. In the case of the Containment Structures, the creep strain will be caused by the post-tensioning forces induced by the tendons on the concrete, as well as the self-weight of the concrete. As the self-weight of the containment structures in the cylindrical walls is higher at the base than, for example, at the apex of the dome, there may be a linear change in creep strain over the height of the structure (whereas shrinkage is expected to be uniform).

Like concrete shrinkage, creep has an asymptotic form, where the creep is initiated at the initial loading of the concrete (in the case of external loads), and the change in creep reduces with time. The total accumulated creep strain can be several times larger than the initial elastic strain upon loading [15].

Creep is influenced by the same intrinsic factors as shrinkage; however, it is also influenced by additional extrinsic factors such as the level of the applied stress, duration of the load, curing, and the age at loading. Creep is dependent on load and environmental factors.

The majority of creep also occurs in the earlier stages of concrete. Although several intrinsic factors influence the creep of concrete, as an example of the time dependant behaviour of creep, the below is used to illustrate the time dependency of creep.

Considering a relative humidity of 70% (which is applicable to Koeberg) the creep of the example presented in reference [15], Figure 8 can be estimated to be:

- 600 µm/m at 1 year;
- 780 µm/m at 10 years; and
- 800 µm/m at 30-years.

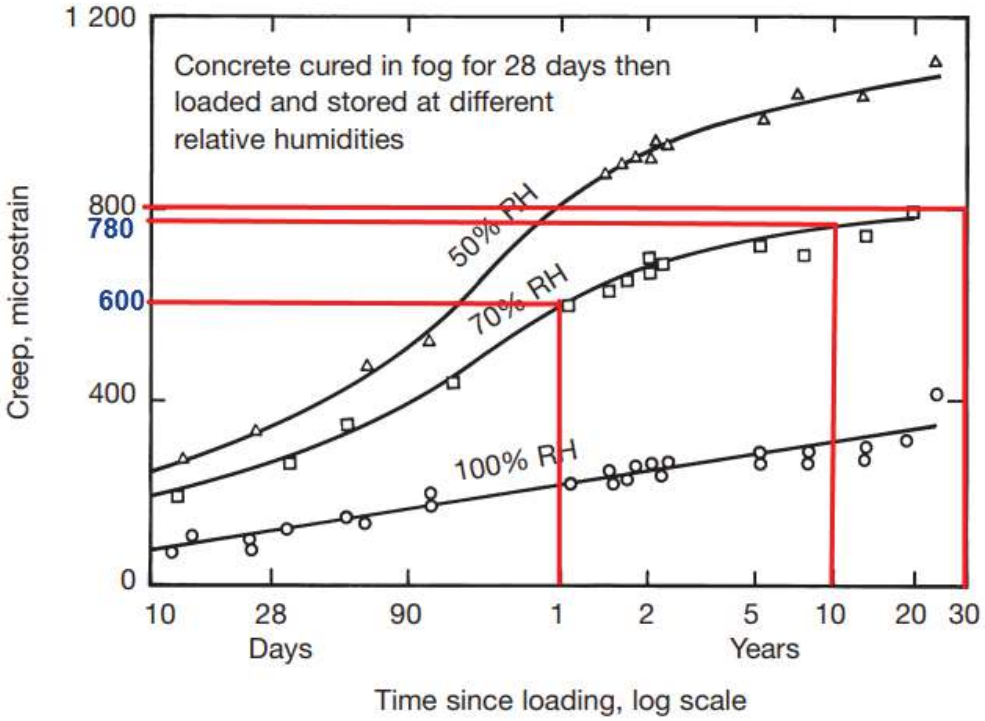

Figure 7: Creep of Concrete from Reference [15]

75% of the 30-year creep has thus developed at 1-year and 97.5% of the creep has developed at 10-years in the aforementioned example.

3.3.5.3 Prediction of Shrinkage and Creep

Design codes such as BS 8110, which is incorporated in SANS 10100-1:2000, use a 30-year timeframe to estimate the shrinkage strain and creep strain factors.

The original design documentation used for Koeberg also refers to a 30-year timeframe for shrinkage and creep, although reference is also made to Shrinkage and Creep at ‘infinity’.

The basis for the 30-year timeframe is not clear through the design codes or standards, although it is postulated that the 30-year timeframe is a conservative estimate at which time a significant portion of a structure’s intended service life shrinkage and creep strain have been achieved. The shrinkage and creep strain are much more significant in the first 30 years, compared to, for example, the next 30 years.

3.3.5.4 Age at Loading

Shrinkage and creep are both time dependent. It is worth noting the construction timelines for the two containment buildings (see Table 2). Both Units were tensioned roughly one year after the concreting was completed. This would mean some shrinkage would have already developed to a large extent and the late age of tensioning would also mitigate the total creep that could develop. Distinction is therefore sometimes drawn between *initial shrinkage* and *residual shrinkage* (see Figure 8). The creep coefficient is also influenced by the age of first loading and therefore creep can be mitigated to some extent by delaying the first loading age.

Table 2: Containment Building Construction Timelines

Event		Unit 1		Unit 2	
		Date	Elapsed Months	Date	Elapsed Months
First Concrete Pour		May 1978	-	October 1978	-
Concrete pour level at Bottom of Ring Beam		May 1979	12	July 1979	9
Threading Tendons	Horizontal	13 March 1980 – 9 August 1980	22-27	29 December 1980 – 2 March 1981	26-29
	Vertical	10 April 1980 – 13 October 1980	23-29	17 December 1980 – 26 March 1981	26-29
	Dome	20 June 1980 – 28 August 1980	25-27	6 February 1981 – 1 April 1981	28-30
Grouting of Tendons	Horizontal	6 May 1980 – 22 August 1980	24-27	22 January 1981 – 2 April 1981	27-30
	Vertical	20 May 1980 – 11 September 1980	24-28	8 January 1981 – 27 March 1981	27-29
	Dome	23 July 1980 – 9 September 1980	26-28	26 February 1981 – 15 April 1981	28-30
Measuring of the four greased tendons		14 October 1980	29	N/A	-
Reference Date for Strain Gauge Zero Measurement		18 September 1980 4 February 1981 17 November 1981	28 33 42	21 April 1981	30
SIT		December 1981	43	October 1982	48

NOTE 1: At the time of tensioning and the first measurement of the tension in the four greased tendons on Unit 1, the average age of the concrete was 1 year and 256 days [33].

Note 2: The reference date for the strain gauge zero measurements were done on different dates for different strain gauges. The dates presented in the table above, represent, in order:

- Unit 1 Strain Gauges Nos. 1 – 57, 18 September 1980
- Unit 1 Strain Gauges Nos. 58 – 59, 4 February 1981 and
- Unit 1 Strain Gauges Nos. 60 – 106 (all gauges including and above 22.89 m), 17 November 1981.

Note 3: The average time which lapsed between the grouting of the vertical tendons (post-tensioning complete) and the first strain measurement (zero measurement) were 14-17 months for Unit 1 and 0-3 months for Unit 2.

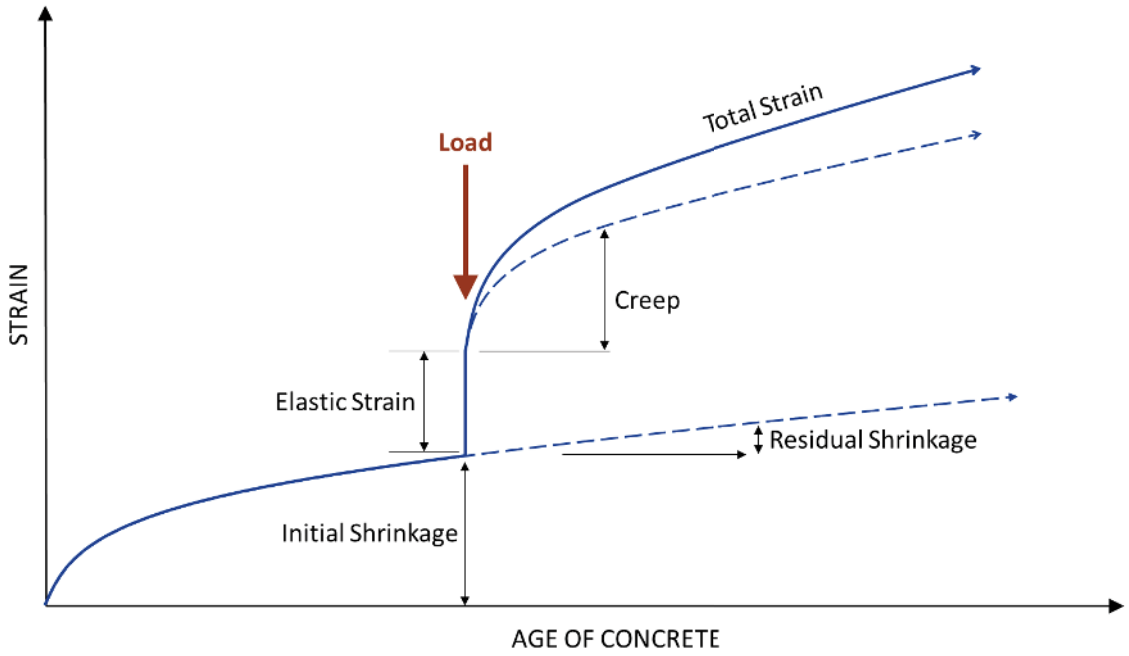

Figure 8: Strain Development of Aged Concrete

3.3.5.5 Steel Relaxation

The steel relaxation of the cables is another time-dependent parameter that influences the cable's long-term performance. Steel relaxation occurs as the material slowly deforms or relaxes under constant stress, similar to creep.

The steel relaxation is also asymptotical and is expected to occur mainly in the initial periods of the structure's life, whereafter the rate of the steel relaxation reduces.

3.4 Original Design Estimation

The original summary of the final containment analysis results [27] provided the stresses in the vertical cables[§], considering the various causes of tension losses, including the tension during a LOCA after the estimated loss of tensioning from all causes. These stresses are shown in Figure 9 and the same values are converted to force in Figure 10.

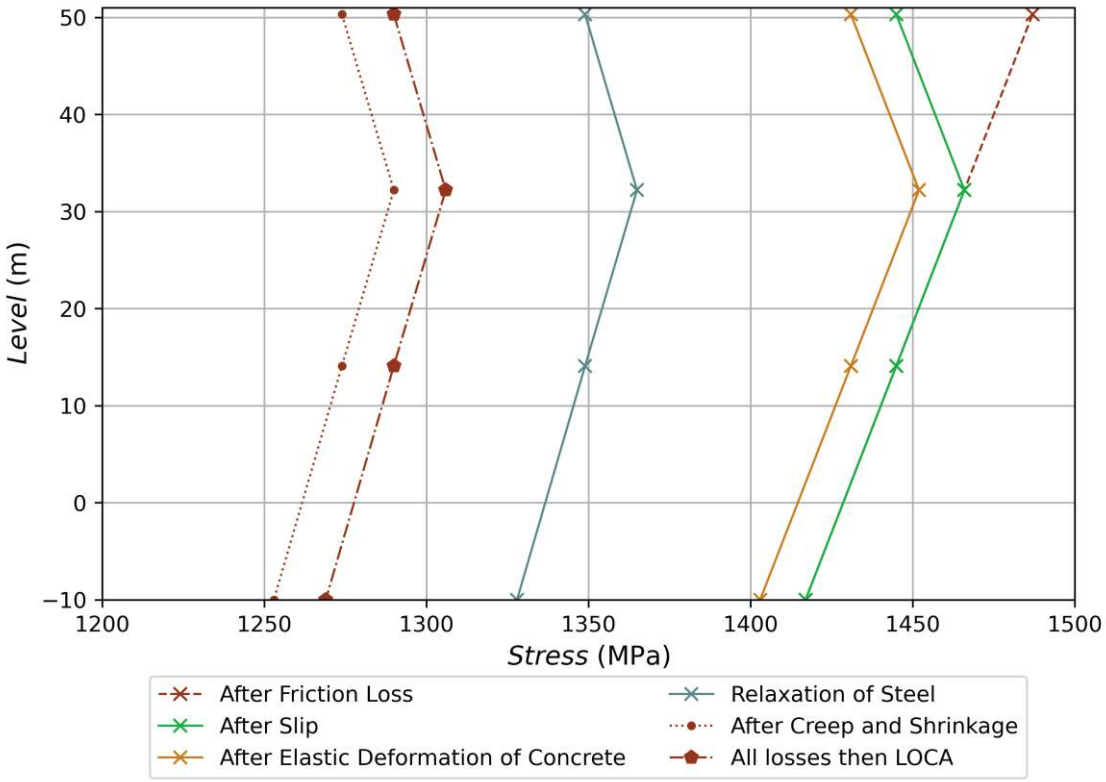

Figure 9: Summary of Design Stress in Vertical Tendons

[§] Only the Vertical Cables are shown. Reference provides the Horizontal Cables' stresses.

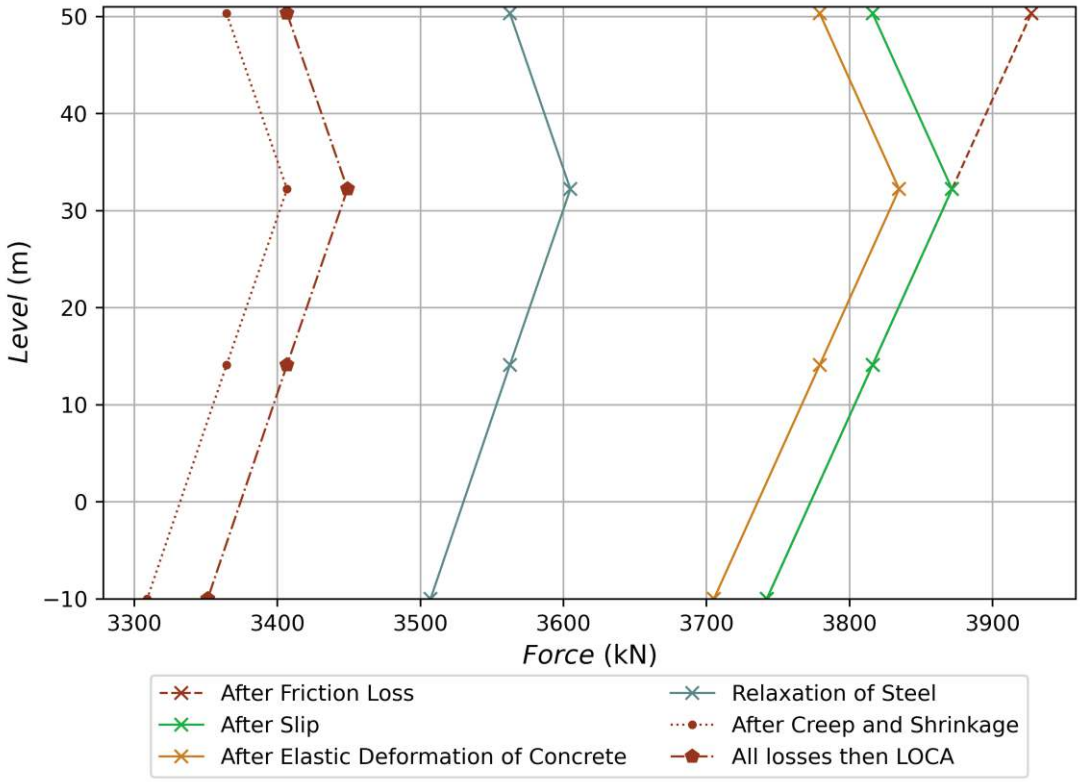

Figure 10: Summary of Design Force in Vertical Tendons

The results of the horizontal and dome tendons, which follows similar methodology to the one presented above can be found in Appendix B.

4. Monitoring and Equipment Installed

The monitoring of 1/2 HRX forms an integral part of the Koeberg Civil Monitoring Programme, which is a surveillance program aimed at ensuring long-term serviceability of all civil buildings, structures and infrastructure.

KAU-030 [1] states that “Periodical monitoring of the containment building is carried out to monitor and trend various parameters that provide information regarding relative movement, level of prestress and local strain in the containment building structure”.

It further states that “*Monitoring of the dynamometers, invar wires, pendulums, strain gauges and thermocouples shall be carried out on a quarterly basis (3 monthly) in accordance with EdF practice.”*

The monitoring of the structures is part of the licence-binding activities of Koeberg and shall be conducted in full compliance with the Nuclear Installation Licence (NIL) as issued by the NNR.

Several different measurement equipment were installed on the containment structures. The original equipment, their function and supporting information are provided in Table 3 below:

Table 3: Installed Monitoring Instrumentation on 1/2 HRX

Equipment		Unit 1		Unit 2		Section Discussed
Topometric Markers		22		22		**§ 4.1**
Invar Wires (Horizontal)		2		2		**§ 4.2**
Invar Wires (Vertical)		4		4		**§ 4.3**
Pendulums		4×3		4×3		**§ 4.4**
Dynamometers		4		0		**§ 4.5**
Strain Gauges	Cylinder & Dome	46	108	56	62	**§ 4.6**
	Raft and Brackets	62		6		
Thermocouples		63		41		**§ 4.7**

Additionally, in general where the *Location* of equipment is used, the following is worth noting:

- The Containment Buildings are practically symmetrical, but orientated differently on the nuclear island,
- For both containment buildings the biological door and gantry structures are at ‘Rib 1’,
- The axis of the containment structures is similar on the nuclear island,
- The location of equipment on the containment structures will be referred to considering the orientation, axis and height, where applicable,
- The layout and orientation of containment structures are illustrated in Figure 11.

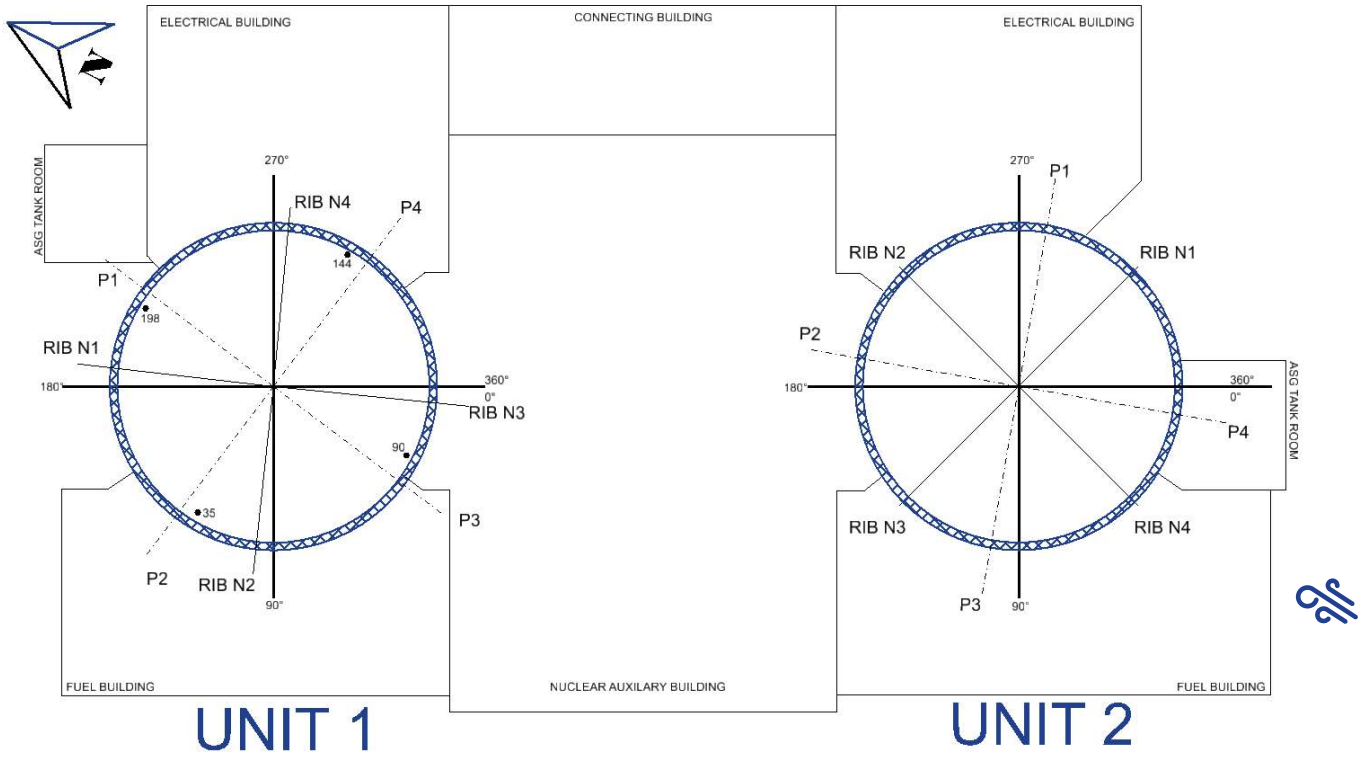

Figure 11: Layout and Orientation of Containment Structures

It is worth noting the local environmental conditions of the structures are different, as the Unit 1 structure is exposed to the sun more than the Unit 2 structure, and vice versa for the predominant wind.

NOTE: The original documents also provide the axis of the containment structures in gradians (100 gradians = 90 degrees).

4.1 Topometric Markers

A network of benchmark that were installed into the underside of the upper raft under 1/2 HRX allows for the deformation at the base of containment to be determined. Refer to Figure 12. The benchmark also allows for the absolute settlement to be measured.

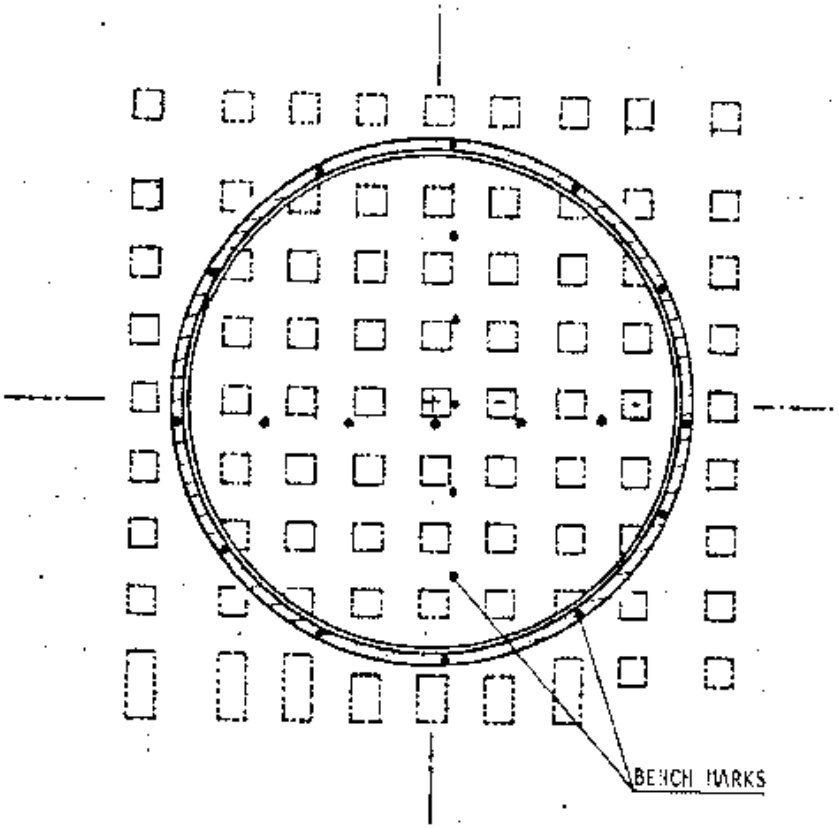

Figure 12: Location of Benchmarks

4.1.1 Topographic Measurements

As part of the ISI programme, the upper and lower rafts are surveyed every five years for deformation and settlement, with the most recent survey conducted in 2021 [22].

4.1.2 Upper and Lower Raft Monitoring

The 5-yearly survey focuses on the settlement and monitoring of the upper and lower rafts and reports the differential movement between the respective rafts.

From the topographic survey, it is noted that both the upper and the lower rafts have settled on average, as follows:

- -0.0018mm Lower Raft
- -0.0019mm Upper Raft (Underneath Unit 1)
- -0.0013mm Upper Raft (Underneath Unit 2)

The latest result is shown in Figure 13 where the 2016 results are compared to 2021.

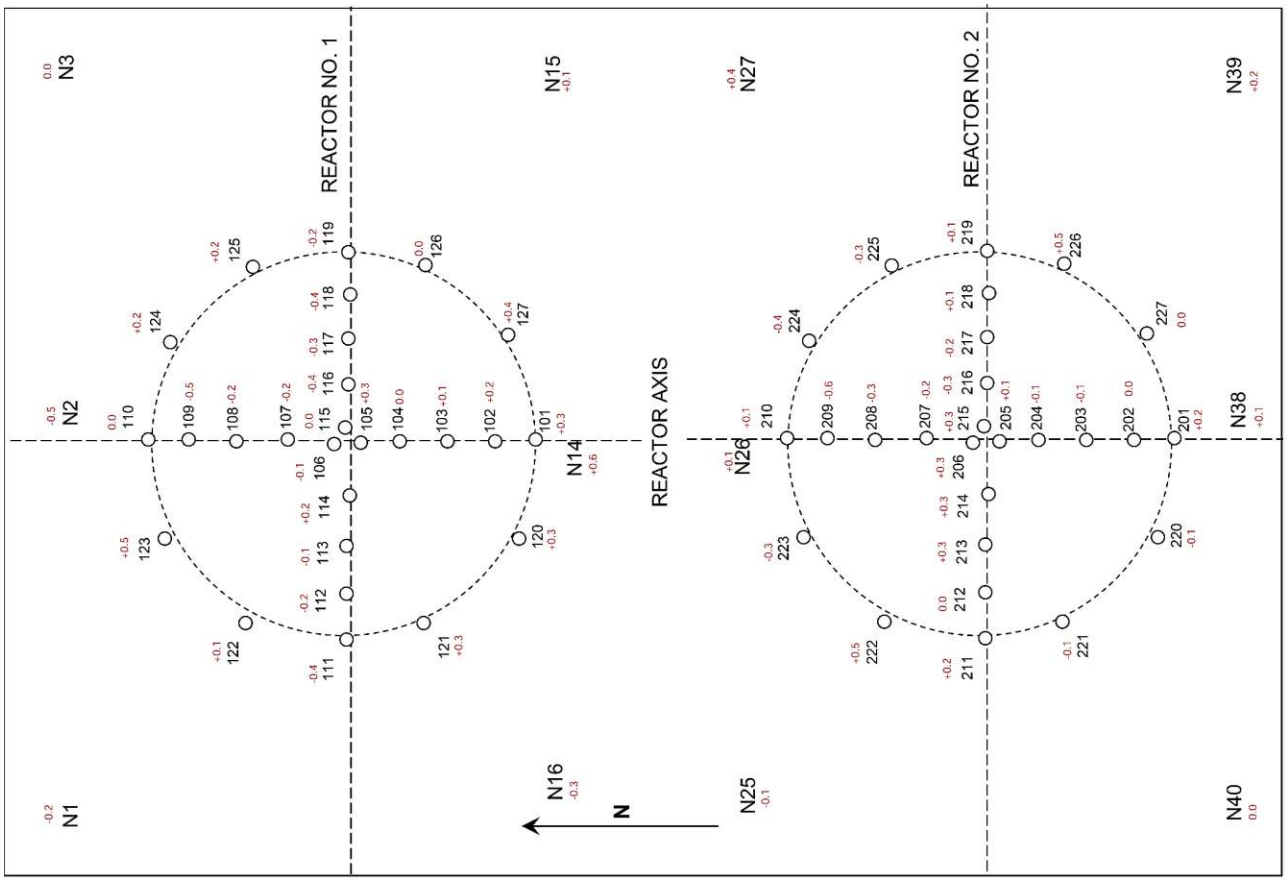

Figure 13: Aseismic Vault – Relative height differences in millimetres, 2016-2021

It is noted that the extreme relative movement between the upper and lower raft (i.e., the residuals) are +0.6mm and -0.5mm. It is concluded in the topographic survey report that the "residuals fall within the precision range of the survey. The settlement was more fully assessed and treated separately under TLAA 304, report L1124-GN-RPT-045.

4.1.3 EdF Experience

To determine the stability of the nuclear island, EdF applies a methodology which is based on the consistency between the design hypothesis / calculations and the measured data and in cases of deviation the surveillance criteria defined by EDF are as follows:

Structures are classified in 3 categories (Vt: Settlement rate – VB: Rotational rate):

- Group 1: Stabilized structure (Frequency of inspection 4 – 8 years)
  - Vt < 0.6 mm/year and/or VB < 0.3 mm/10m/year
- Group 2: Structure in the process of being stabilized (Frequency of inspection 2 – 4 years)
  - 0.6 mm/year < Vt < 1.2 mm/year and/or 0.3 mm/10m/year < VB < 1 mm/10m/year
- Group 3: Un-stabilized structure (Frequency of inspection 1 – 2 years)
  - Vt > 1.2 mm/year and/or VB > 1 mm/10m/year

4.1.4 Koeberg Results

Eskom determined the rate of settlement to compare the results to the EdF methodology and determined that the rate of settlement is within the EdF acceptance criteria for Group 1: Stabilised structures which supports the survey interval of 5-yearly as well as the acceptance criteria, considering a vertical displacement rate per year.

The maximum absolute settlement for the upper raft is 7.1 mm and occurs underneath unit 2 containment building and maximum absolute settlement of 5.3 mm for the lower raft. The results also indicate the movement of the nuclear island has plateaued out. The current absolute settlement measurement is still consistent with design hypothesis/calculation of the maximum static settlement for the nuclear island in range of 10 mm ± 1 mm. The expected settlement rate for the nuclear island is 0.12 mm / year [14].

4.2 Invar Wires (Horizontal)

Originally, 2 invar wires were installed, for each structure, at the raft level of the structures. The wires were placed in ducts in the concrete base along the diameter of the structure, orthogonally.

These wires were used to measure the deformation of the structures' diameter at the base; however, the equipment was discontinued, and the ducts closed. These parameters are now measured under the topographical survey.

4.3 Invar Wires (Vertical)

Four (4) sets of Invar Wires [35] are installed on each Unit. These Invar Wires are installed below the *ring beam* (Figure 3) at a level of +45.37m and hangs to the -3.70m level, on every quarter turn. The invar wires are used to measure the vertical movement of the HRX structures.

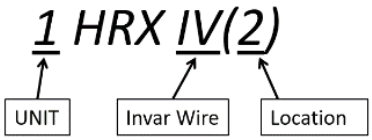

4.3.1 Koeberg Experience and Results

The invar wires at Koeberg have degraded with time and the measurements and/or the documentation of the invar wire results has been poor in the past. These invar wires were refurbished and will be monitored every 5 years in accordance with the ageing management programme. The degradation of the invar wires led to some invar wires breaking and the datum for the measurements were lost. As such, long-term monitoring results since commissioning are not available for the invar wires or not useful. Since circa 2009 the on-line monitoring has been performed quarterly in accordance with the In-Service Inspection (ISI) programme [3], however the results do not provide a holistic overview of the containment behaviour since commissioning.

The results are therefore not considered as part of this report.

4.4 Pendulums (Plumblines)

The Pendulums [34] are installed near the vertical Invar wires. The Pendulums are installed in four (4) groups of three (3), with each group installed a quarter turn from the previous. Each group consists of 3 lines, installed at full height, midway and at the bottom of the structures.

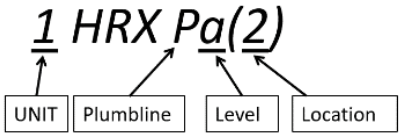

The levels refer to the height at which the pendulums are connected, where:

a = + 42m

b = + 26m

c = + 10m**

4.4.1 Koeberg Experience and Results

Like the invar wires, the pendulums at Koeberg have degraded with time and the lifetime measurements and/or the documentation of the pendulum results had been poor and the long-term monitoring results since commissioning is not available or not useful. The pendulums have since been refurbished, and data will be useful in monitoring the structures for the intended period of LTO. Since circa 2009 the on-line monitoring has been performed quarterly in accordance with the ISI programme [3], however the results do not provide a holistic overview of the containment behaviour since commissioning. The results are therefore not considered as part of this report.

Refurbishment of unit 1 and unit 2 Invar wires and Pendulums was successfully completed in 2024. New baseline readings post refurbishment has since been established.

4.5 Dynamometers

There are four (4) un-grouted vertical tendons on 1HRX to allow the force in the cables to the concrete to be monitored (all other tendons, in all orientations on Unit 1 and Unit 2 are grouted). These cables are used to measure the tension forces in the four individual cables which is sometimes referred to as the ‘relaxation tests’, as it is expected that the force in the cables will relax (reduce) over time.

The respective cables are labelled cables. 35, 90, 144 and 198, as illustrated in Figure 11, and their initial force development is illustrated in Table 4. Each cable is fitted with three (3) dynamometers with a capacity of 150t each [31].

Operational experience has shown that the equipment requires calibration to ensure the readings are not erratic. In 2023, recalibration of the dynamometers was completed. The measurements taken on site in (mV/V) are then correlated during the calibration of the equipment to a force (kN).

The monitoring results are discussed in more detail in § 5 - Dynamometers.

4.6 Strain Gauges

Vibrating wire strain gauges (also sometimes referred to as acoustic strain gauges) were incorporated into the concrete allowing local strains in the concrete to be measured and then determining the corresponding stresses. They are positioned in various locations in the walls and rafts of the structures, points selected to be indicative of the overall behaviour of the structure.

** Only 1 HRX Pc (3) is at + 9.2m

As illustrated in Table 3, there is a notable difference in the number of gauges installed on the respective structures. There are 20% more gauges in the 1HRX wall and dome as compared to 2HRX and 165% more in the raft. A complete list of the installed strain gauges is presented in Appendix A.

Importantly, the strain results can be corrected for temperature, although for the long-term trending the seasonal effects are neglected, as seasonal variations will simply cancel out.

Furthermore, additional modern technology Vibrating Wire Strain Gauges (VWSGs) with automatic data logging capabilities were installed on the external facade of the containment domes and walls. In addition, modern technology optical fibres are currently being installed on the external facade of the dome and walls of the containment building. The installation of these modern technologies forms part of the bridging strategy prior to the implementation of a modification aimed at improving the quality of data obtained from the online monitoring system. Currently, 10 modern VWSGs and 4 optical fibres are installed on each containment building.

4.7 Thermocouples

The thermocouples were embedded alongside pairs of the original strain gauges to measure the concrete temperate at the moment the strain is measured, to allow the effects of the concrete temperature to be included in the stress calculations. There are 42% more thermocouples on 1HRX compared to 2HRX.

4.8 In-Service Inspections

The monitoring of 1/2 HRX is currently performed by qualified personnel. The monitoring readings are taken and tracked on a database, then a report is compiled. The inspection reports are used to update this report. The last reports are the following for unit 1 and 2 respectively.

- [23] JN848-NSE-ESKB-L-8443: 1HRX online monitoring results for Q1 (2021), and
- [24] JN848-NSE-ESKB-L-8524: 2HRX online monitoring results for Q2 (2021)

These reports however do not provide a comparison between the respective structures.

5. Dynamometers Analysis

5.1 Cable Force and Trending

The ‘shrinkage and creep’ of the concrete and the ‘relaxation of steel’ as mentioned are both time-dependent parameters and therefore will occur over time. For the original analysis [27][††], the ultimate time frame at which the losses were estimated is not clear and reference is made to 30 years. The basis for the 30-year period is likely due to the shrinkage and creep coefficient prediction models in codes and standards (for example SANS 10100) which are limited to a 30-year period. Reference [33], however, predicts the ultimate (or infinite) shrinkage and creep of the concrete in accordance with the original design rules[‡‡].

[††] This Report was Authorized on 7 February 1980

[‡‡] This Report was Authorized on 21 July 1982

The initial force in the cables was measured during the tensioning process and was subsequently measured at 1 000, 3 200 and 15 000 hours after the initial tensioning. These results are summarized in Table 4.

Table 4: Initial In-Service Relaxation Tests

Cable	Load Cell	14-10-1980 0 hours (kN)		26-11-1980 1,000 hours (kN)		25-02-1981 3,200 hours (kN)		28-06-1982 15,000 hours (kN)	
35	151	1,252.90	**3,773.1kN**	1,228.90	**3,694.1kN**	1,210.40	**3,645.9kN**	1,206.05	**3,632.9kN**
	152	1,275.20		1,246.80		1,226.30		1,223.87	
	153	1,245.00		1,218.40		1,209.20		1,202.97	
90	154	1,239.80	**3,757.0kN**	1,210.50	**3,668.1kN**	1,202.00	**3,606.3kN**	1,195.85	**3,615.4kN**
	155	1,262.00		1,234.90		1,198.80		1,220.79	
	156	1,255.20		1,222.70		1,205.50		1,198.77	
144	157	1,196.30	**3,716.7kN**	1,177.30	**3,649.9kN**	1,138.70	**3,601.4kN**	1,149.08	**3,599.4kN**
	158	1,251.50		1,224.30		1,221.20		1,211.28	
	159	1,268.90		1,248.30		1,241.50		1,239.04	
198	160	1,203.20	**3,721.5kN**	1,171.90	**3,620.5kN**	1,167.30	**3,595.7kN**	1,166.36	**3,589.9kN**
	161	1,245.40		1,211.80		1,206.90		1,204.41	
	162	1,272.90		1,236.80		1,221.50		1,219.09	
Average Force (KN)		**3,742.08**		**3,658.15**		**3,612.33**		**3,609.40**	
Average Relaxation				**2.25 %**		**3.50 %**		**3.55 %**	
Relaxation Limit				**3.4 %**		**4.0 %**			

Note: The relaxation limits are as specified for the specific time of measurement as per the original relaxation analysis per reference [33].

The initial forces measured in Table 4, and the limits of the various measuring units, are plotted.

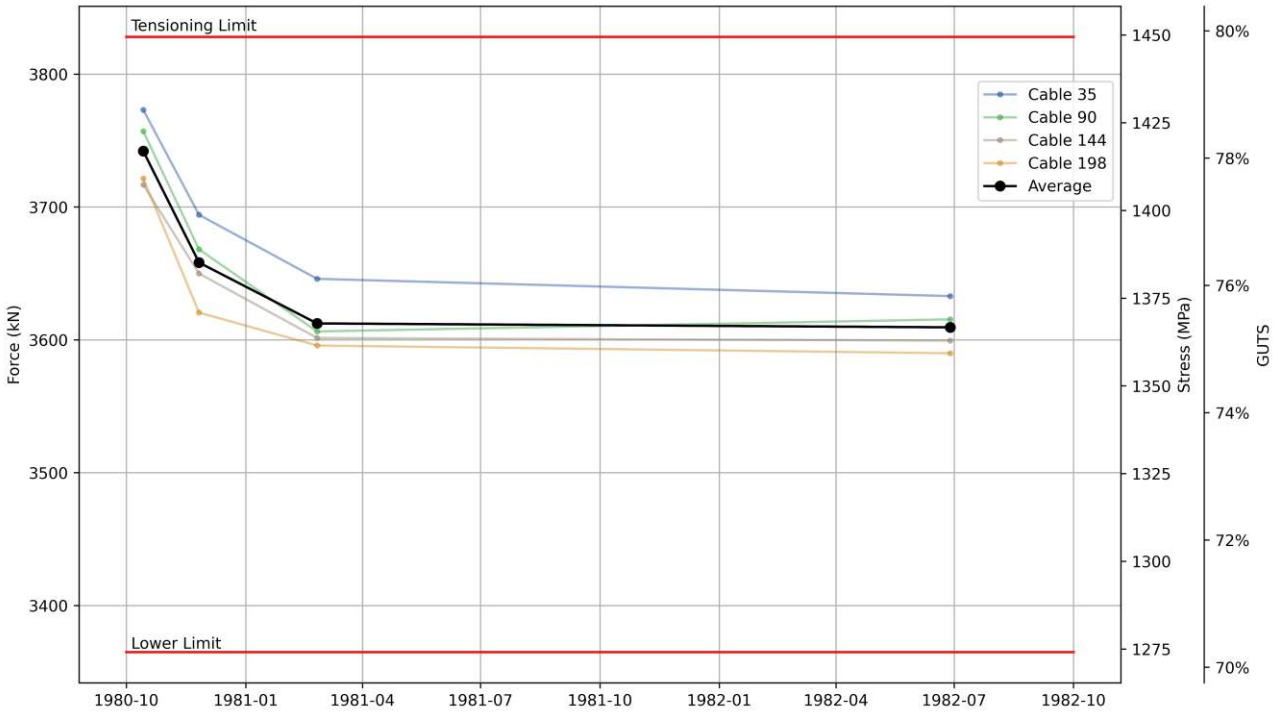

Figure 14: Cable Relaxation During First 15,000 Hours

The steel relaxation noted in Figure 14 is due to a combination of the instantaneous and time-related mechanisms listed in §3.3.5. It is however not possible to differentiate completely between these mechanisms by only considering the cable force.

Notwithstanding, the behaviour of tensioning loss over time is consistent with expectations, where the majority of the loss is expected at the beginning of the structure's life. The creep behaviour of the concrete and the creep relaxation of the steel occurs more dramatically initially; however, the rate of loss reduces consistently over time.

The lower limit indicated in Figure 14 is the lower limit for the force as assumed in the design documents (reference [27]) and corresponds to Table 1.

5.2 Individual Dynamometer Readings and Anticipated Error

To measure the total force in each un-grouted cable, the respective cables' three (3) dynamometers are correlated to force, and then summed to represent the total force in each cable.

Circa 2005, Eskom adapted the testing procedure to measure each dynamometer twice. The final measurement is averaged between the two readings. The precision of the measurements can therefore be determined by comparing the absolute difference in the respective readings (referred to as ΔmV/V). These differences in readings are shown in Figure 15.

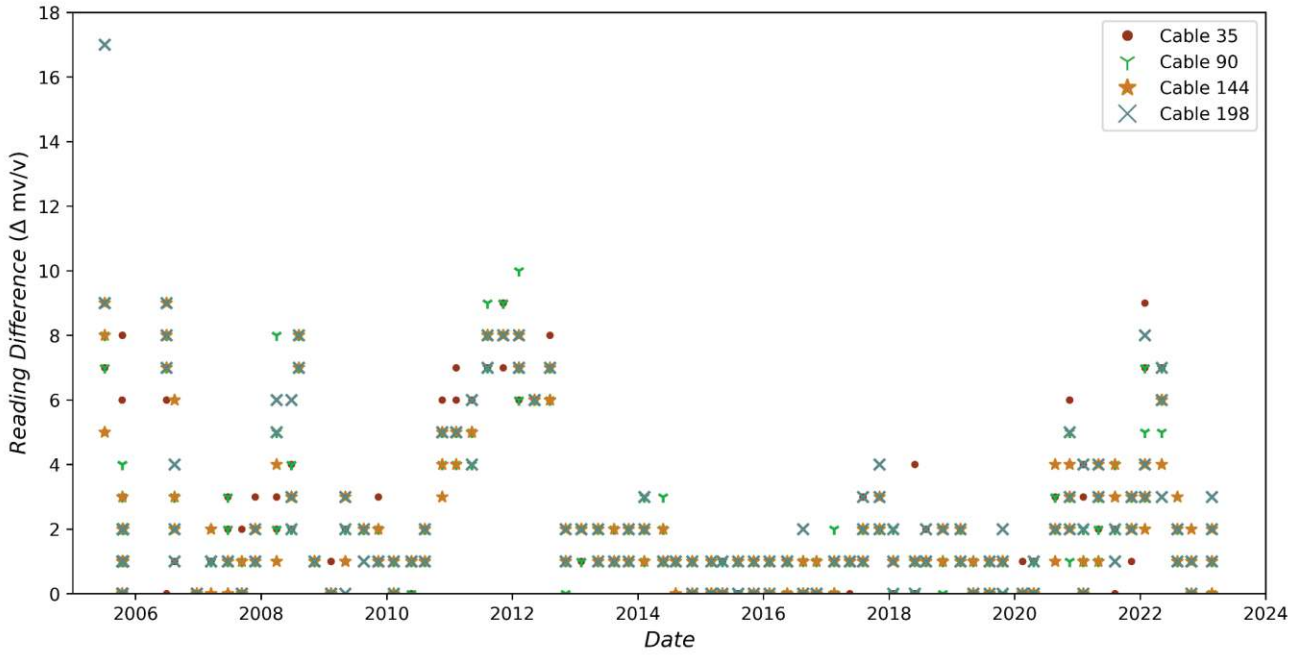

Figure 15: Differences in Respective Dynamometer Readings

There is no distinct trend in the respective ΔmV/V readings. There may be some subjectivity in the measuring of the readings, considering the readings taken circa 2006 and 2022.

Further statistical analysis of the differences in readings (ΔmV/V values) yields the following results:

Table 5: Statistical Analysis of ΔmV/V

Statistical Parameter	mV/V	kN
Mean	2.220	3.60
Median	1	1.62
Mode	1	1.62
Standard Deviation	2.393	3.88
Sample Variance	5.727	9.29
Minimum	0	0.00
Maximum	17	27.57
Count	888	

NOTE: Force was correlated to the dynamometer average calibration

NOTE: The ‘count’ (888 readings) represents 1776 total readings, 74 different quarterly measurements spanning 18.5 years

Furthermore, the ΔmV/V values are plotted in a histogram, Figure 16, to illustrate the precision of the readings, with the force.

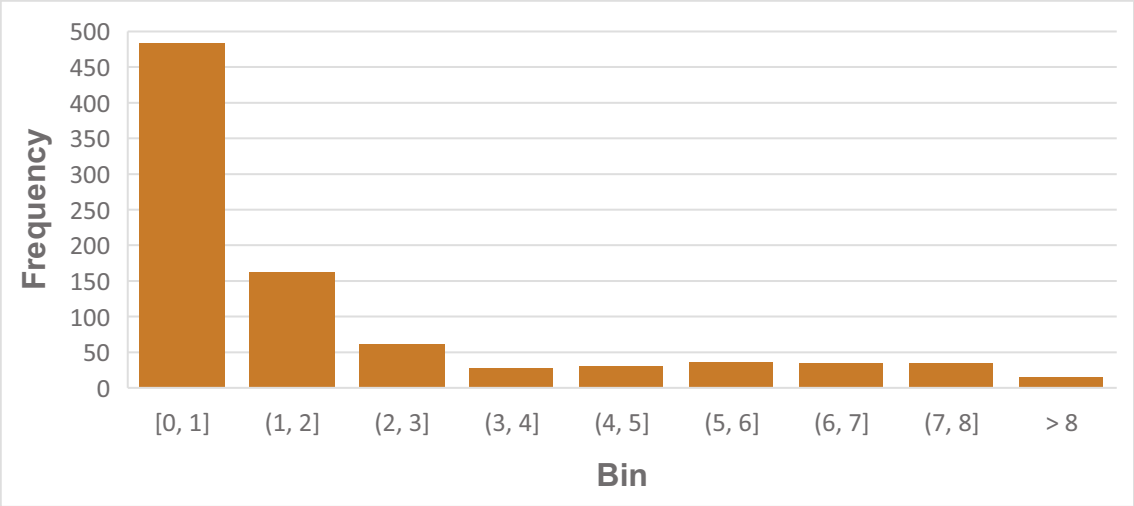

Figure 16: Histogram of ΔmV/V readings

The standard deviation of the force is expected to be 1σ ≈ 4 kN for each Dynamometer and the three-sigma value for a cable (3σ) is therefore 36 kN. Assuming a cable force of 3,400 kN in each cable, the error (or precision) is estimated to be 1.059%[§§], which is below the dynamometer's original accuracy of 3% [33].

5.3 History

Since commissioning, the dynamometers have been used to measure the force in the respective loadcells for the four greased tendons. However, as can be seen in Figure 17 and 18, the data available was erratic during certain periods most likely due to the dynamometers' calibration being out of specification and in other instances the wire holding the load cells being faulty resulting in gaps in the data.

In 2023, recalibration of the dynamometers was completed. Additionally, the instrument used to perform the measurements of the dynamometers was upgraded from Vishay P-3500 to modern Vishay P-3 strain indicator, which has a data logging capability. The dynamometers re-calibration was successful.

The data prior to 2023 recalibration was obtained using the Vishay P3500 and from the containment dome measuring terminal. The data post-calibration, October 2023 onwards, was obtained using the Vishay P3 and from the NAB roof measuring terminal. This upgraded method of obtaining data introduced a consistent difference between data before and after calibration. A new trend for the data post-calibration is apparent, as shown in Figure 17 and Figure 18.

[§§] With the assumption that the readings are normally distributed.

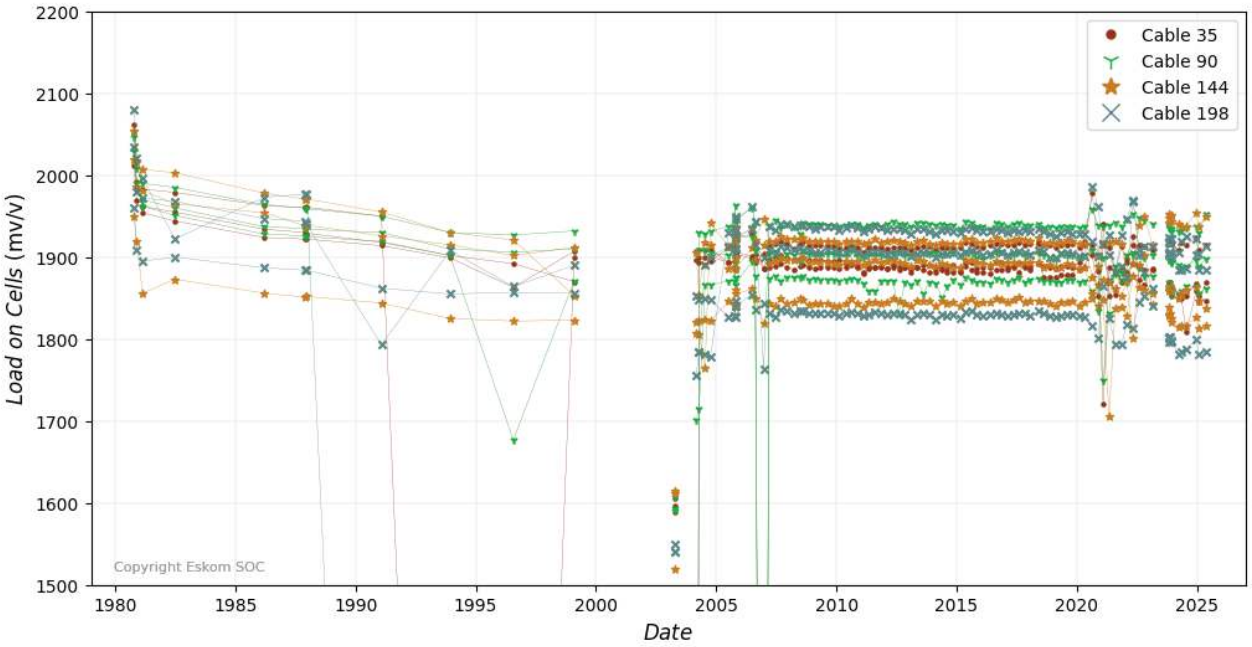

Figure 17: Measurements of Each Load Cell

The three respective loadcells on each greased tendon are combined to provide the total force as measured by the dynamometers, as shown in Figure 18:

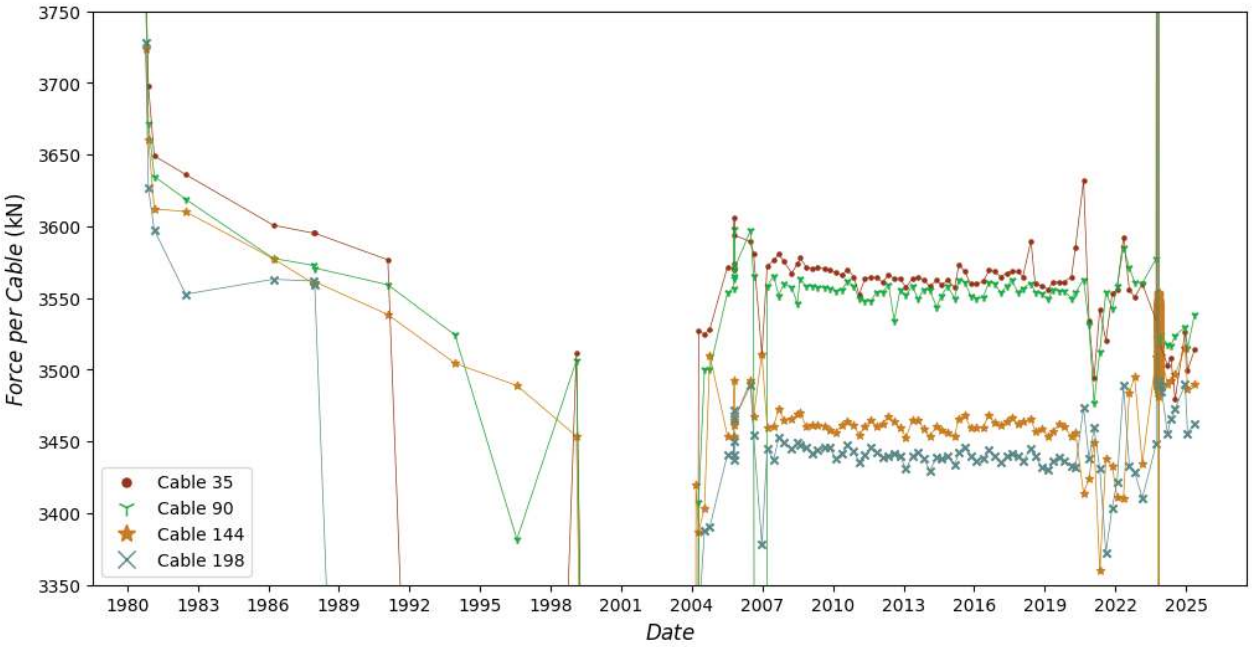

Figure 18: Summation of Each Load Cell

The force in the cables is however direct measurements of the actual force in the tendons and the datum for the force cannot be lost (unless external factors influence the tendons). Therefore, a gap in the data, or issues with calibration, is not a long-term concern, as once the measurements continue, or the calibration is addressed, the measurements should again read the actual force in the tendons.

After the measurements were restarted circa 2005, it was noted that the calibration of the equipment was lost, and the readings were erratic. This can be determined by inspection, for example, one reading can show a significant decrease in the tension, while the next may show a significant increase – which is not possible, as the tension cannot be regained if significant tension is lost (in the case of a broken strand for example).

By inspecting the results post 2020, it again can be deduced that the calibration of the monitoring equipment has been lost as the forces in the cables increase and decrease erratically. The dynamometers were however recalibrated in October 2023 and the post-calibration results will normalise as well.

To provide a clearer picture of the calibration issue, the tendon forces were normalized to each's average for the period where the calibration was sufficient (2008 – 2020) as presented in Figure 19.

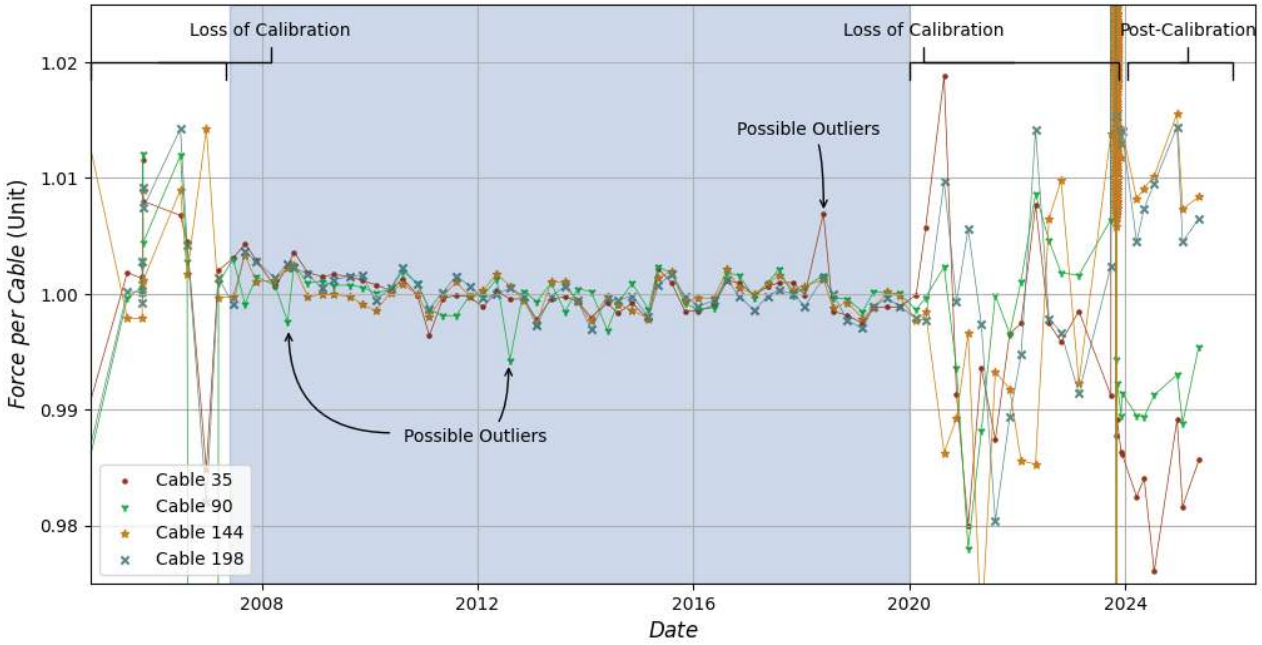

Figure 19: Normalized Tendon Forces

5.4 Trending of Tendon Forces

The trend of the cable force is clear for the period 2008 – 2020 where the calibration of the monitoring of the equipment was not disputed.

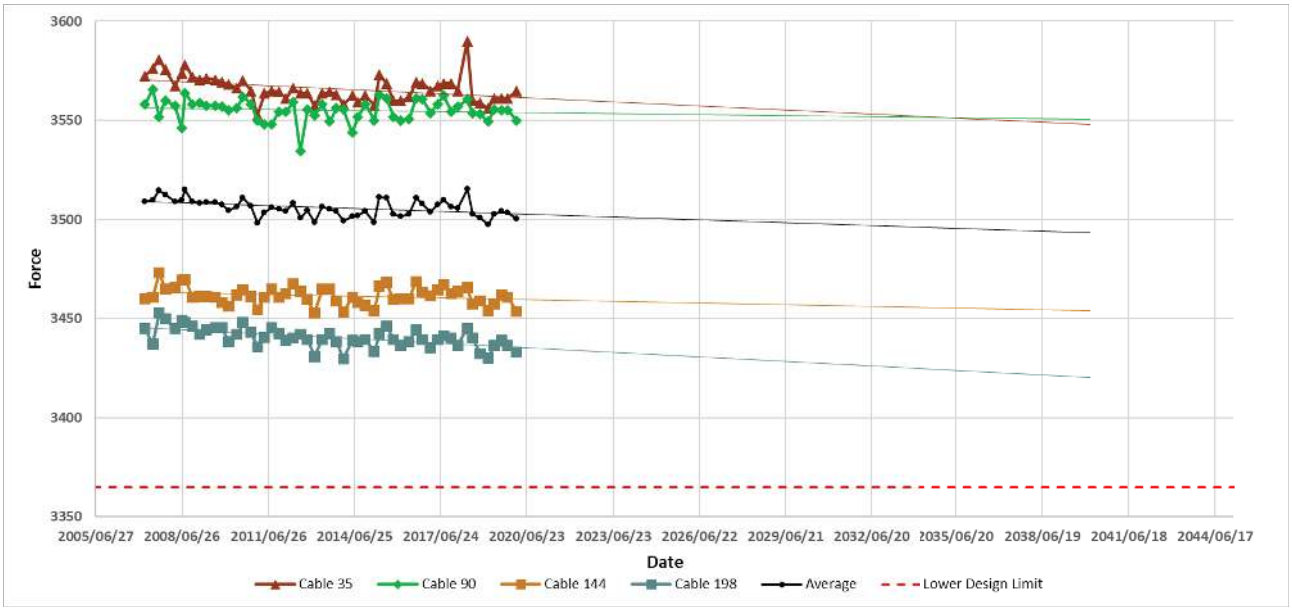

Figure 20: Linear Regression of Calibrated Tendon Forces

The original design documentation [33] makes it clear that the *average* tendon force needs to be considered, however for completeness, the individual tendon forces as well as the average tendon force regression are presented below.

When considering the linear regression of the two sets of data and extrapolated to 60-year operation, i.e., 2044 the following results are obtained:

Table 6: Extrapolated 60-Year Tendon Force Estimates

Cable	Slope [kN/day]	40-Year [kN]	60-Year Extrapolated [kN]
Cable 35	-0.0019	3,558	3,544
Cable 90	-0.0005	3,553	3,550
Cable 144	-0.0008	3,457	3,451
Cable 198	-0.0021	3,432	3,416
Average	**-0.0013**	**3,500**	**3,491**

Note: The start date is 14 October 1980, the day of the first measurement)

Figure 10 can then be compared to the results in Table 6 to illustrate the expected (design) tension forces expected in the tendons, versus the measurements to date and the linearly extrapolated prediction based on the calibrated period from 2008 to 2020. This is presented in Figure 21.

It can be seen that the extrapolated 60-year tendon force of 3,491 kN (1,322 MPa) is still expected to be above the original calculated minimum tension force of 3,365 kN (1,274 MPa) [27].

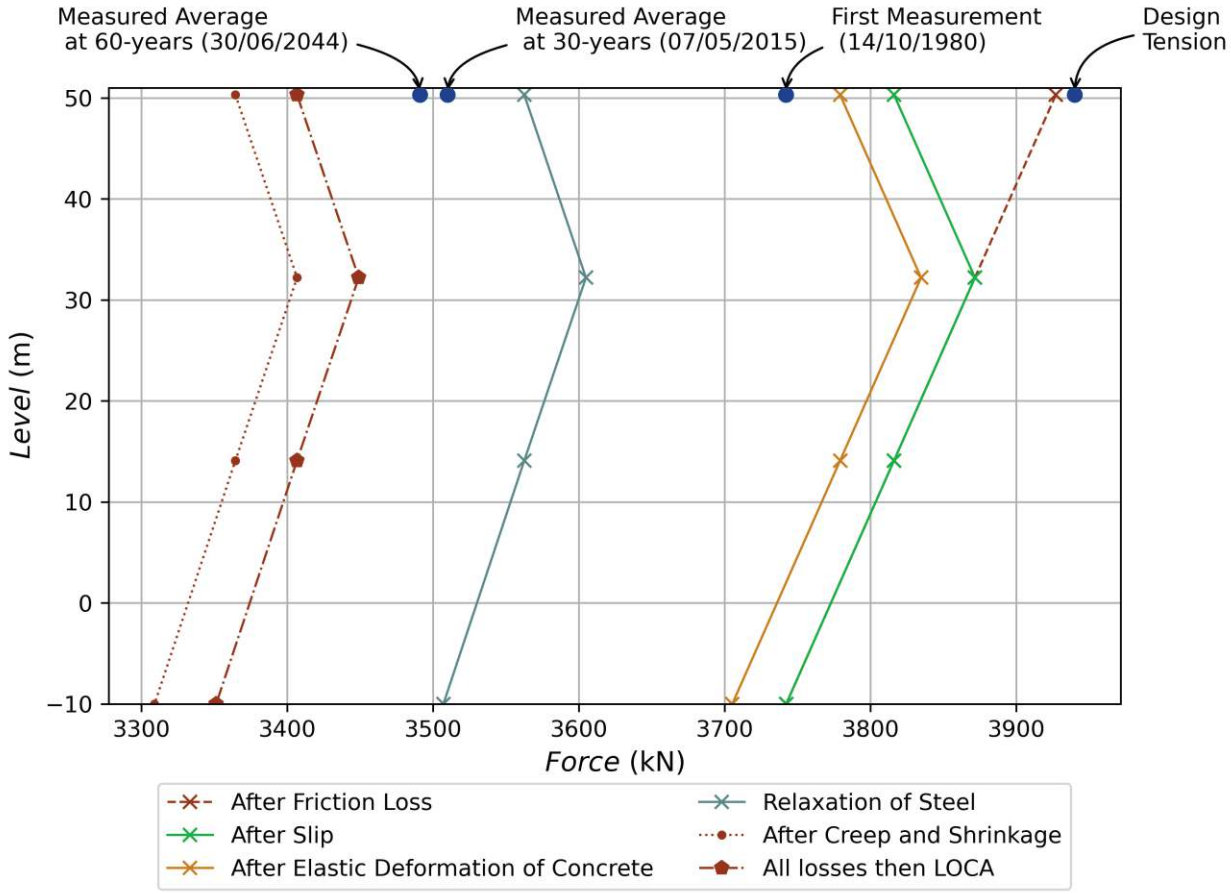

Figure 21: Design Prediction of Tension Forces and the Measured and Estimated Results

The above results indicate:

1) The measured average tension in the tendon after 30 years (**3,510 kN**, as measured on 07/05/2015) is higher than expected in terms of the original design after 30 years based on a 8.9 % relaxation (3,409 kN) [33].
2) The additional loss of tension during LTO is not expected to be significant and will not challenge the original estimate.
3) Based on the measured and predicted tension in the tendons as noted above, there is sufficient margin for the period of LTO before the minimum design tension of 3,365 kN is reached compared to a 60-year extrapolated tendon force of 3,491 kN.

6. Strain Monitoring

The strain results are investigated to determine the development of movement on the containment structures. It is common practice to consider strain gauges above the +20m level, because at this height the effect of the raft is considered negligible.

Furthermore, the data for the strain is discussed in ‘hours’ after commissioning for ease of data processing. The zero hour is on **1980/09/18**.

6.1 Containment Structures Cylindrical Walls Vertical Strain

The raw vertical strain data for the +22.89m level gauges are presented below in Figure 22 for both Unit 1 and Unit 2. For Unit 2, a strain gauge can be seen to be an outlier (circled in Figure 22) which skews the data when inspecting the 'jump' in the average of the strain. This strain gauge (Unit 2, No. 10) is located at +22.89m on Grade 110. The strain gauge is however paired with No.12 at the same location which fits the data and is not excluded.

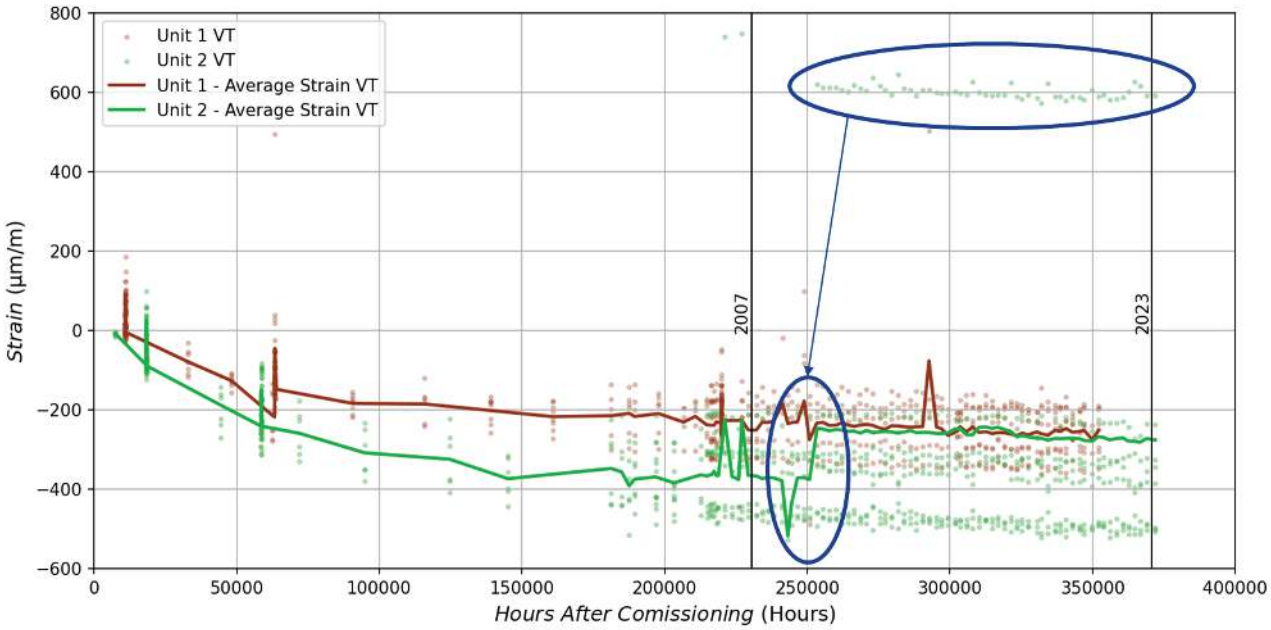

Figure 22: Raw Vertical Strain Data at +22.89m

With the exclusion of strain gauge Unit 2, No. 10, the data and the average strain are repeated in Figure 23. It is seen by inspection that the average of the data follows an expected trend and that the exclusion of strain gauge Unit 2, No. 10 is justified. Besides the instantaneous peaks which represent ILRTs, it is noted that the other peaks (deviations from the average trend) do not represent structural anomalies because the increases/decreases return to the expected average trend.

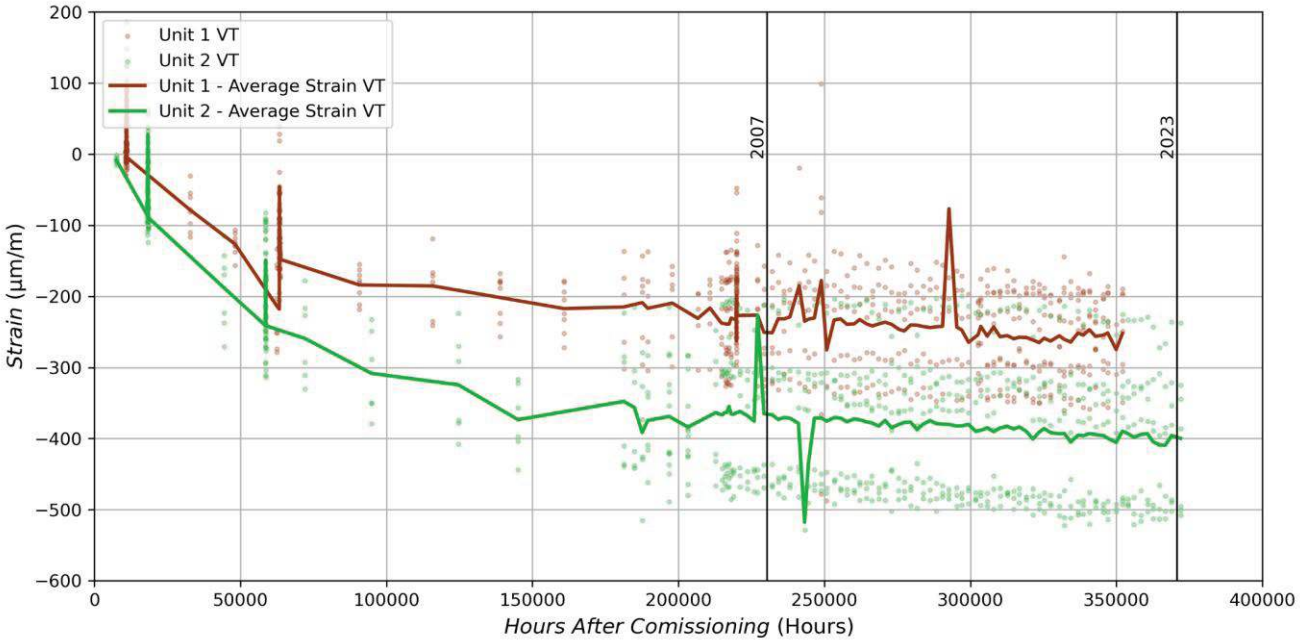

Figure 23: Vertical Strain Data at +22.89m

6.1.1 Linear Estimation of Linear Portion of Data

It is assumed that the expected exponential strain development has already occurred and that the remainder of the strain development that will occur can be represented by a linear regression. This was done from circa 2009 onward (250 000 hours), and the linear trend and extrapolation to 2044 (525 600 hours) is presented in Figure 24. 2009 was selected as the beginning mark for the linear extrapolation as it is the end of the 30-year period of the published strain predictions and by inspection, the start of the linear strain development.

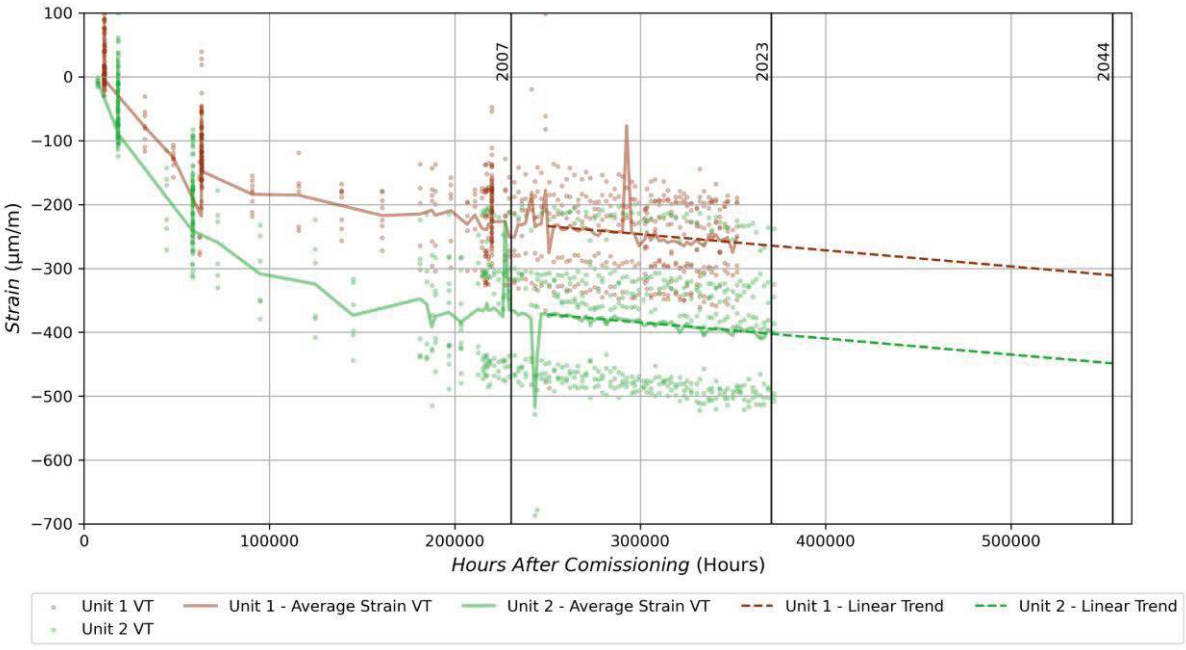

Figure 24: Linear Extrapolation of the Vertical Strain Development

CONTROLLED DISCLOSURE

6.1.2 Exponential Regression of all Data

It is understood that the complete trend is exponential for the lifetime of the strain development, an exponential regression can be performed on the strain data to replicate the entire range of the data (not only the last linear portion). The results are presented below:

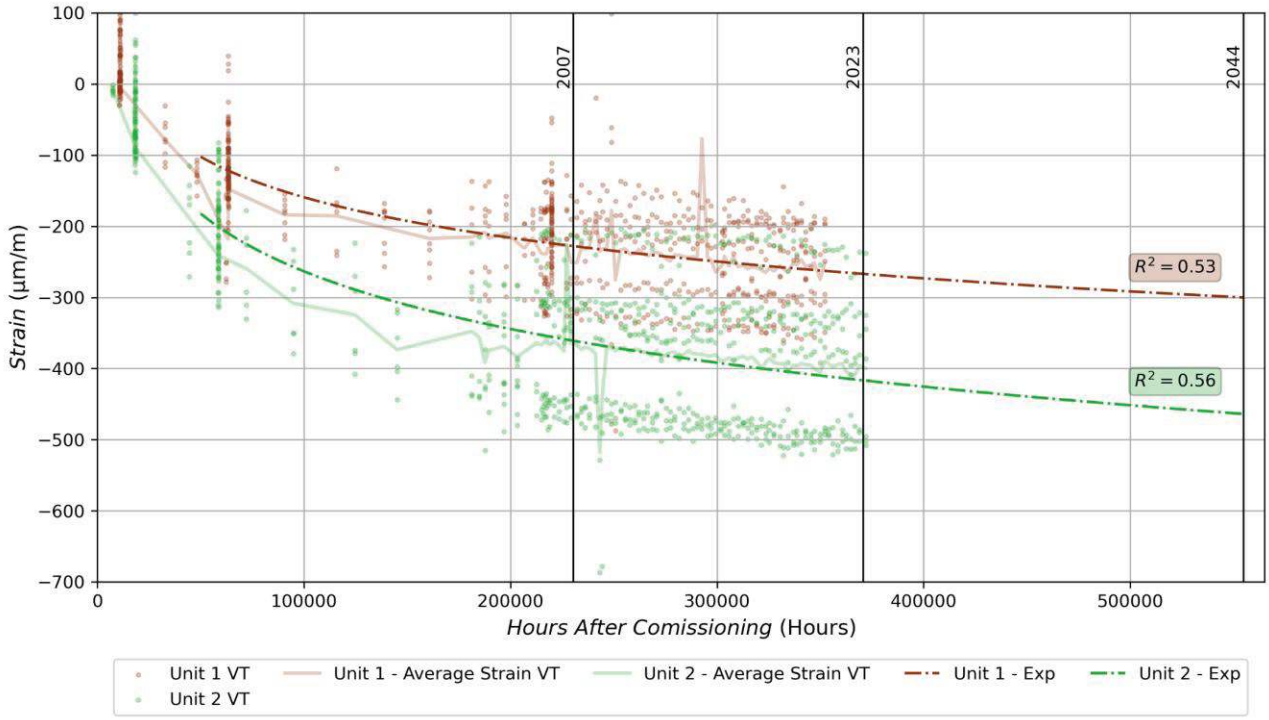

Figure 25: Exponential Extrapolation of the Vertical Strain Development

6.1.3 Addition of 20% Factor

A simplified approach may be to simply consider the average strain at 40 years and add a factor of 20% to the average strain to predict the strain at 60 years. The basis for the 20% is a conservative estimation of the strain that may further develop over the next 20 years. This was also performed considering the latest measurements' average and projecting the 60-year strain by including a 20% factor to test the suitability of the simplified method. The result is presented below, and clearly shows more conservative predicted strain.

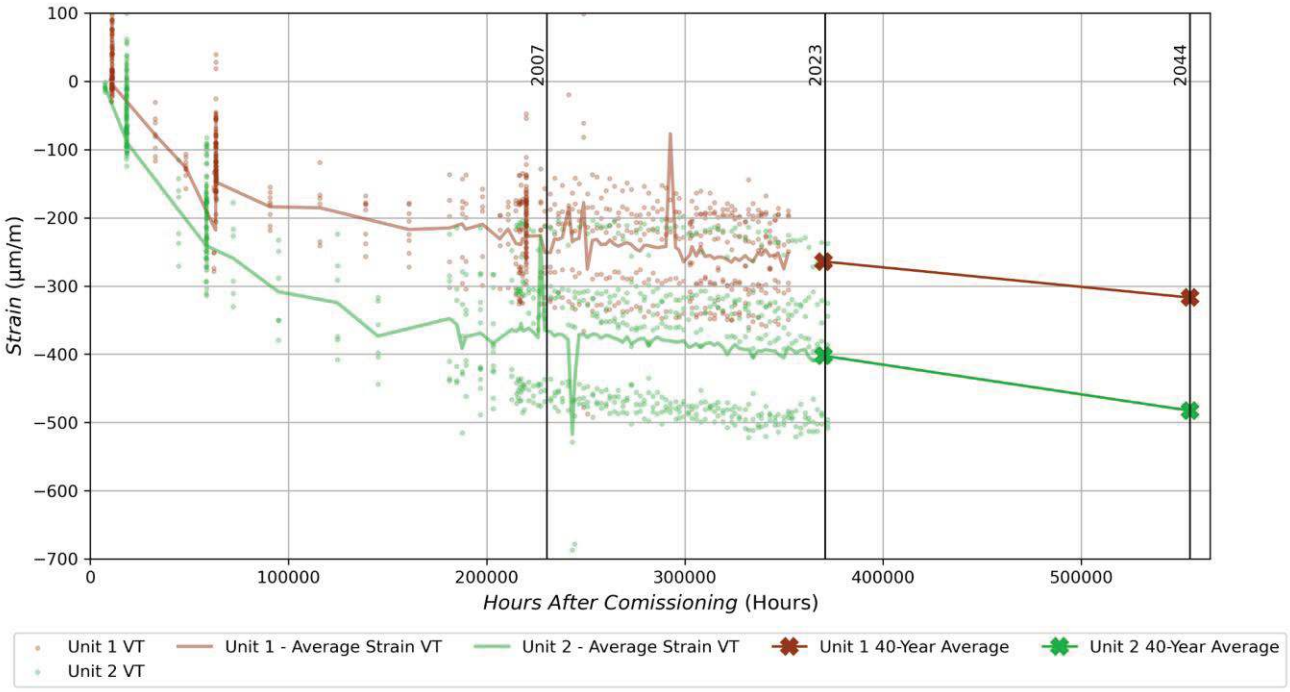

Figure 26: 20% Extrapolation of the Vertical Strain Development

6.1.4 Summary of Vertical Strain Extrapolations

The combined results of all three methods described above is depicted below in Figure 27 and the numerical values for the different analysis is summarized in Table 7.

Table 7: Extrapolation of Vertical Strain Development

Method	Unit 1 (µm/m)		Unit 2 (µm/m)	
	40-year	60-year	40-year	60-year
Linear	-264.31	-310.77	-402.29	-448.72
Exponential	-266.99	-299.77	-416.90	-463.36
20% Factor	-264.14	-316.97	-402.29	-482.75

Note: Data in the green highlighted cells are used as input to the TLAA.

The different extrapolation methods provide good correlation, although the exponential extrapolation is the preferred method for extrapolation as it is the expected behaviour of the time-dependent parameters and considers the data holistically.

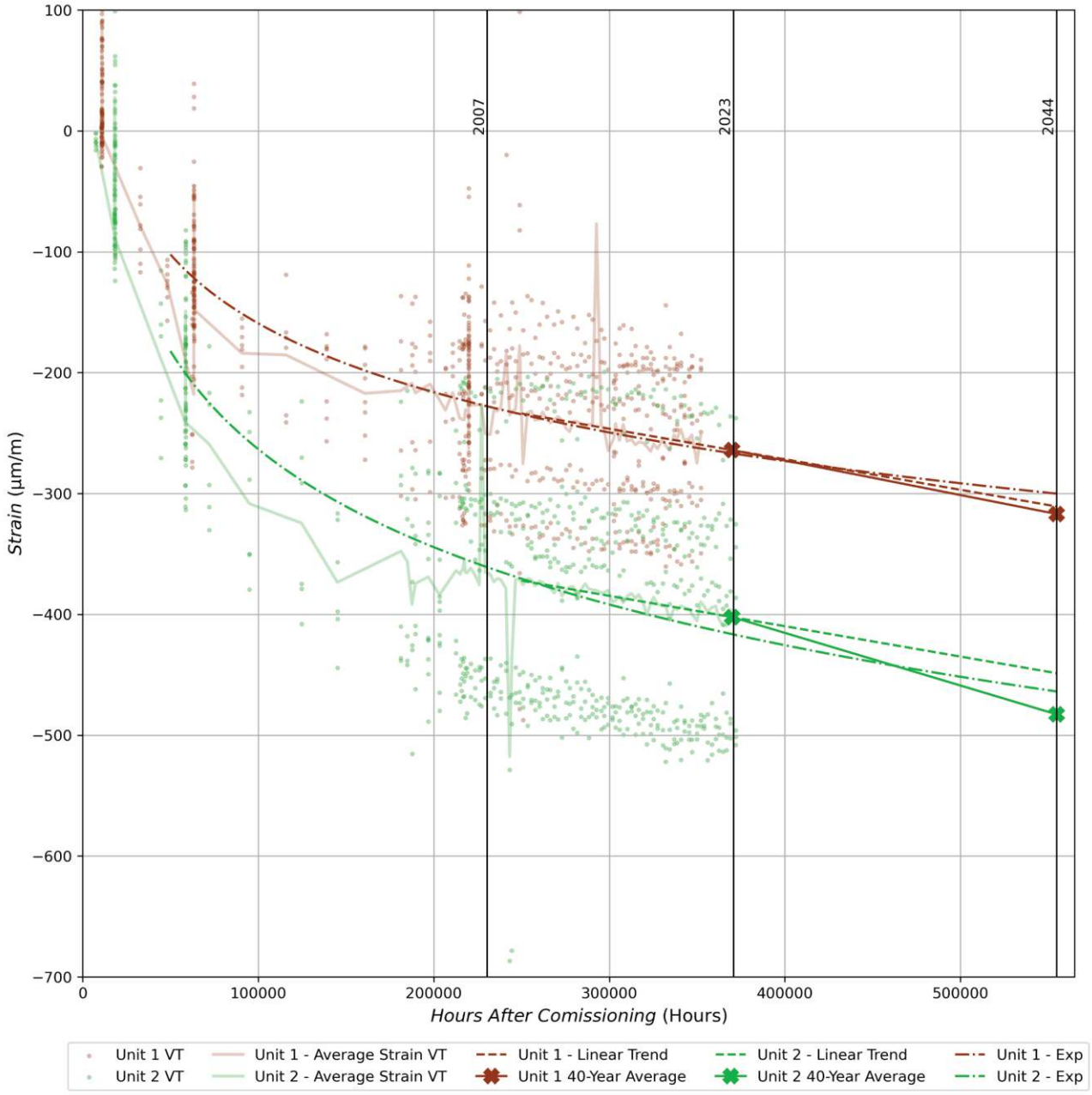

Figure 27: Combined Extrapolation Methods of the Vertical Strain Development

6.2 Containment Structures Cylindrical Walls Horizontal Strain

Similarly to the vertical strain, the horizontal strain development is considered by investigating the different extrapolation methods. For the horizontal strain development, however, no strain gauges are excluded. No structural anomalies can be identified from the trends.

6.2.1 Linear Estimation of Linear Portion of Data

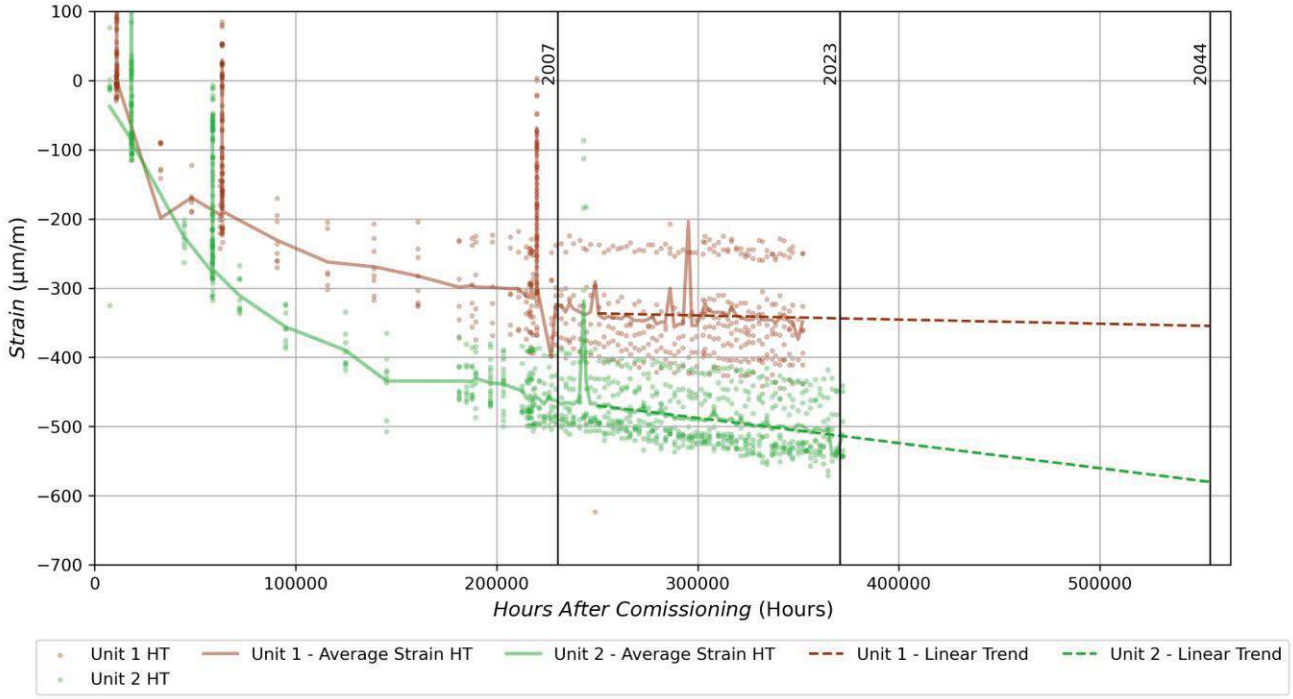

Figure 28: Linear Extrapolation of the Horizontal Strain Development

6.2.2 Exponential Regression of all Data

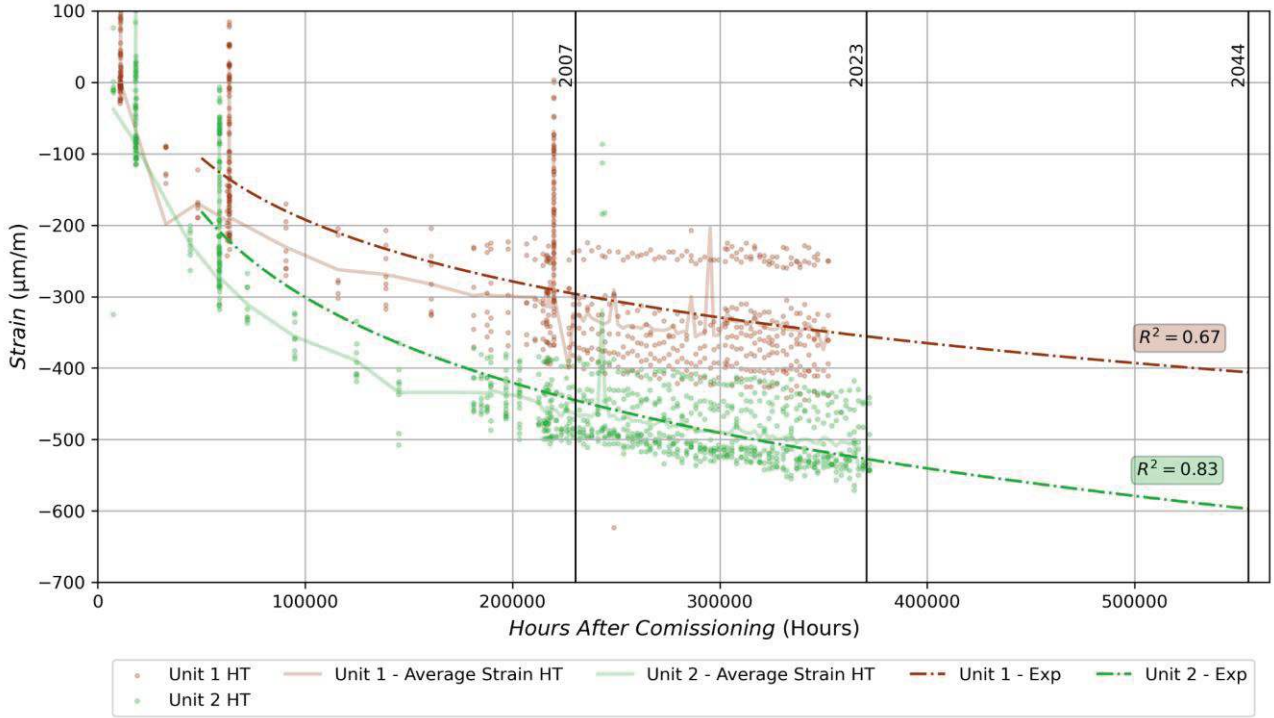

Figure 29: Exponential Extrapolation of the Horizontal Strain Development

6.2.3 Addition of 20% Factor

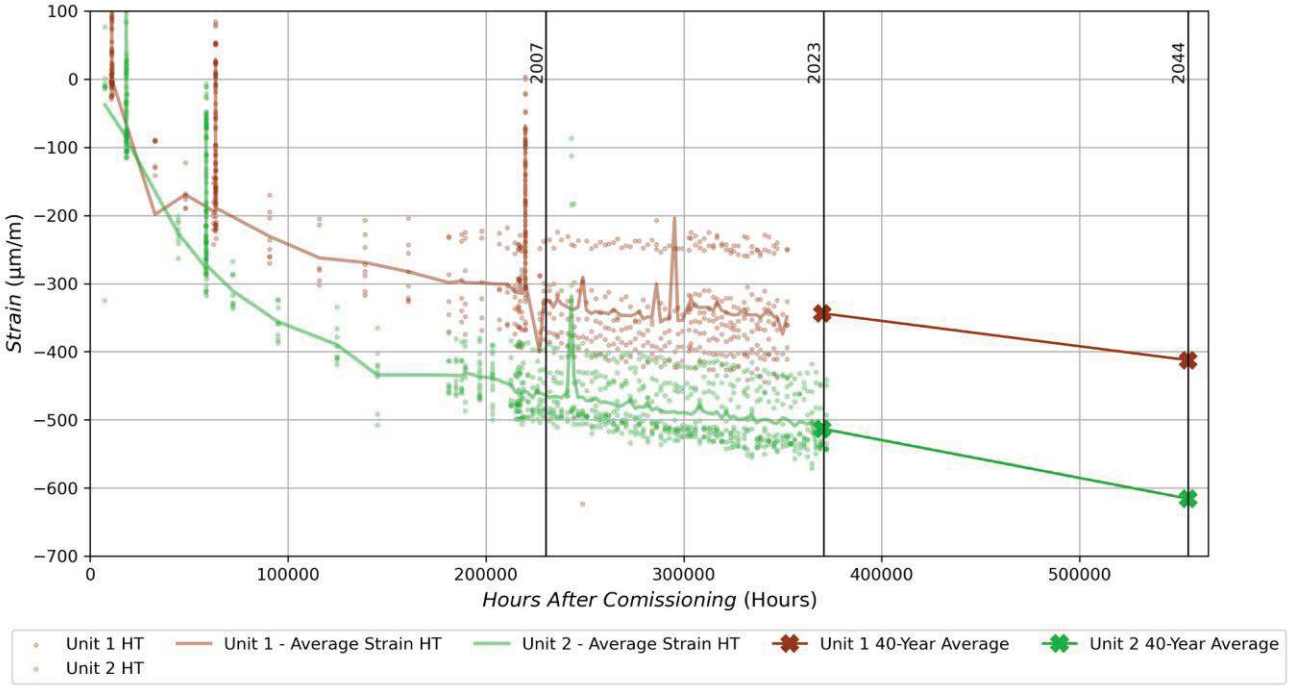

Figure 30: 20% Extrapolation of the Horizontal Strain Development

6.2.4 Summary of Horizontal Strain Extrapolations

The extrapolated horizontal strain is summarized below in Table 8 and Figure 31:

Table 8: Extrapolation of Horizontal Strain Development

Method	Unit 1 (µm/m)		Unit 2 (µm/m)	
	40-year	60-year	40-year	60-year
Linear	-343.67	-354.69	-513.10	-580.09
Exponential	-354.47	-403.73	-526.20	-594.07
20% Factor	-343.67	-412.41	-513.10	-615.72

Note: Data in the green highlighted cells are used as input to the TLAA.

The holistic exponential extrapolation is preferred for the prediction of strain development at 60 years, and it is the expected behaviour of the time-dependent parameters.

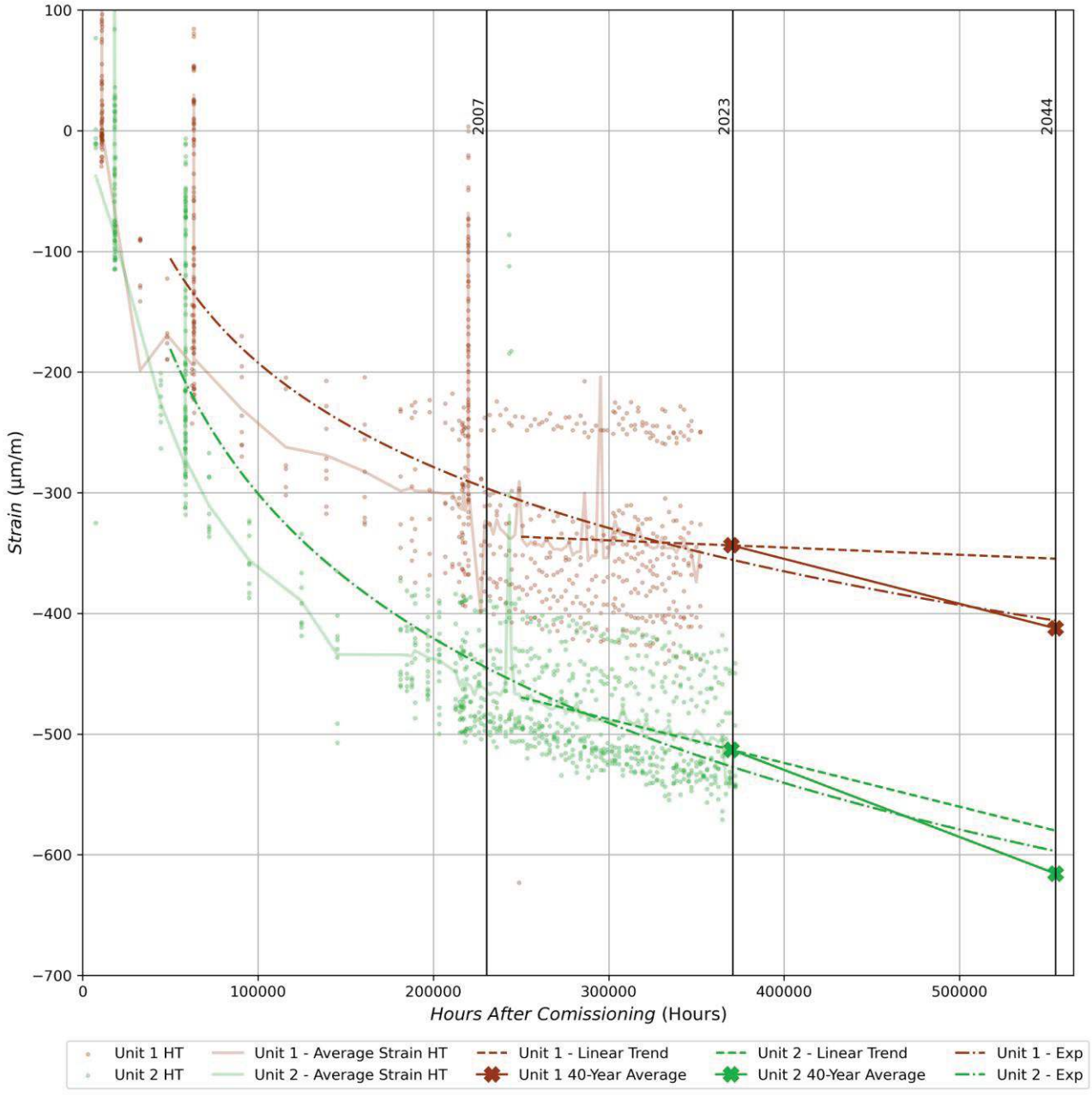

Figure 31: Combined Extrapolation Methods of the Horizontal Strain Development

6.3 Dome Strain

The strain measurements for the domes exhibit some variability compared to the more consistent readings observed in the vertical and horizontal strain measurements on the walls. The data is sparse with numerous gaps and outliers. Therefore, the strain gauge results need to be closely considered and scrutinized.

Unit 2 has no meaningful readings that can be compared with the Unit 1 strain. Note the figure below (Figure 32) for the 8 strain gauges on the domes (4 per Unit). The Unit 2 data is limited and is disregarded for the remainder of the report.

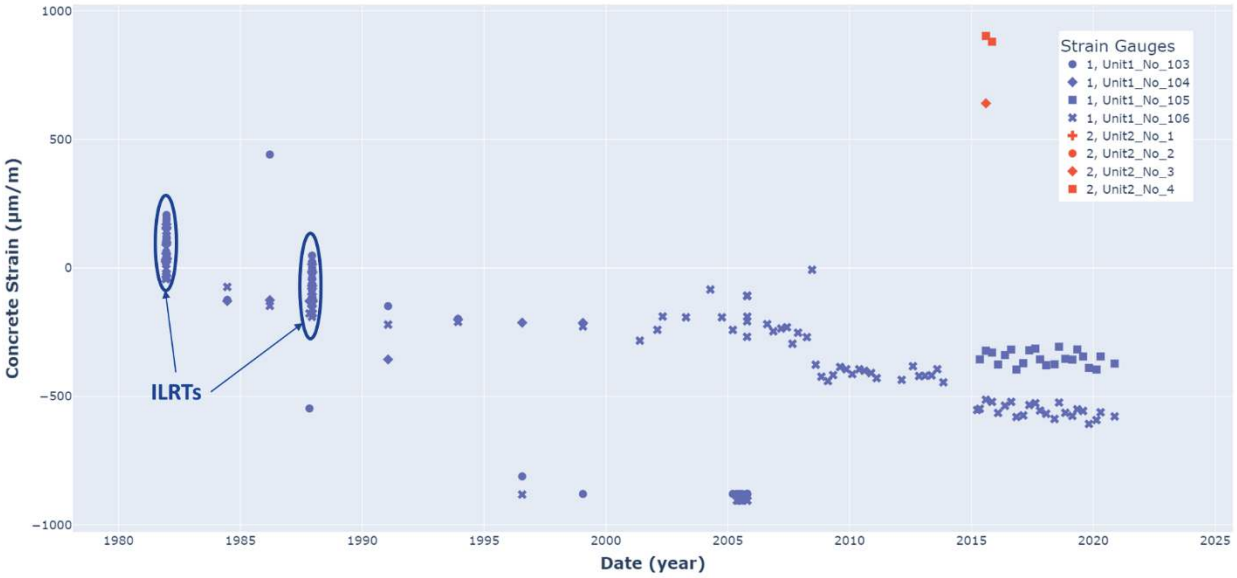

Figure 32: All dome strain gauge data at +56.00m level

Considering the Unit 1 data individually for each strain gauge the following conclusions are drawn (refer to Figure 33 – Figure 36 below):

Strain Gauge 103 and Strain Gauge 104 do not have sufficient data to consider usable and therefore will be excluded from the analysis.

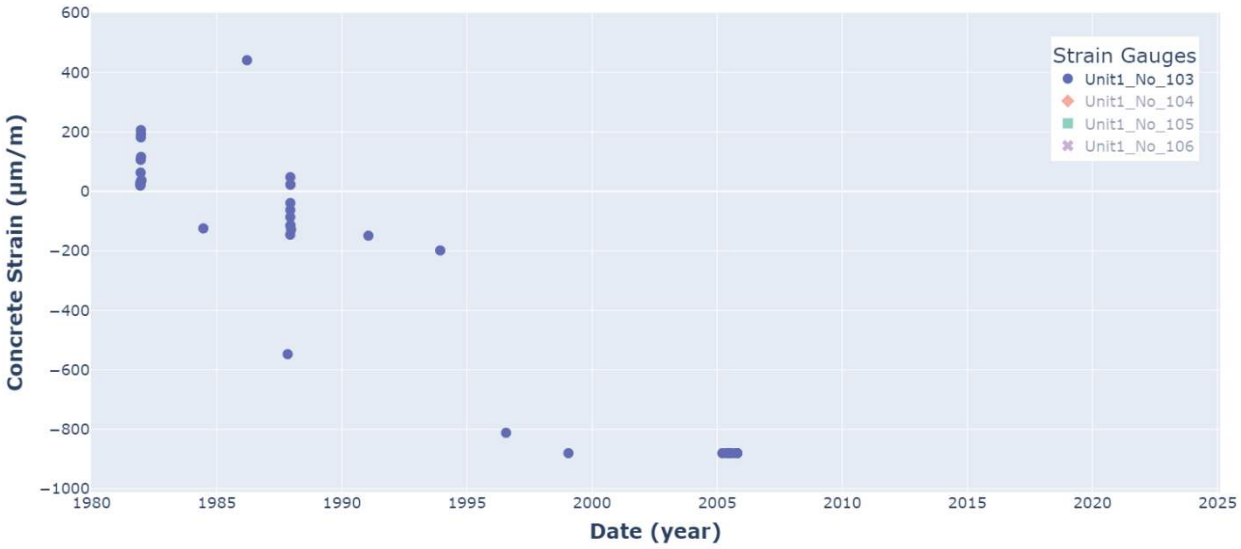

Figure 33: Strain Data for Unit 1 Gauge 103

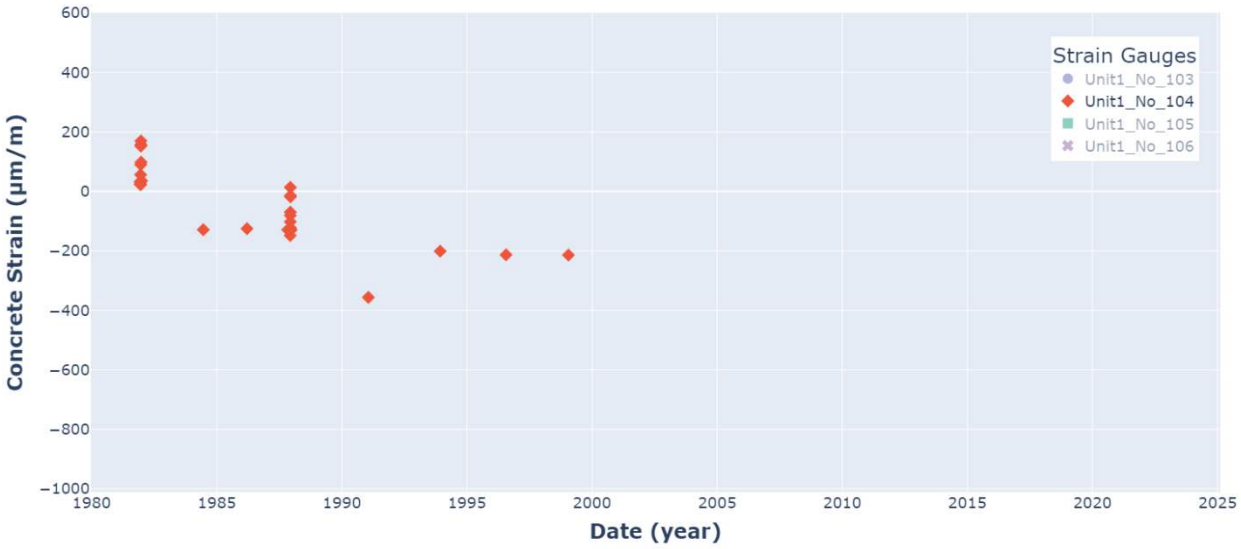

Figure 34: Strain Data for Unit 1 Gauge 104

Strain Gauge 105 has no data prior to 2015 available. The available data (from 2015 onward) does however seem plausible and may be used for a linear extrapolation to 60 years. Alternatively, a zero value may be taken at the origin and an exponential regression may be performed.

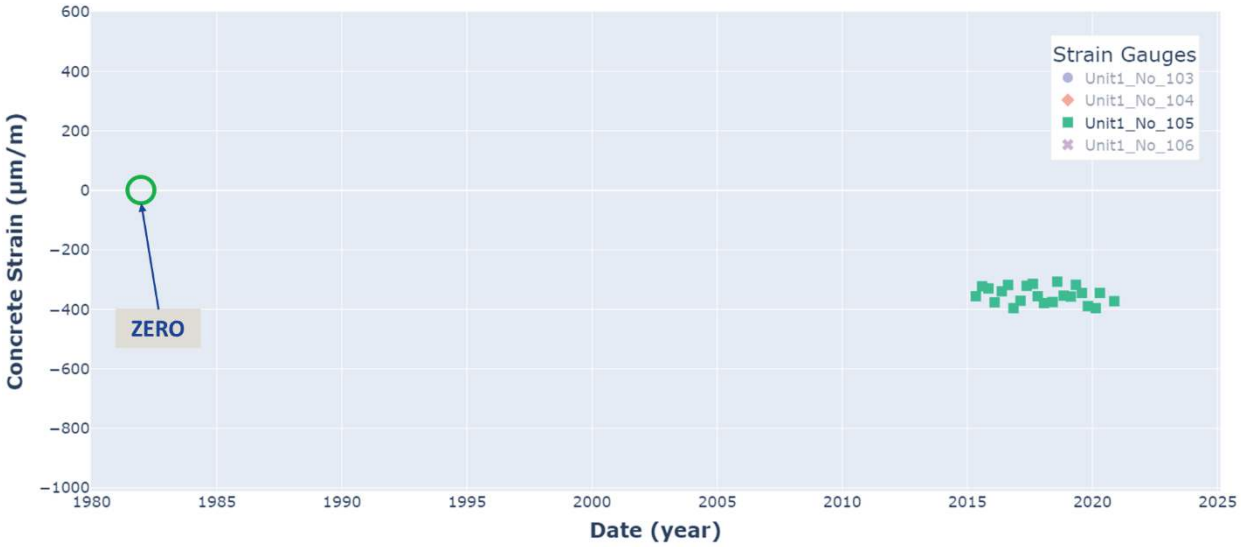

Figure 35: Strain Data for Unit 1 Gauge 105

Strain Gauge 106 has the most amount of data. The data includes some ILRT data and outliers as indicated in Figure 36. Additionally, it is noted that two 'jumps' are seen in the data. The Unit 1 dome was inspected, and no significant delamination or local degradation was identified at the apex (+56m level) therefore the jumps cannot be due to degradation.

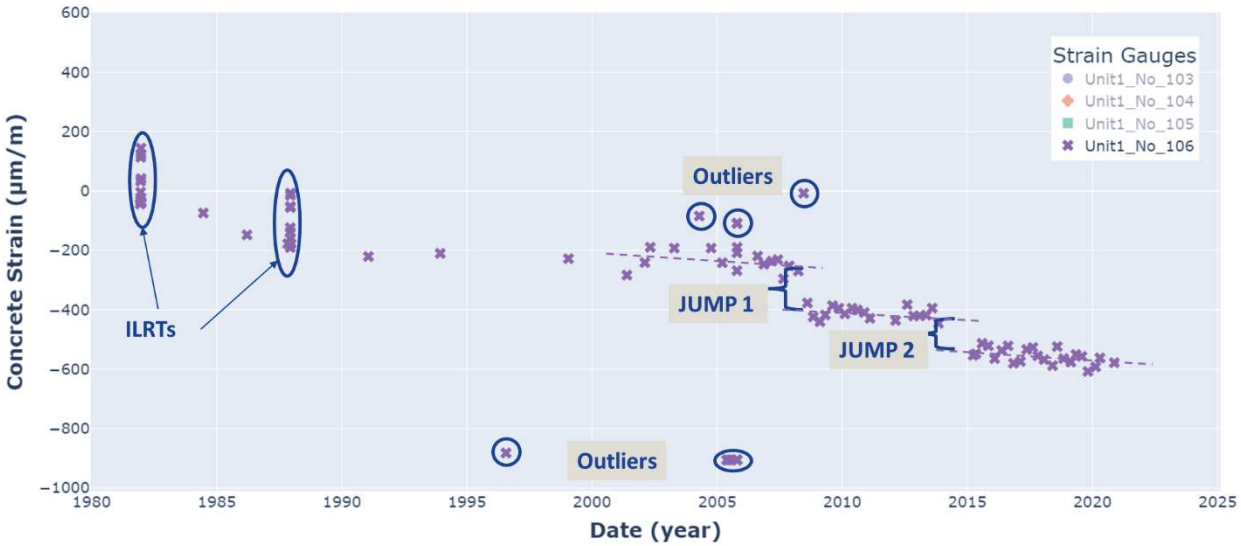

Figure 36: Strain Data for Unit 1 Gauge 106

To investigate the possible cause of the jumps, the following was considered:

1. Change in strain due to axial stress changes, and
2. Change in strain due to bending moments.

For the jumps to represent changes in axial stresses due to, for example, a release in tendon force from a cable snapping, the dome section would see a change in direct axial stress. This stress would reduce the strain and cause a jump in the opposite direction to what is seen (in a similar manner to how the ILRT decreases the strain). Therefore, the jump cannot be due to a reduction in direct axial stress.

To investigate the change in strain due to bending moments, a simple 2D analysis was performed to determine the possible changes in strain due to a change in the induced distributed load applied by the tendon across the dome. The bending moment diagram for the analysis is shown in Figure 38.

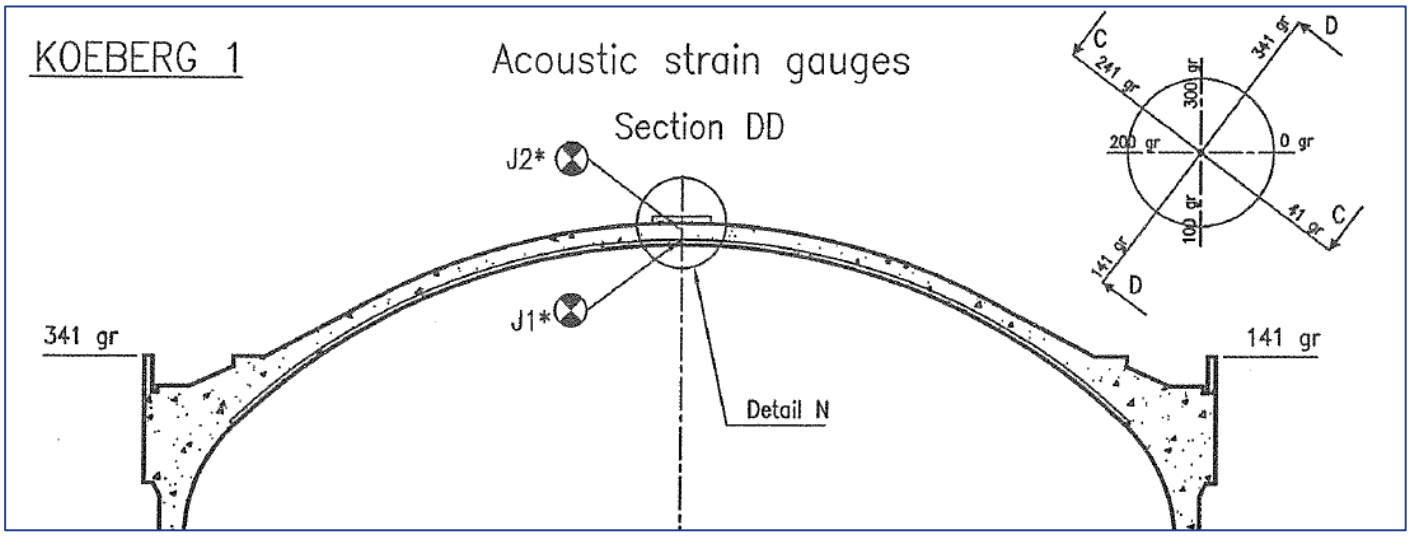

Figure 37: Location of Dome Strain Gauges

CONTROLLED DISCLOSURE

The dome has two locations where the strain gauges were placed referred to as **J1*** and **J2***. The **J1*** (Strain Gauges 103 & 104) are located at the lower section of the dome while **J2*** (Strain Gauges 105 & 106) are located in the upper portion. This is illustrated in Figure 37.

A unit distributed load would induce a moment factor of **-0.286** and a reduced distributed force will experience a proportional reduction in moment factor, i.e., a 20% reduction in load yields a 20% reduction in moment factor.

The bending moment diagram indicates sagging in the dome which implies compression on the upper face of the dome.

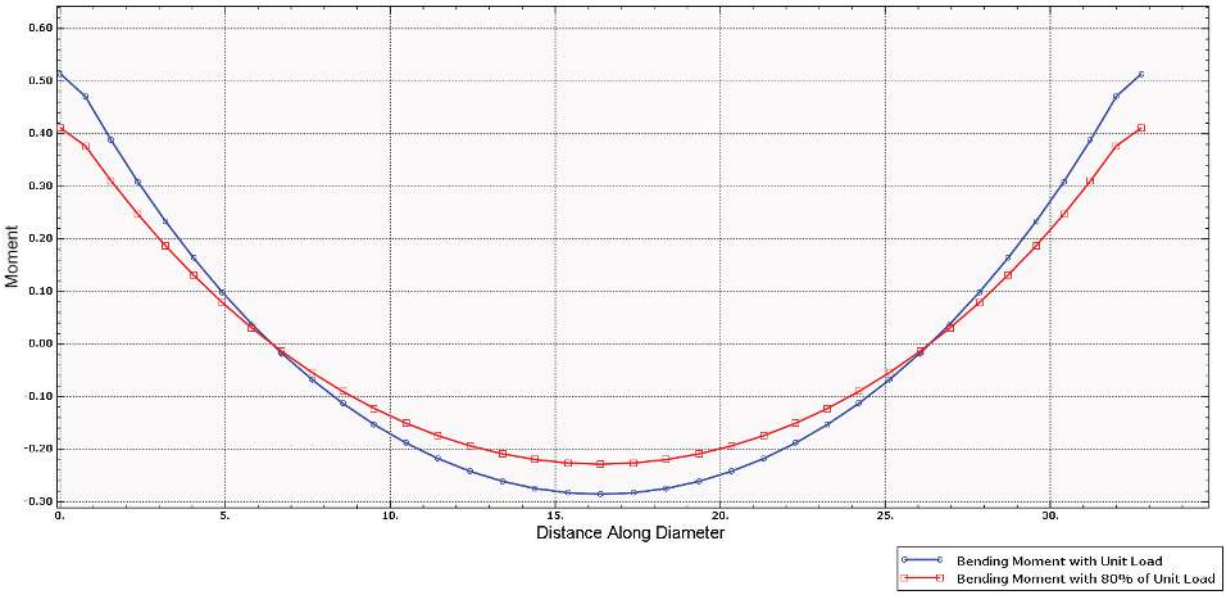

Figure 38: Bending Moment in the dome due to a unit load

Accordingly, a reduced induced distributed force (for example, due to a ruptured tendon) on the dome would relieve compression stress at the upper section of the dome and indicate a reduction in strain, i.e., an upward movement of the strain data (and not a downward "jump" as seen in Figure 36).

The origin of these jumps in the data is therefore postulated to be due to faulty strain gauges. Accordingly, the strain gauge measurements for Strain Gauge 106 is ignored from circa 2008, or from the first jump onward. The remaining data used to represent the domes are presented in Figure 39. No structural anomalies can be identified from the trends.

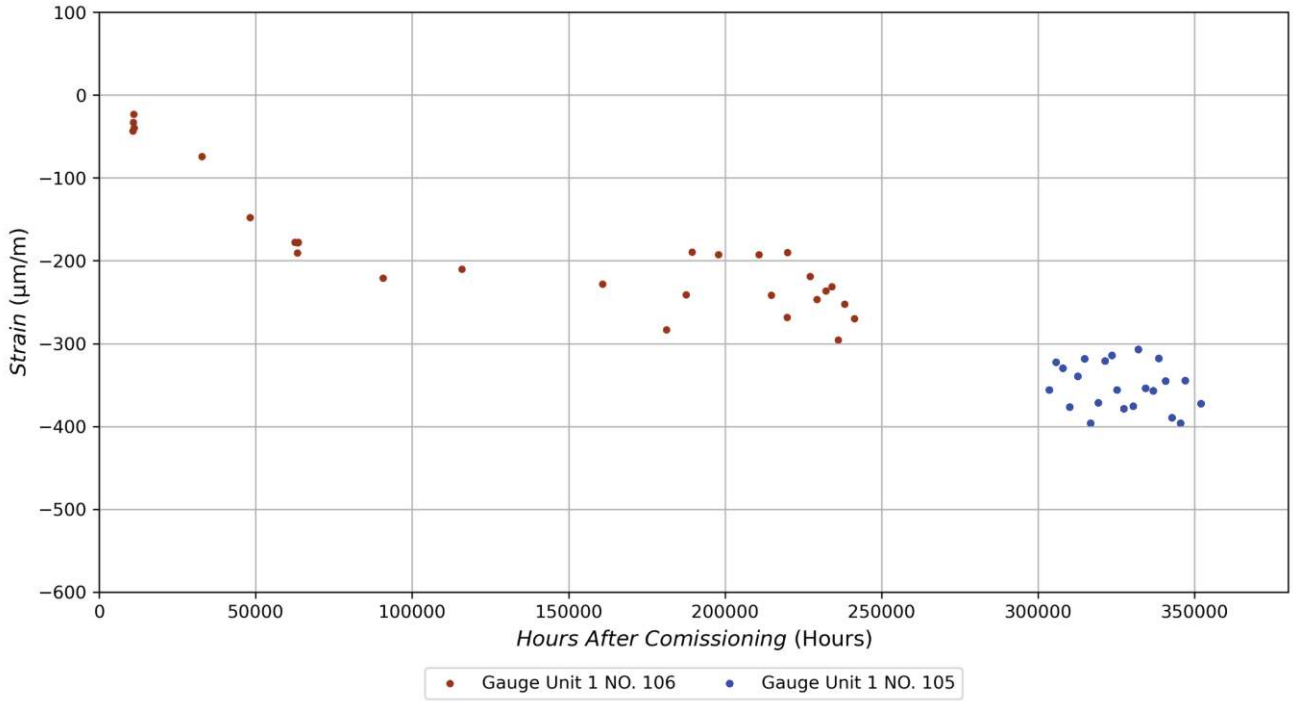

Figure 39: Cleaned Data for the Dome

An alternative option is also considered where the measurements were adjusted by the average of the first five readings after the jump occurred. The data for the Unit 1 dome, adjusted for the 'jumps', are illustrated in Figure 40.

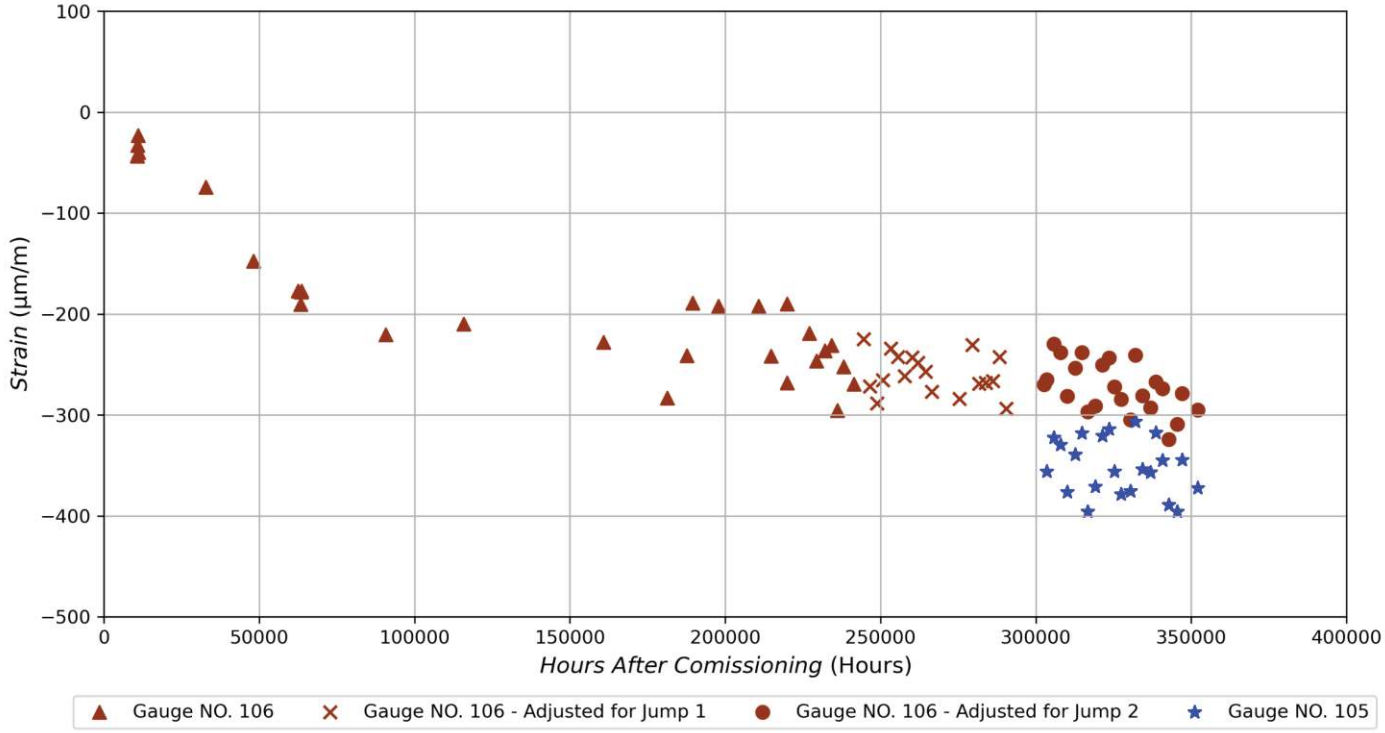

Figure 40: Cleaned and Adjusted Data for the Dome

6.3.1 Linear Estimation if Linear Portion of Data

From the remaining data, the linear extrapolation could be performed. Note that, conservatively, only the strain data of Gauge No. 105 is extrapolated to 60 years.

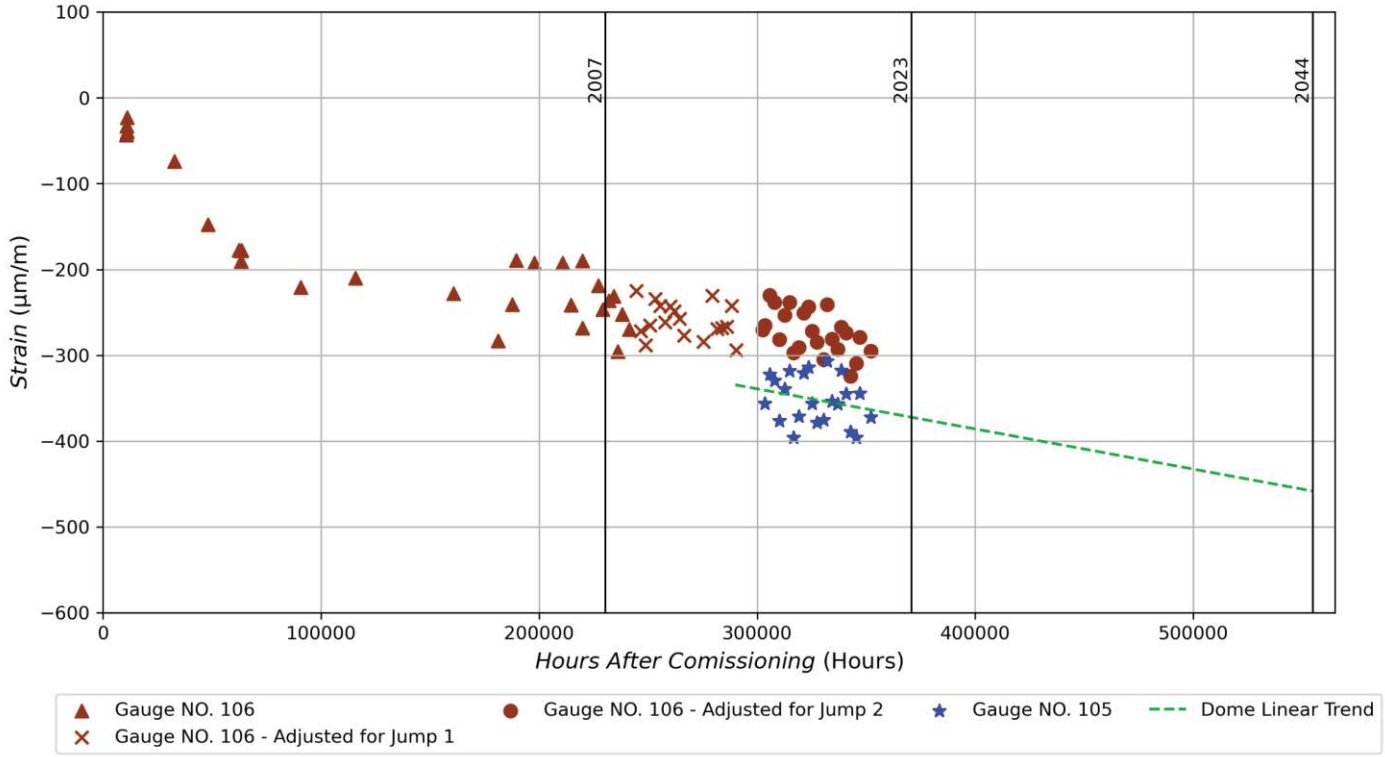

Figure 41: Linear Extrapolation of the Dome Strain Development

6.3.2 Addition of 20% Factor

Similarly, to the linear extrapolation, the 40-year average of Gauge No. 105 was used to determine the estimated strain at 60 years by adding an estimation factor of an additional 20%.

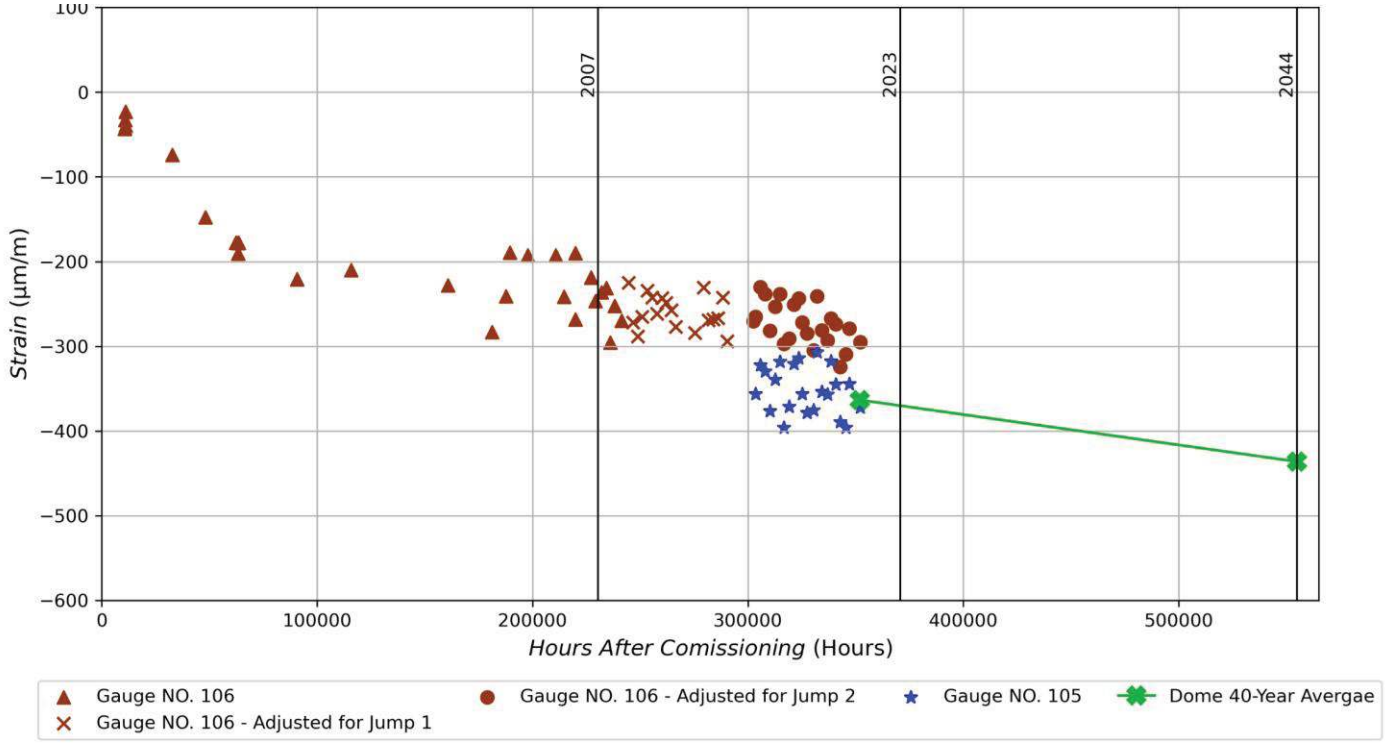

Figure 42: 20% Extrapolation of the Dome Strain Development

6.3.3 Exponential Regression of Cleaned Dome Data

All the available data could however be used to develop an exponential regression of the data:

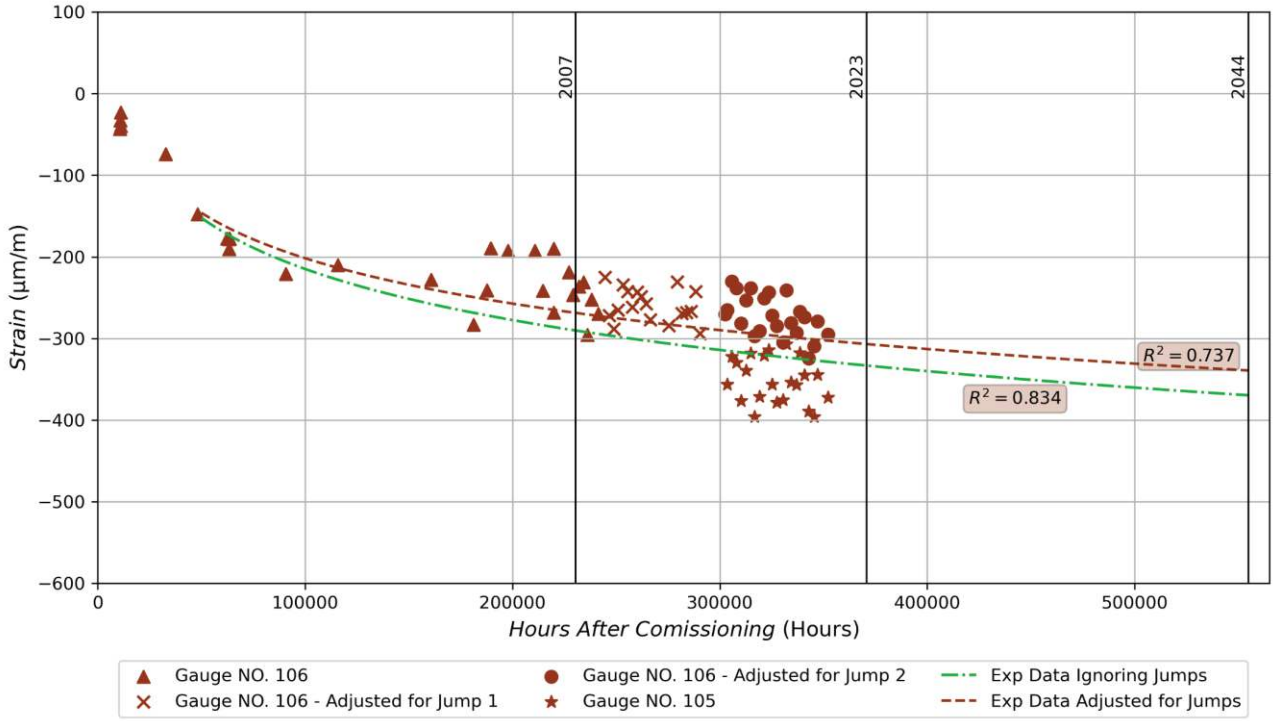

Figure 43: Exponential Extrapolation of the Horizontal Strain Development

6.3.4 Summary of Dome Strain Extrapolations

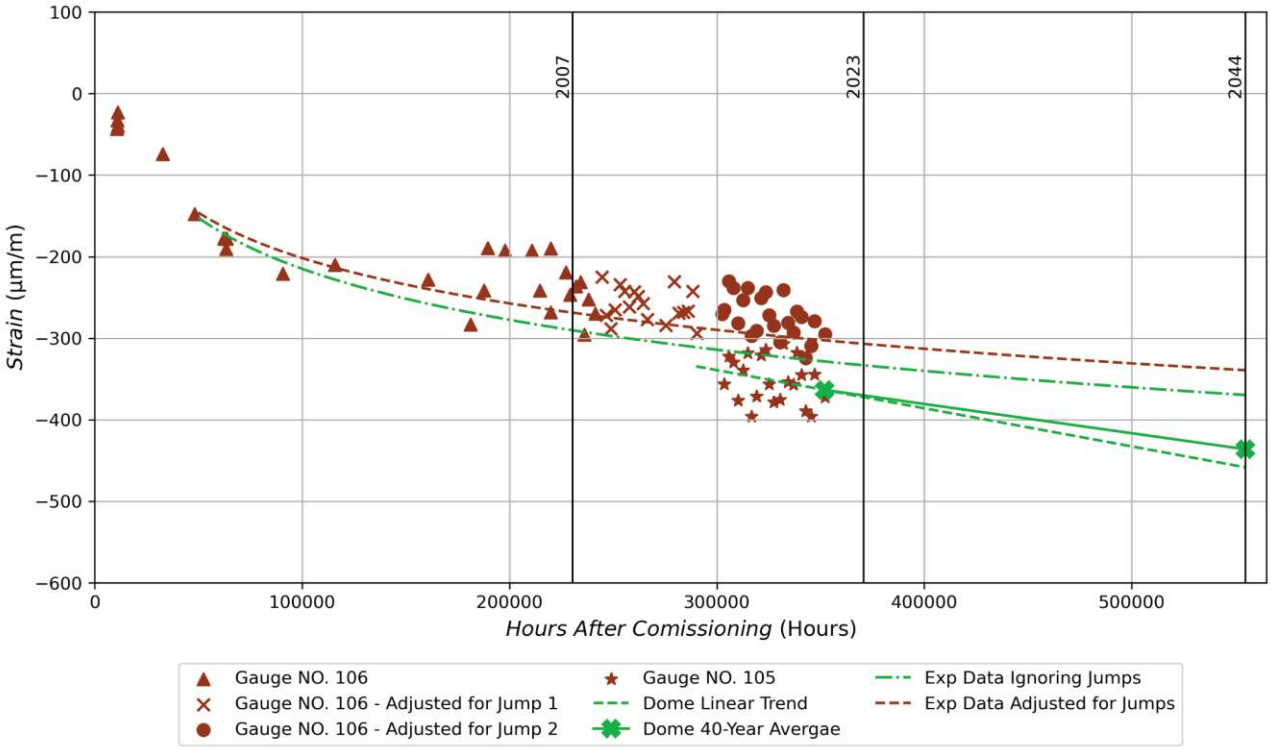

Figure 44: Combined Extrapolation Methods of the Horizontal Strain Development

The differences in the different extrapolation methods are shown in Table 9. The Unit 1 strain values for the dome were considered non-conservative and were therefore not used as input to the TLAA analysis (see § 6.4.2).

Table 9: Extrapolation of Dome Strain Development

Method	Unit 1 (µm/m)	
	40-year	60-year
Linear	-363.45	-458.25
20% Factor	-363.45	-436.14
Exponential Ignoring 'Jumps'	-328.79	-369.26
Exponential Adjusted for 'Jumps'	-302.70	-339.21

6.4 Summary of All Strain Data

6.4.1 Summary of Extrapolation Results

A summary of the strain data considering the use of the exponential prediction models are provided in Table 10, and for comparison, the predicted strain calculated from the assumed losses as documented in § 4.2.1 of reference [27] is also provided.

Furthermore, for all three sections of the Containment (vertical and horizontal wall section and the dome), the exponential extrapolation was considered the most applicable as it considers the available data holistically and not only last part of the data. For the dome, the data adjusted for the jumps is taken as the best estimate for the strain development of the dome. Note that in the succeeding § 7 (TLAA section) the worst case is also considered for reference. Adjustments are also made to consider Unit 2.

Table 10: Summary of All Strain Data

Parameter		Unit 1	Unit 2	% Difference between Units
40-year Design Prediction Strain [µm/m]	Vertical	-78.00		-
	Horizontal	-118.67		-
	Dome	-157.00		-
Strain at 40 years [µm/m]	Vertical	-266.99	-416.90	**43.8 %**
	Horizontal	-354.47	-526.20	**39.0 %**
	Dome	-302.70	-454.06***	**40%**
Strain at 60 years [µm/m]	Vertical	-299.77	-463.36	**42.9 %**
	Horizontal	-403.73	-594.07	**38.2 %**
	Dome	-339.21	-508.71***	**40%**

Note: Data in the green highlighted cells, i.e., Unit 2 strain data, are used as input to the TLAA.

The 40-year predicted strain values provided in Table 10 is calculated from reference [27]. It is noted that the vertical strain measured at 40 years of **-266.99 µm/m (Unit 1) and -416.9 µm/m (Unit 2)** is higher (i.e., more negative) than the strain predictions.

*** Values calculated for a 40% difference to Unit 1

6.4.2 Adjustment for Unit 2 Dome

As discussed in § 3.3.5.4 – Age at Loading (Table 2) the measurement of the strain development in Unit 2 commenced shortly after the tendons were tensioned while there was a delay in the initial measurements on Unit 1. This delay in the measurements for Unit 1 is most likely the reason for the difference in the strain development for Unit 1 and Unit 2 seen throughout the report and, the strain development for Unit 1 would be closer to that of Unit 2 if the readings were done closer to the tensioning date.

Accordingly, the Unit 1 data cannot be deemed representative of both domes without adjustment. Considering the differences in respective strain values for Unit 1 and Unit 2 in Table 10, the Unit 2 dome strain was determined by assuming a 40% difference in the dome data of Unit 1 and Unit 2.

7. Time-Limited Ageing Analysis

7.1 Six Criteria for Time-Limited Ageing Analysis

It is required to fulfil the six criteria for TLAA according to the safety standards in IAEA Specific Safety Guide No.SSG-48 [1], chapter 5.64, (1) to (6). The six criteria are discussed individually below:

1. Time limited ageing analyses should involve SSCs within the scope of ageing management. Scope setting is described in paragraphs 5.14–5.21 and illustrated in Fig. 3.

TLAA 301 considers the concrete containment structure. The current TLAA 301 involves the prestress of the unit 1 and unit 2 containment structures that are within the scope of aging management for LTO at Koeberg.

2. Time limited ageing analyses should consider ageing effects. Ageing effects include, but are not limited to: loss of material, changes in dimension, changes in material properties, loss of toughness, loss of pre-stress, settlement, cracking, and loss of dielectric properties.

The ageing effects considered in the TLAA for the structural ageing are the time-dependent parameters i.e., (1) concrete creep and shrinkage (C+S) and (2) the prestressing steel relaxation.

The delamination of the containment wall surfaces is discussed in depth in § 11.1 of this report. It is discussed that delamination does not have a detrimental impact on the integrity of the containment structures and Eskom is actively pursuing mitigation measures to enhance their long-term durability.

3. Time limited ageing analyses should involve time limited assumptions defined by the current operating term. The specified operating term should be explicit in the analysis. Simple assertion that a component is designed for a particular service life or for the lifetime of the plant is not sufficient. Any such assertion should be supported by calculations or other analyses that explicitly include a time limit or a time based assumption.

The time limited assumption defined by the current operational term is the structural integrity of the containment structure at the end of the initial planned lifetime of 40 years considering LOCA conditions. The planned lifetime including LTO is a total of 60 years after commissioning. The LTO term is specified in the TLAA analysis and the calculations for the containment structural integrity duly considers the full 60-year period.

4. Time limited ageing analysis should have been determined to be relevant by the operating organization in making a safety determination as required by national regulations. Relevancy is a determination that the operating organization makes on the basis of a review of the information available. A calculation or analysis is relevant if it can be shown to have a direct bearing on the action taken as a result of the analysis performed. Analyses are also relevant if they provide the basis for the safety determination for the plant when, in the absence of the analyses, the operating organization might have reached a different safety conclusion or taken a different safety action.

The relevancy of the TLAA 301 is confirmed by using the available and historic monitoring data of the containment structures and by extrapolating the monitoring data to predict the future development of the strain. The monitoring data enable a safety determination regarding the structural integrity at the end of LTO in LOCA condition. The safety determination is based on evaluation of monitoring data, the containment ageing analysis based on these data including prediction to LTO and the fulfilment of the design criteria defined in the original design in accordance with the national regulations. The outcome of the ageing analysis, results in a safety conclusion regarding the containment structural behaviour.

5. Time limited ageing analyses should involve conclusions or provide the basis for conclusions relating to the capability of SSCs to perform their intended functions.

The TLAA 301 constitutes the verification that the loss of containment concrete prestress remains within the design limits, including under LOCA conditions for the full 60-year period. On this basis, it can be concluded that containment structural integrity will be ensured.

6. Time limited ageing analyses should be contained or incorporated by reference in the current licensing basis. The current licensing basis includes the technical specifications and the design basis information, or the commitments of the operating organization documented in the plant specific documents contained or incorporated by reference in the current licensing basis, including, but not limited to: safety analysis reports, regulatory safety evaluation reports, the fire protection plan or hazard analysis, correspondence with the regulatory body, the documentation of the management system, and topical reports included as references in the safety analysis reports. If a code of record is in the safety analysis report for a particular group of structures or components, the reference material should include all the calculations called for by that code of record for those structures or components.

The current TLAA demonstrates that the compressive requirement, i.e., that the containment concrete should remain in compression under containment design basis conditions after considering the time related loss of tendon prestress remains valid for the period of LTO (i.e. after 60 years). The analysis includes shrinkage and creep of the concrete, steel relaxation of the tendons, and loss of posttensioning forces. The TLAA 301 “Concrete Containment Tendon Pre-Stress” is referenced in the Initial List of Time Limited Ageing Analysis [27], chapter 4.1.3. The bulk work of ageing management evaluation is described in the Technical Requirement Specification (TRS) [1] and more comprehensive in the SALTO Ageing Management Assessment Report (Interim) [5]. The TLAA 301 is based on the Safety Analysis Report (SAR), part II, chapter 4.2.2 Containment Tests and Inspections [4]. Based on this, it is required to manage the loss in pre-stressing force in the tendons during the LTO. The Pre-stress magnitude must be higher than the regulatory limit or criterion during the LTO.

7.2 TLAA Methodology

A Time Limited Ageing Analysis (TLAA) can be performed by considering the estimated concrete strain in the different sections of the containment structures as determined in the preceding sections of this report.

The time limited assumption defined by the current operating term is the structural integrity of the containment structure under LOCA conditions at the end of the initial planned 40-year lifetime. In the current case, it is required that the mean concrete stresses in the wall must remain in compression under LOCA conditions when considering the time dependent loss of tendon pre-stress over the full period of LTO. The planned additional lifetime in LTO is 20 years, i.e. a total of 60 years after the end of construction. TLAA-301 was performed previously, and this report re-performs that TLAA and expands on the work done previously in reference [16].

The TLAA is performed on the principle of bi-axial equilibrium by considering the structural mechanics to balance the forces in the structure. Accordingly, the calculations applied in the TLAA considers the strain, tendon forces, stress in the concrete, liner and reinforcement and the material properties of all the components.

Bi-axial equilibrium calculations are performed through an iterative method by ensuring the bi-axial forces balance to pre-determined target values. This methodology is shown visually in Figure 45 and is based on reference [16].

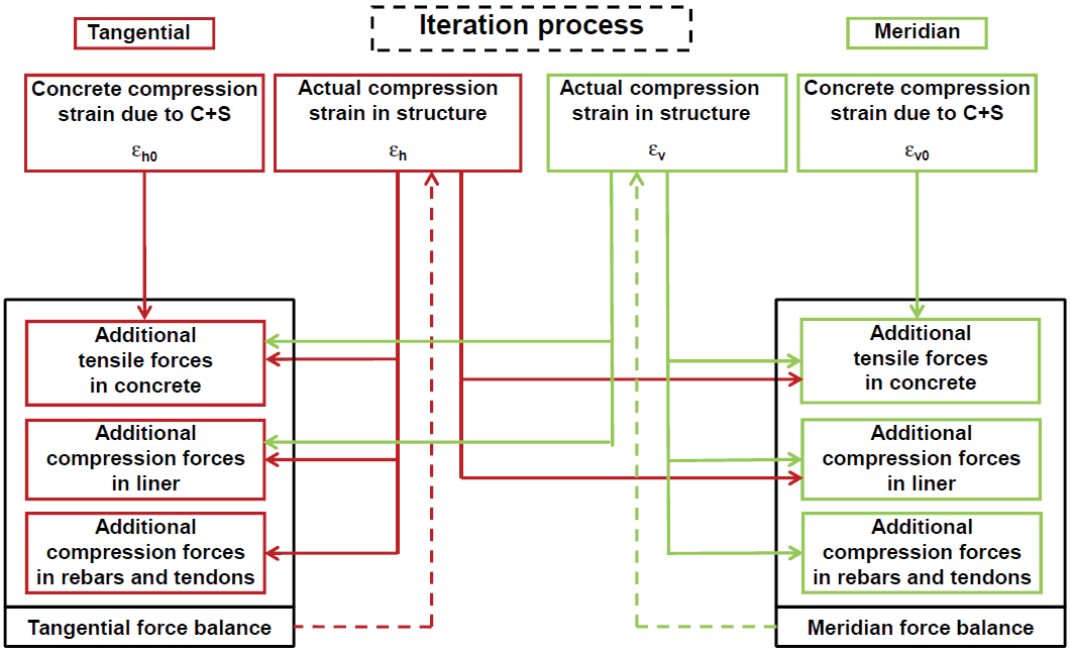

Figure 45: Iteration Process to Balance Bi-Axial Forces

The analysis and calculations from reference [16] was reproduced in Microsoft Excel to be able to perform the TLAA and a sensitivity study of the results. The calculations were repeated for three different scenarios, namely:

(1) Using the predicted concrete strain at 40 years;

(2) Using the measured concrete strain at 40 years; and

(3) Using the measured concrete strain extrapolated to 60 years.

Note - 1: For the measured concrete strain extrapolated to 60 years the exponential predicted concrete strain was used in the analysis for each case.

Note - 2: The Unit 2 strain values were applied in the analysis as this is the best-estimate strain as summarized in Table 10.

Note - 3: The analyses in § 7.5 Cylindrical Wall Analysis and § 7.6 Dome Analysis considers the best-estimate strain, however the analysis is expanded in § 7.7 Results discussion to also consider the Unit 1 and the average strain between the Units.

7.3 Material properties

For the TLAA analysis, the material properties are used for the bi-axial equilibrium analysis. The material properties used for the analysis are [27]:

Table 11: Material Properties Used in the TLAA

Material	Young's Modulus [GPa]	Poisson's ratio	$A_{Hotrizontal}$ [mm²/m]	$A_{Vertical}$ [mm²/m]	Dome [mm²/m]
Concrete	15	0.2	900,000	900,000	800,000
Liner	210	0.28	7,000	6,800	9,000
Reinforcement	200	N/A	1,610	2,790	7,060
Tendons	190	N/A	9,900	4,910	6,830

NOTE: The concrete Young's modulus (E_{Mod}) is considered a time dependant parameter and reduces with time. The original design documents used 15 GPa as the long-term E_{Mod}. 15 GPa is conservative and estimating the long-term E_{mod} using modern codes such as the French RCC-CW code, the E_{mod} for the concrete may be in the region of 19 GPa. Regardless, the original design values of 15 GPa is used in the analysis.

A refinement of the concrete Material properties and its impact on the outcome of the TLAA is explored in §9. A higher Young's Modulus and Poisson's ratio was confirmed.

7.4 Assumptions

The following is assumed for the TLAA:

1. The post tensioning tendons are not affected by corrosion over the evaluated 20 years.
2. The full concrete section is assumed, and no delamination is considered during the analysis.
3. Assumptions with respect to the strain development predictions are discussed accordingly in the below sections.

Importantly, Point 1 above is checked for validity throughout the life of the structure through the approved ISI programme including the online monitoring and the 10-yearly performance of the ILRT test (see § 12.3).

Point 2 is validated as the assumption is conservative. A reduced concrete section, counterintuitively, distributes the compressive stress over a smaller section of the concrete, therefore increasing the axial compressive stress in the section.

Other mitigation efforts are not required to validate the TLAA, and if the assumptions are invalidated through the approved ISI programme, the re-analysis will require to be re-visited.

7.5 Cylindrical Wall Analysis

7.5.1 Cylindrical Wall – Predicted Strain at 40 years

Redacted - PAIA Section 36 (1)(b); PAIA Section 37 (1)(a)

Materials	[MN/m²]	[MN/m²]	[MN/m²]	[MN/m²]	[MN/m²]	[MN/m²]
Concrete	-12.14	-7.03	-11.33	-6.39	**-3.85**	**-2.56**
Liner	-182.63	-115.60	-202.31	-130.80	-160.32	-106.78
Rebars	-143.11	-61.39	-157.80	-70.62	-124.21	-58.94
Tendons	1256.00	1431.00	1199.04	1340.23	1230.95	1351.33

The tendon stress due to initial prestressing are calculated from initial tendon stresses after friction and slip losses and after elastic deformation of the concrete as provided in reference [27], § 4.1.2. In order to get the strains, the stresses can be divided by the Young's Modulus of the prestressing steel.

- Vertical tendon strain: 1431 MPa/190,000 MPa = 0,00753
- Horizontal tendon strain: 1256 MPa/190,000 MPa = 0,00661

7.5.2 Cylindrical Wall – Measured Strain at 40 years

Redacted - PAIA Section 36 (1)(b); PAIA Section 37 (1)(a)

Total Stresses	Begin of Lifetime		End of Lifetime		LOCA end of Life	
	σ_h	σ_v	σ_h	σ_v	σ_h	σ_v
Materials	[MN/m²]	[MN/m²]	[MN/m²]	[MN/m²]	[MN/m²]	[MN/m²]
Concrete	-12.14	-7.03	-9.83	-5.28	**-2.35**	**-1.44**
Liner	-182.64	-115.60	-293.93	-216.19	-251.93	-192.17
Rebars	-143.12	-61.39	-222.28	-127.52	-188.69	-115.84
Tendons	**1256.00**	**1431.00**	**1137.79**	**1286.18**	**1169.71**	**1297.27**

7.5.3 Cylindrical Wall – Extrapolated Strain at 60 Years

Redacted - PAIA Section 36 (1)(b); PAIA Section 37 (1)(a)

Total Stresses	Begin of Lifetime		End of Lifetime		LOCA end of Life	
	σ_h	σ_v	σ_h	σ_v	σ_h	σ_v
Materials	[MN/m²]	[MN/m²]	[MN/m²]	[MN/m²]	[MN/m²]	[MN/m²]
Concrete	-12.14	-7.03	-9.59	-5.12	**-2.10**	**-1.29**
Liner	-182.63	-115.60	-308.63	-228.54	-266.63	-204.52
Rebars	-143.11	-61.39	-232.99	-135.35	-199.40	-123.68
Tendons	**1256.00**	**1431.00**	**1127.62**	**1278.73**	**1159.53**	**1289.83**

7.5.4 Summary of Cylindrical Wall Analysis

The summary of the three different analyses performed on the cylindrical walls is provided in Table 12, below:

Table 12: Summary of the Cylindrical Wall TLAA Results

Final Stress		Begin of Lifetime		End of Lifetime		LOCA end of Life	
Material	Analysis	σ_h	σ_v	σ_h	σ_v	σ_h	σ_v
		MPa	MPa	MPa	MPa	MPa	MPa
Concrete	40a P	-12.1	-7.03	-11.33	-6.39	-3.85	-2.56
	40a M	-12.1	-7.03	-9.83	-5.28	-2.35	-1.44
	60a	-12.1	-7.03	-9.59	-5.12	-2.10	-1.29
Liner	40a P	-182.6	-115.60	-202.33	-130.80	-160.33	-106.78
	40a M	-182.6	-115.60	-293.93	-216.19	-251.93	-192.17
	60a	-182.6	-115.60	-308.63	-228.54	-266.63	-204.52
Rebars	40a P	-143.1	-61.39	-157.81	-70.62	-124.22	-58.94
	40a M	-143.1	-61.39	-222.28	-127.52	-188.69	-115.84
	60a	-143.1	-61.39	-232.99	-135.35	-199.40	-123.68
Tendons	40a P	1256.0	1431.00	1199.04	1340.23	1230.95	1351.33
	40a M	1256.0	1431.00	1137.79	1286.18	1169.71	1297.27
	60a	1256.0	1431.00	1127.62	1278.73	1159.53	1289.83

The analysis performed on the cylindrical wall are validated by comparing the results of the TLAA (which uses strain data as input parameters) to the extrapolation of the tendon force as determined in § 5.3 – where the average tendon force was estimated to be **3,500 kN** and **3,491 kN** (or 1,325.3 MPa and 1,278.7 MPa) for the 40-year and 60-year predictions respectively. The tendon force is however measured and predicted at the anchor head (where the dynamometers are) at the +56m.

As indicated in Table 12, the measured 'End of Life' vertical tendon stress is predicted to be **1,286.18** MPa (40 years) and **1,278.73** MPa (60 years), which is within 2.07% and 3.32% of the estimated tendon forces from Section 5.4 of this report. The predicted vertical tendon forces based on the analysis are however based on a reference height of +22m.

Although the reference heights are not the same, the analysis provides confidence in the results of the TLAA methodology, as the two different methods are similar, and the correlation in the results justifies for the use of the dynamometers to support the strain gauges.

A further consideration is done by comparing the percentage loss of stress and force:

For the stress calculated at 22m:

Beginning of life = 1,431 MPa

at 40 years: = 1,286.18 MPa

% loss = (1,431-1,286.18)/1431 = 10.12%

Force measured (even though at the top):

- Beginning = 3,742 kN

- Estimated at 40 years = 3,500 kN

% loss = (3,742 – 3,500)/3,742 = 6.47%

(Thus, stress estimate is taken as conservative)

7.6 Dome Analysis

The analysis was repeated for the dome section of the containment structures. It is noted that the dome has limited strain gauges available and that only the strain gauges at the uppermost peak of the containment structures are considered (where the dead load is considered zero). Furthermore, it should be noted that the dome is considered symmetric and the strain in both the circumferential and the radial directions are considered equal.

As noted previously, the adjusted Unit 1 data was used where the strain was increased to be a best estimate of the actual strain.

7.6.1 Dome – Predicted Strain at 40 Years

Redacted - PAIA Section 36 (1)(b); PAIA Section 37 (1)(a)

Total Stresses	Begin of Lifetime		End of Lifetime		LOCA end of Life	
	σ_h	σ_v	σ_h	σ_v	σ_h	σ_v
Materials	[MN/m²]	[MN/m²]	[MN/m²]	[MN/m²]	[MN/m²]	[MN/m²]
Concrete	-8.03	-8.03	-7.07	-7.07	**-1.77**	**-1.77**
Liner	-124.94	-124.94	-155.61	-155.61	-124.73	-124.73
Rebars	-85.68	-85.68	-106.71	-106.71	-85.53	-85.53
Tendons	**1 194.0**	**1 194.0**	**1 143.0**	**1 143.0**	**1 163.1**	**1 163.1**

The tendon stress due to initial prestressing are calculated from initial tendon stresses after friction and slip losses and after elastic deformation of the concrete as provided in reference [27], § 4.1.2. In order to get the strains, the stresses can be divided by the Young's Modulus of the prestressing steel.

- Vertical tendon strain: 1,194 MPa /190,000 MPa = 0,00628

7.6.2 Dome – Measured Strain at 40 Years

Redacted - PAIA Section 36 (1)(b); PAIA Section 37 (1)(a)

Total Stresses	Begin of Lifetime		End of Lifetime		LOCA end of Life	
	σ_h	σ_v	σ_h	σ_v	σ_h	σ_v
Materials	[MN/m²]	[MN/m²]	[MN/m²]	[MN/m²]	[MN/m²]	[MN/m²]
Concrete	-8.03	-8.03	-5.60	-5.60	**-0.31**	**-0.31**
Liner	-124.94	-124.94	-219.60	-219.60	-188.72	-188.72
Rebars	-85.68	-85.68	-150.58	-150.58	-129.40	-129.40
Tendons	**1 194.0**	**1 194.0**	**1 101.3**	**1 101.3**	**1 121.5**	**1 121.5**

7.6.3 Dome – Extrapolated Strain at 60 Years

Redacted - PAIA Section 36 (1)(b); PAIA Section 37 (1)(a)

Total Stresses	Begin of Lifetime		End of Lifetime		LOCA end of Life	
	σ_h	σ_v	σ_h	σ_v	σ_h	σ_v
Materials	[MN/m²]	[MN/m²]	[MN/m²]	[MN/m²]	[MN/m²]	[MN/m²]
Concrete	-8.10	-8.10	-5.34	-5.34	**-0.05**	**-0.05**
Liner	-126.04	-126.04	-231.42	-231.42	-200.54	-200.54
Rebars	-86.43	-86.43	-158.69	-158.69	-137.52	-137.52
Tendons	**1 204.5**	**1 204.5**	**1 094.4**	**1 094.4**	**1 114.5**	**1 114.5**

7.6.4 Summary of Dome Analysis

A summary of the final, three different analyses performed as part of the TLAA is provided in Table 13.

Table 13: Summary of the Dome TLAA Results

Total Stresses		Begin of Lifetime		End of Lifetime		LOCA end of Life	
Material	Analysis	σ_h	σ_v	σ_h	σ_v	σ_h	σ_v
		MPa	MPa	MPa	MPa	MPa	MPa
Concrete	40a P	-8.03	-8.03	-7.07	-7.07	-1.77	-1.77
	40a M	-8.03	-8.03	-6.35	-6.35	-1.05	-1.05
	60a	-8.10	-8.10	-5.34	-5.34	-0.05	-0.05
Liner	40a P	-124.94	-124.94	-155.61	-155.61	-124.73	-124.73
	40a M	-124.94	-124.94	-187.03	-187.03	-156.15	-156.15
	60a	-126.04	-126.04	-231.42	-231.42	-200.54	-200.54
Rebars	40a P	-85.68	-85.68	-106.71	-106.71	-85.53	-85.53
	40a M	-85.68	-85.68	-128.25	-128.25	-107.07	-107.07
	60a	-86.43	-86.43	-158.69	-158.69	-137.52	-137.52
Tendons	40a P	1194.00	1194.00	1143.02	1143.02	1163.14	1163.14
	40a M	1194.00	1194.00	1122.55	1122.55	1142.67	1142.67
	60a	1204.50	1204.50	1094.35	1094.35	1114.47	1114.47

The data is also represented for the concrete stress criteria. It is seen that with the analysis as discussed above, all the concrete sections fall in the design criteria at 60 years.

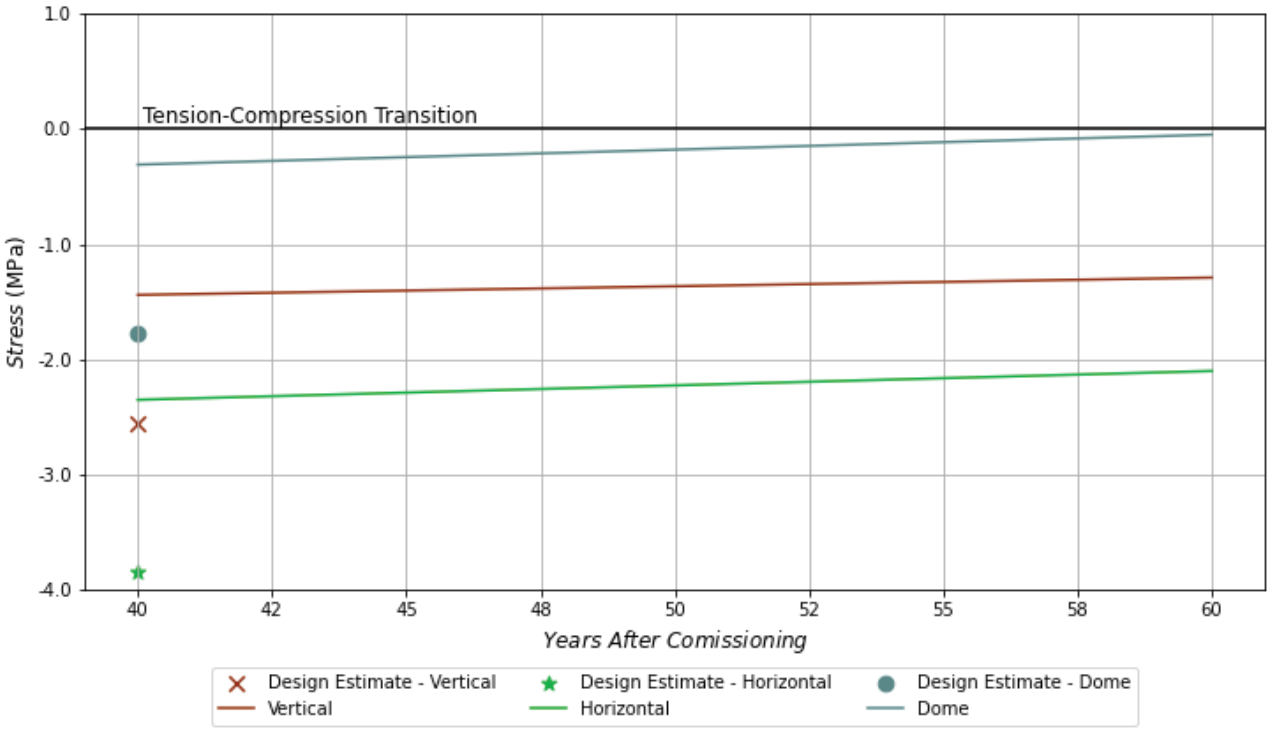

Figure 46: Graphical Summary of TLAA Results

The above results indicate that the containment structures meet the compressive requirement for LTO.

7.7 Results discussion

When considering the strain results, the Unit 1 and Unit 2 data differ by ±40% (Table 10). It is believed that the difference stems from the delay in the initial monitoring onset for the Unit 1 structure.

The calculation of the strain is based on Equation 1:

$$\frac{\Delta l}{l} = 625 \cdot 10^{-5} \cdot K\left(F^2 - {F_0}^2\right) [\mu/m]$$

Equation 1

Where: $\frac{\Delta l}{l}$ = Relative Strain in [µm/m]

$K = 0.3$ = Characteristic Coefficient for the Strain Gauges

$F \; and \; F_0$ = Frequency Measurements in [Hz]

The F_0 measurement is the baseline measurement for the strain measurements taken directly after tensioning, i.e., the 'zero-hour reading'. Table 2 provides the reference dates for when the baseline readings were taken. For the Unit 1 strain gauges above the +22.89m level, which are the gauges considered in this report, the 'zero-hour reading' were taken 14 months after the final tensioning was done. While for Unit 2 the measurements were taken during the same month. This delay experienced in Unit 1 is likely the cause of the differences in the strain gauge measurements.

Accordingly, the Unit 2 data was used as representative for both units. The percentage difference between the respective results for the units was calculated to be approximately 40%. Therefore, the Unit 2 dome strain is estimated by increasing the unit 1 dome strain by a percentage difference of 40%, to be **-456 µm/m** and **-521 µm/m** for 40 and 60 years respectively as applied in the aforementioned analysis.

The analysis was re-performed for both Units and a range of strain data values were used to indicate the upper and lower limit range for the data used. This is provided in Figure 47.

The analysis included the following:

- Each aspect of the TLAA, namely, 'Horizontal', 'Vertical', and 'Dome', is plotted by a range of values. The range is highlighted with similar colours for each aspect.
- The Unit 2 strain values for 40 and 60 years, which is similar to Figure 46. In each case this is labelled with an annotation "Unit 2" next to the line.
- The Unit 1 strain values 40 and 60 years, as indicated in Table 10. In each case this is labelled with an annotation "Unit 1" next to the line.
- The average of Unit 1 and Unit 2 strain values, annotated by the dashed line inside each range.
- An additional range is indicated for each aspect of the TLAA, which is annotated in the legend as "Worst-Case". The worst-case values are presented if the strain values were based on the prediction method of simply adding an additional (non-scientific) 20% to the measured strain at 40 years per Table 7, Table 8 and Table 9 for the vertical, horizontal and dome strain respectively.

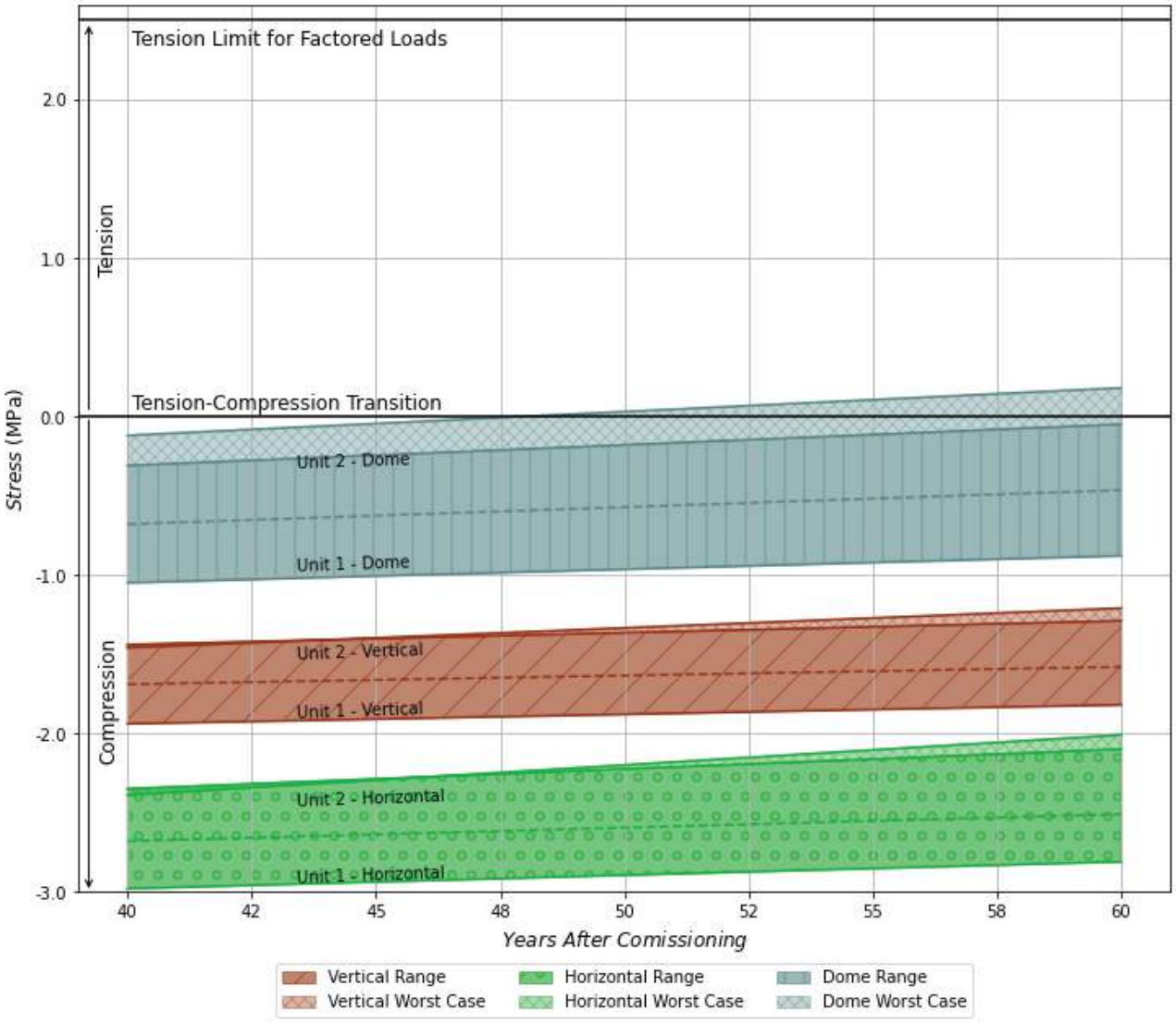

Figure 47: Graphical Summary of TLAA Results with Ranges for All Sections Analysed

From the analysis the following can be concluded:

1. The cylindrical walls of the containment structures are validated for an additional 20 years and based on the current analysis and the strain development; no design limits are exceeded (as shown in Figure 46).
2. The domes of the containment structures are validated for an additional 20 years based on the current analysis and the strain development. When considering the adjustment that needed to be made to accommodate the uncertainties for Unit 2, the design margins are still not exceeded (as shown in Figure 46).
3. If more conservative estimates are applied for the purposes of analysis and to assess available margins, the design limit is exceeded (**by 0.18MPa**). This is however marginal and not a concern for the safe operation of the Koeberg containment structures.
4. The quality of the available data for the cylindrical wall is deemed sufficient, only 1 defective strain gauge was removed from the analysis.

5. For the dome, the data available was limited and needed engineering interpretation. The available data for unit 1 dome was increased by a 40% to represent the Unit 2 dome and the conclusion is conservative and based on sound engineering interpretation of the data. Notwithstanding the limited number of available strain gauges on the dome, recommendations are made with respect to the installation of additional strain gauges in § 12.6 of this report. The additional strain gauges are however not needed prior to LTO.

8. TLAA with 3rd ILRT's data

Eskom has considered the results of the previous ILRTs (performed in 2015 on both units, also referred to as the 3rd ILRTs, with the first being performed at commissioning and the second in 2005 and 2008 on unit 1 and unit 2 respectively) to cross-validate the TLAA calculation, specifically considering the effect of the LOCA containment pressure. The monitoring of the structures during the 3rd ILRTs were performed by EDF experts using automatic monitoring equipment. EDF measured the invar wires, pendulums and strain gauges with good precision and the results have been shared with the NNR.

The results were not incorporated into the TLAA (§7) nor considered for cross validating the TLAA calculations. This is now performed below:

EDF advised Eskom to carefully consider which gauges to use in simplistic calculations and avoid using data from gauges that may be influenced by the equipment hatch. Eskom was advised to specifically investigate the behaviour of gauges **I-1** and **I-5** of Unit 1 and gauges **I-2** and **I-6** of Unit 2 as they might be influenced by the hatch during pressure tests, and/or determine if there are outliers in the data by inspection. The location of the gauges that might be influenced by the equipment hatch is shown in Figure 48 and Figure 49 .

EDF also disregards clear outliers from their analysis.

It is also confirmed that it is common practice for EDF to consider the 'common parts' (i.e., the +22.89m gauges) of the containment structures when calibrating analytical models.

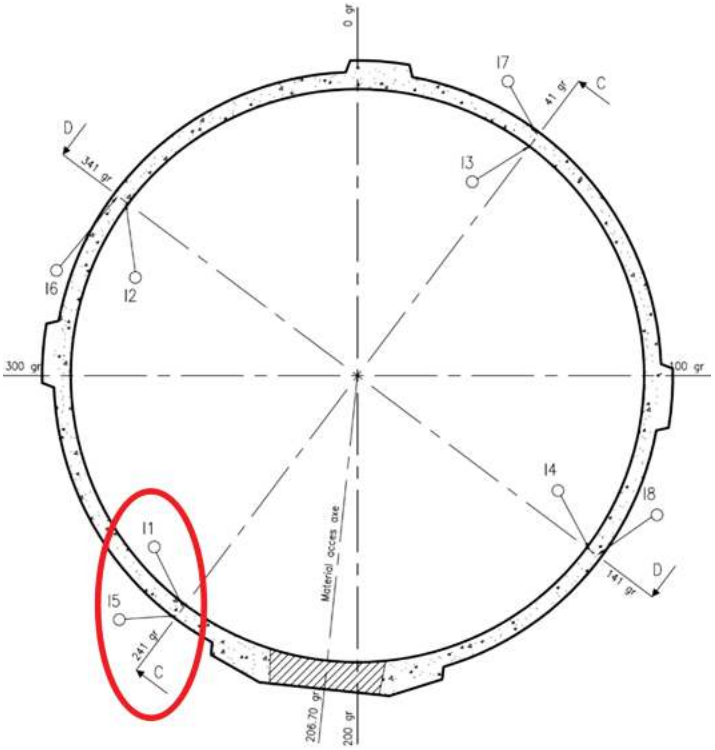

Figure 48: Location of Unit 1 +22.89m Strain Gauges

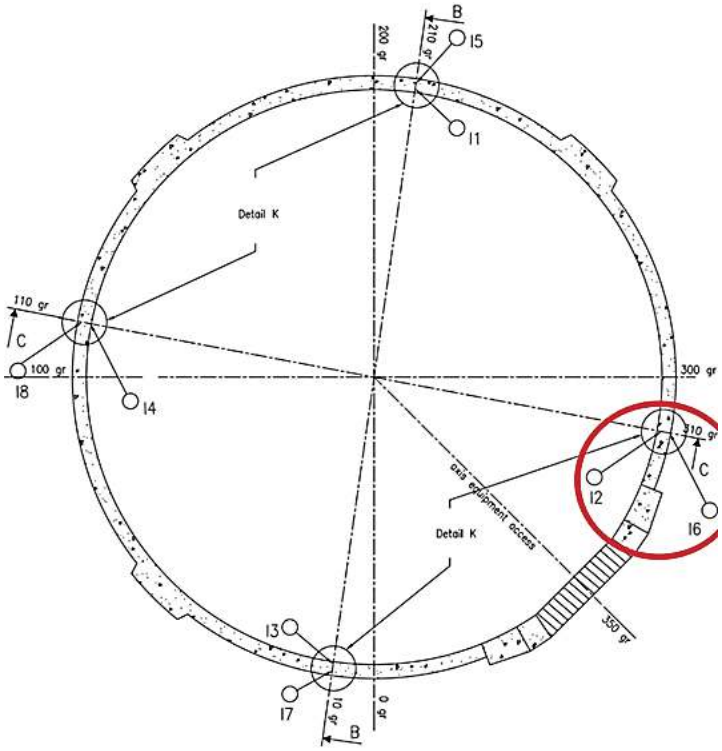

Figure 49: Location of Unit 2 +22.89m Strain Gauges

8.1 Unit 1 3rd ILRT Data

Consider the 3rd ILRT data for the +22.89m strain gauges below. The strain is 'adjusted' to have a common start point only, and no other manipulation is done. This is purely to consider the data relative to a common initial strain to see the impact of the ILRT.

For the vertical gauges:

- **I-5** gauge can be ignored as it is influenced by the hatch, and
- **I-6** & **I-7** is ignored as outliers.

For the horizontal gauges, all the gauges are considered. See Figure 50 and Figure 51.

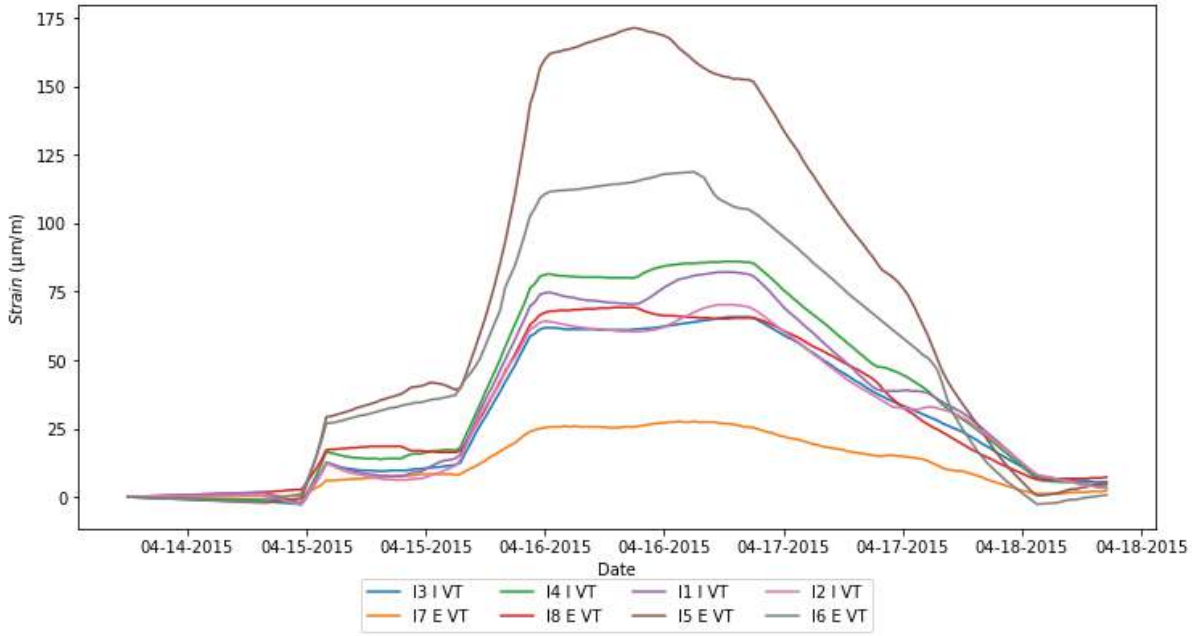

Figure 50: Unit 1 Adjusted Strain Data at +22.89m - Vertical

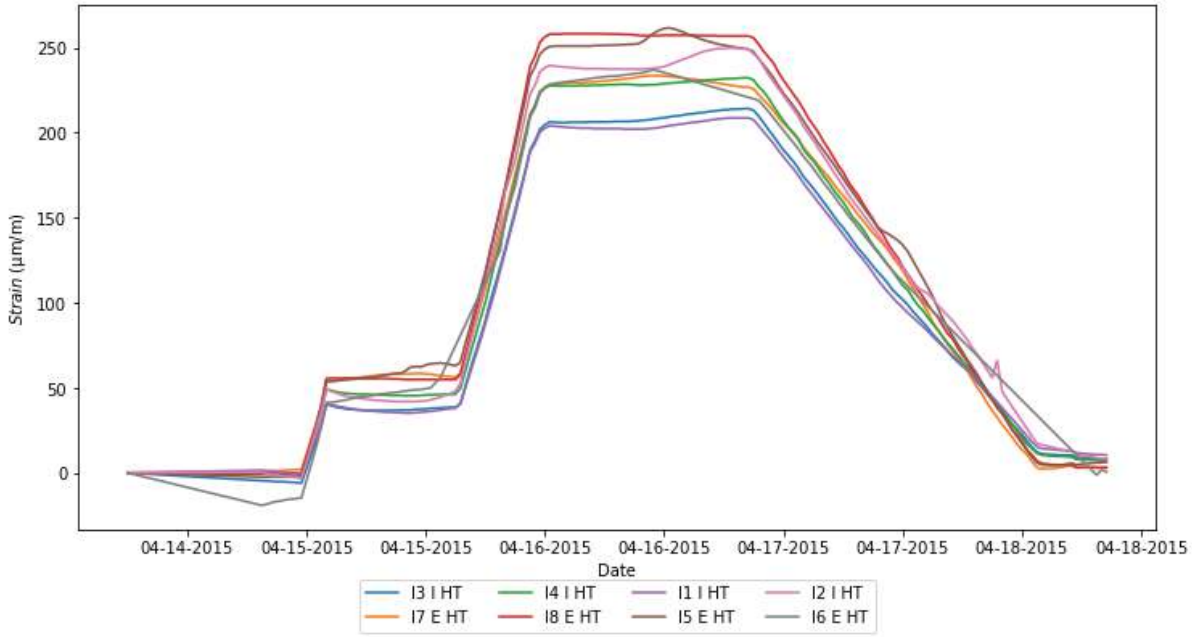

Figure 51: Unit 1 Adjusted Strain Data at +22.89m - Horizontal

8.2 Unit 2 3rd ILRT data

The adjusted Unit 2 strain is provided below for the 3rd ILRT.

For the vertical gauges:

- **I-6** gauge can be ignored as it is influenced by the hatch.

For the horizontal gauges, all the gauges are considered. See Figure 52 and Figure 53.

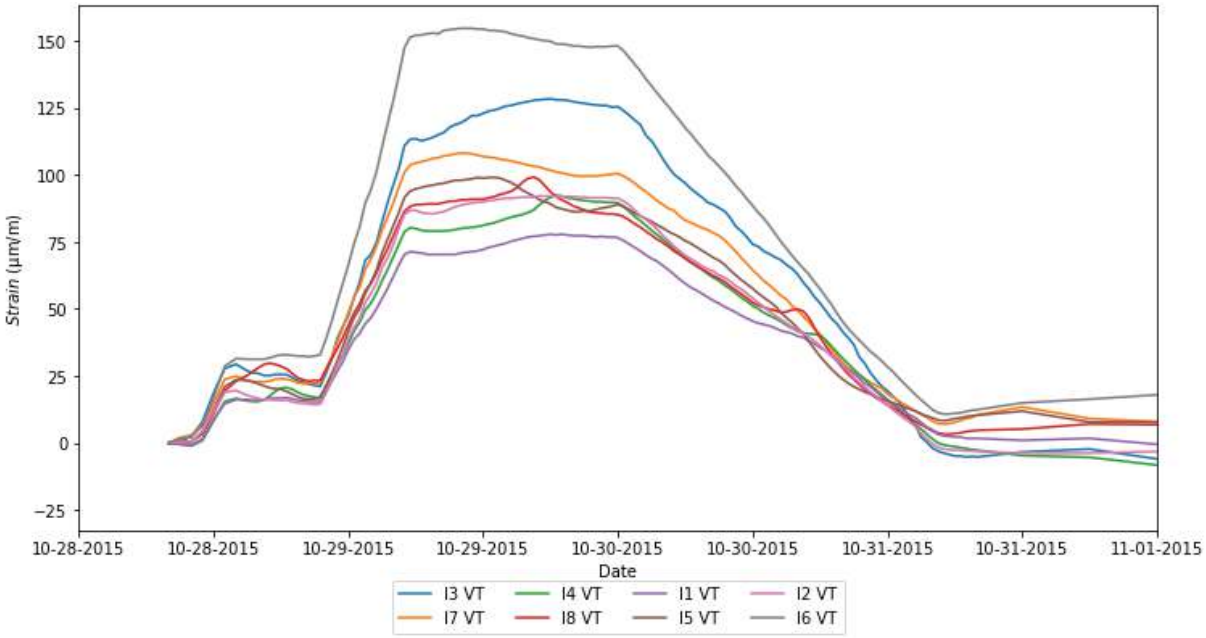

Figure 52: Unit 2 Adjusted Strain Data at +22.89m - Vertical

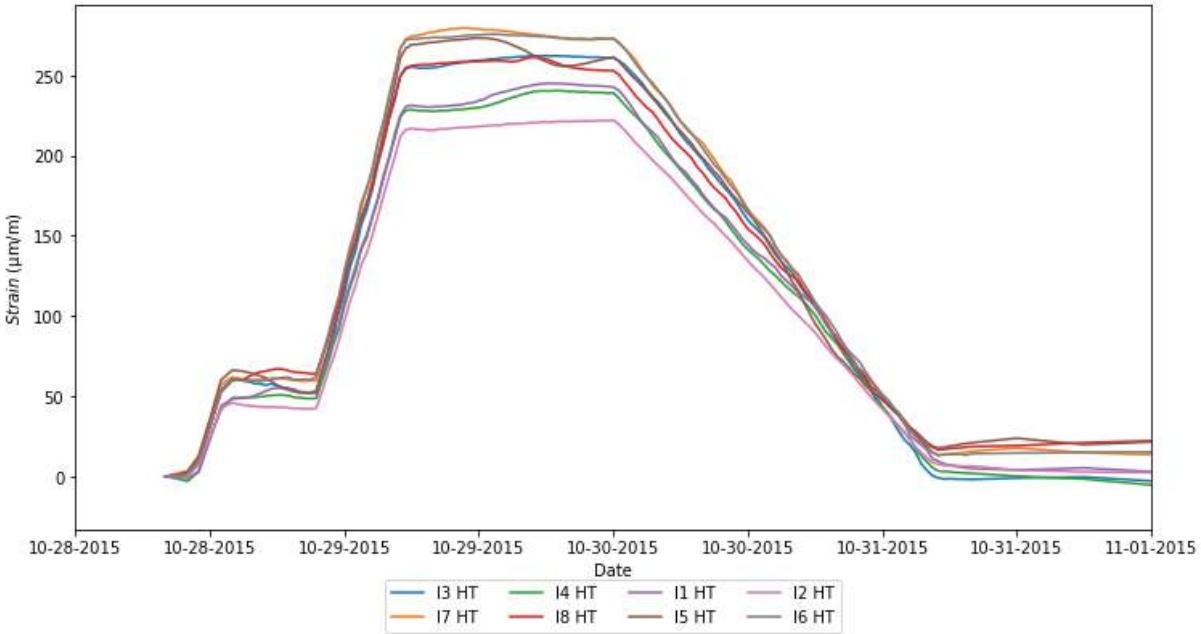

Figure 53: Unit 2 Adjusted Strain Data at +22.89m – Horizontal

8.3 Average Strain Curves

The average strain of the respective Units is presented in Figure 54 and Figure 55 below, with the outliers removed as discussed above:

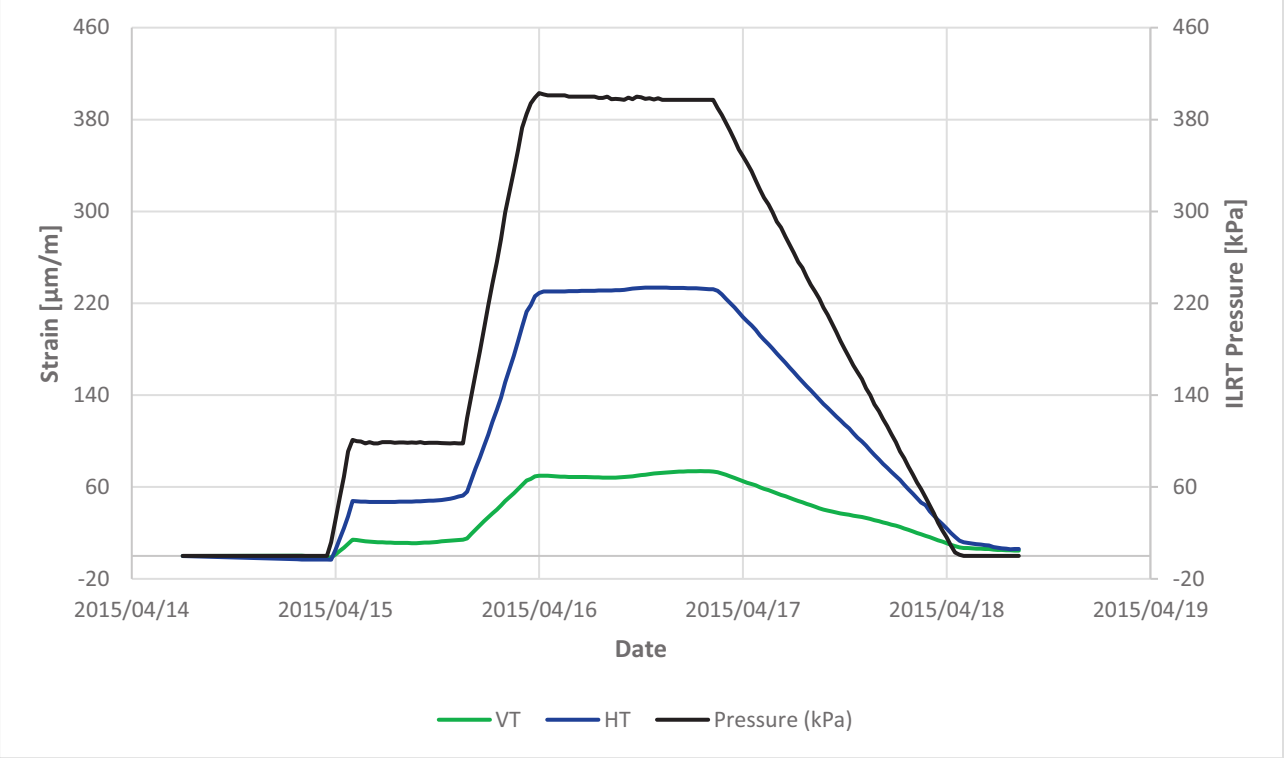

Figure 54: Unit 1: +22.89m 3rd ILRT Strains

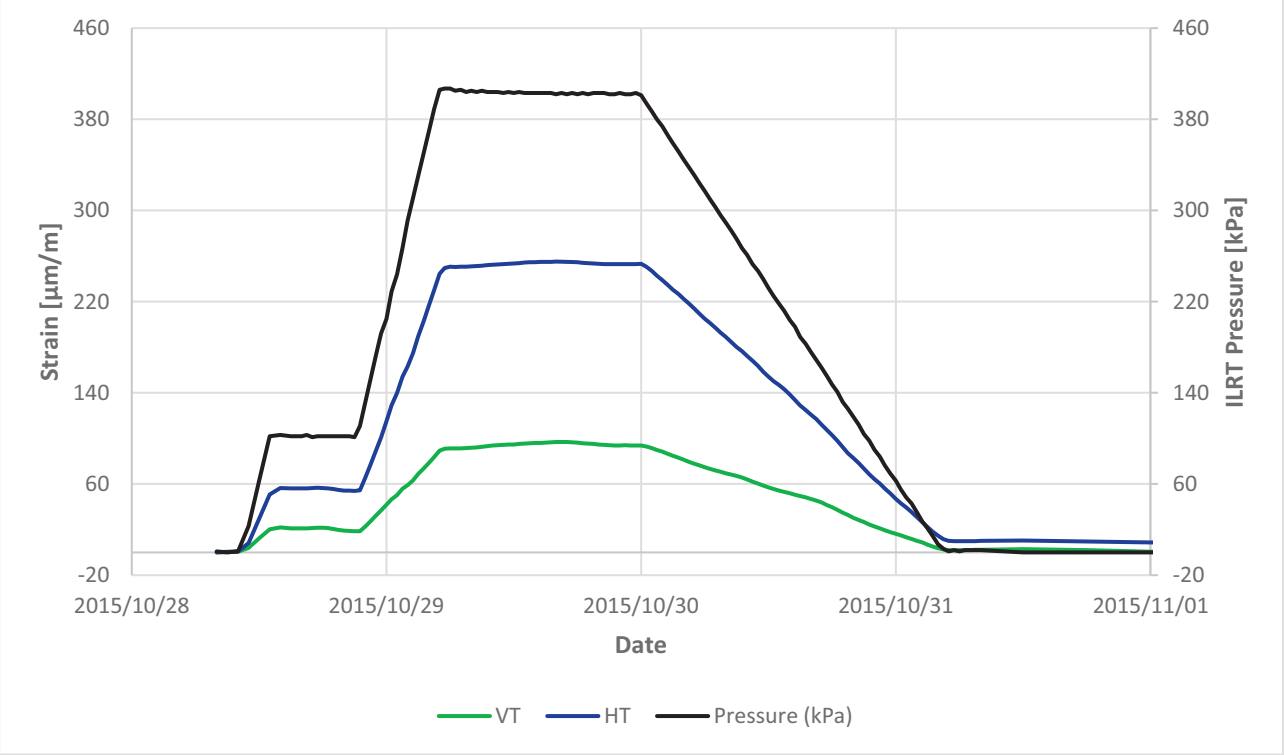

Figure 55: Unit 2: +22.89m 3rd ILRT Strains

The average strains obtained during the previous ILRTs were used to calibrate the TLAA calculations, as several material properties were assumed based on conservative estimates. The calibration of the analytical model is done to reduce the level of conservatism assumed during the TLAA calculations and to show the safety margin available. The analytical model is calibrated by using the strain measured during the 3rd ILRTs to calculate the E_{Mod} for each unit and each strain direction. The result is shown below:

Table 14: Calculated Concrete EMod from 3rd ILRTs – Walls

Unit	Direction	Measured ε from 3rd ILRTs [μm/m]	Result of ε obtained during back-calculation [μm/m]	% Diff	E_{mod} [GPa]
U1	Horizontal	231.90	231.55	0.152%	27.9
	Vertical	70.65	70.70	0.069%	32.65
U2	Horizontal	252.80	252.91	0.045%	25.2
	Vertical	94.19	94.28	0.092%	23.9

The original Structural Integrity (SIT) report (KBA1206D00102) calculated the E_{Mod} of the concrete based on the +22.89m strain gauge data and the invar wire data and obtained the following results:

Table 15: SIT Calculated Concrete EMod, 1982 – Walls

Unit	Instrumentation	E_{Mod} [GPa]
Unit 1	Strain Gauges	22.8
	Invar wires	23.6
Unit 2	Strain Gauges	20.7
	Invar wires	24.2

By comparison, the results obtained in the back-calculation using the strains of the 3rd ILRTs and the original SITs, compare well and demonstrate the conservatism in using 40 GPa for the E_{Mod} of the concrete in the TLAA.

8.4 Containment Domes

During the 3rd ILRTs, data was obtained from two strain gauges on each dome. Therefore, a similar exercise as above was performed to calibrate the TLAA calculations based on the ILRT strain data for the domes. See Figure 56 and Figure 57.

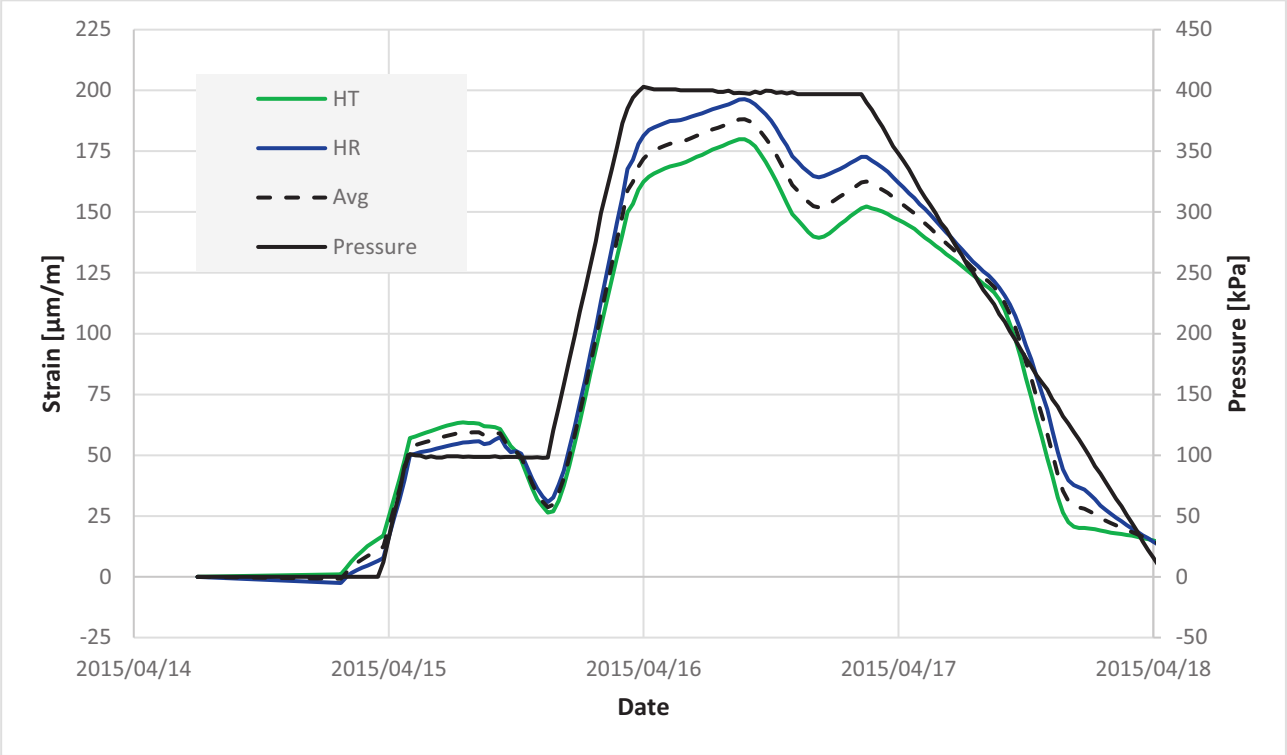

Figure 56: Unit 1 3rd ILRT Data – Strain and Pressure

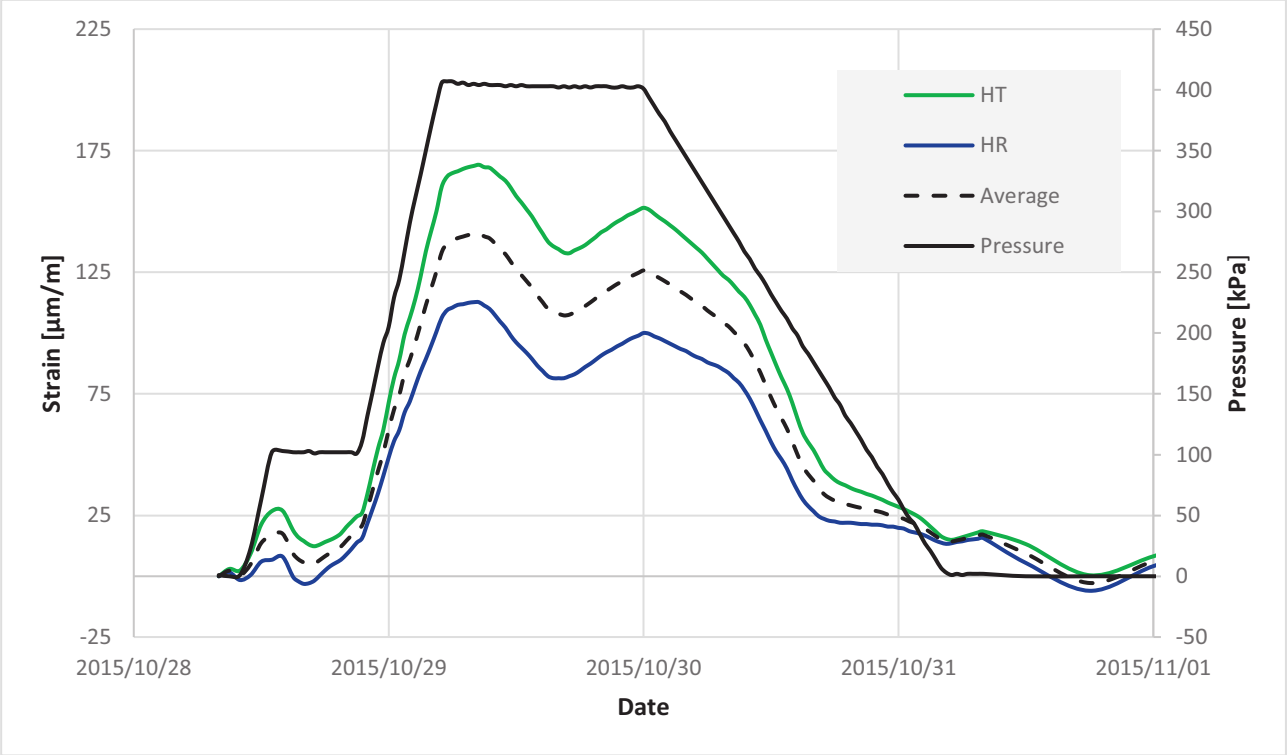

Figure 57: Unit 2 3rd ILRT Data – Strain and Pressure

It is clear, in Figure 58 and Figure 59, that the domes are more susceptible to temperature variations when comparing the strain and temperature data:

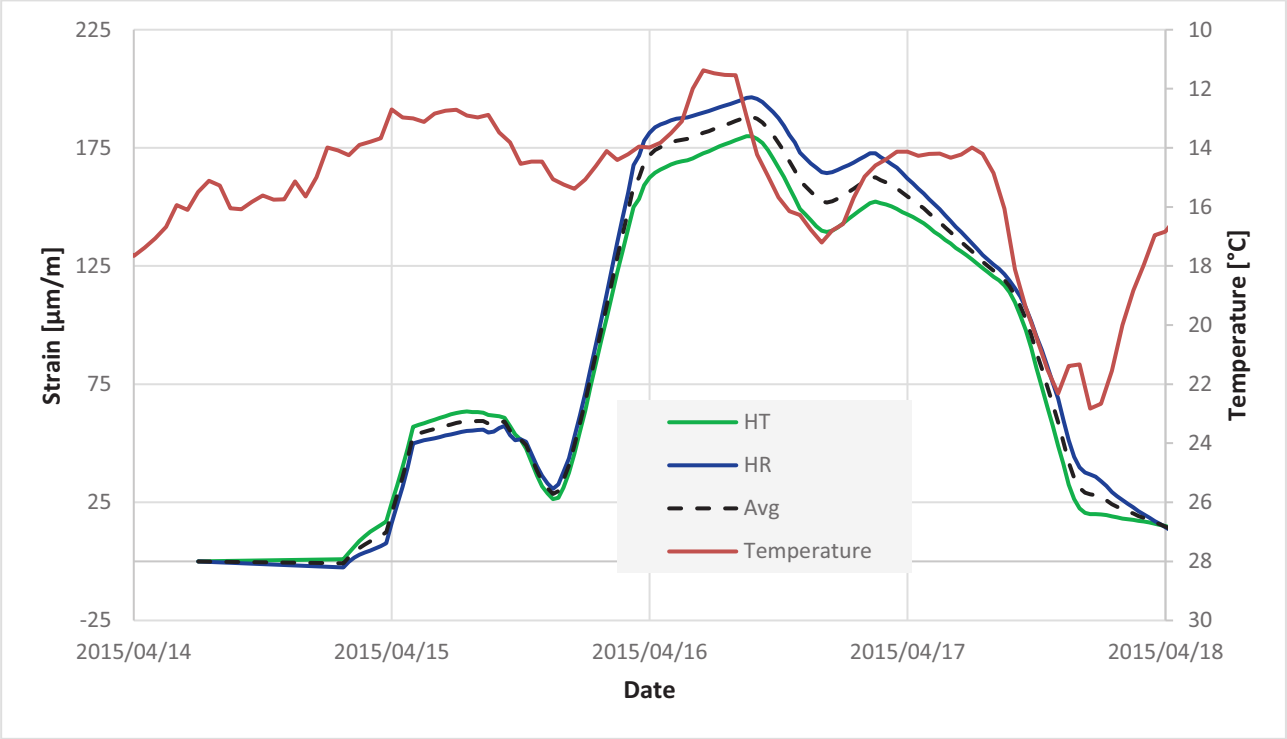

Figure 58: Unit 1 3rd ILRT Data – Strain and Temperature

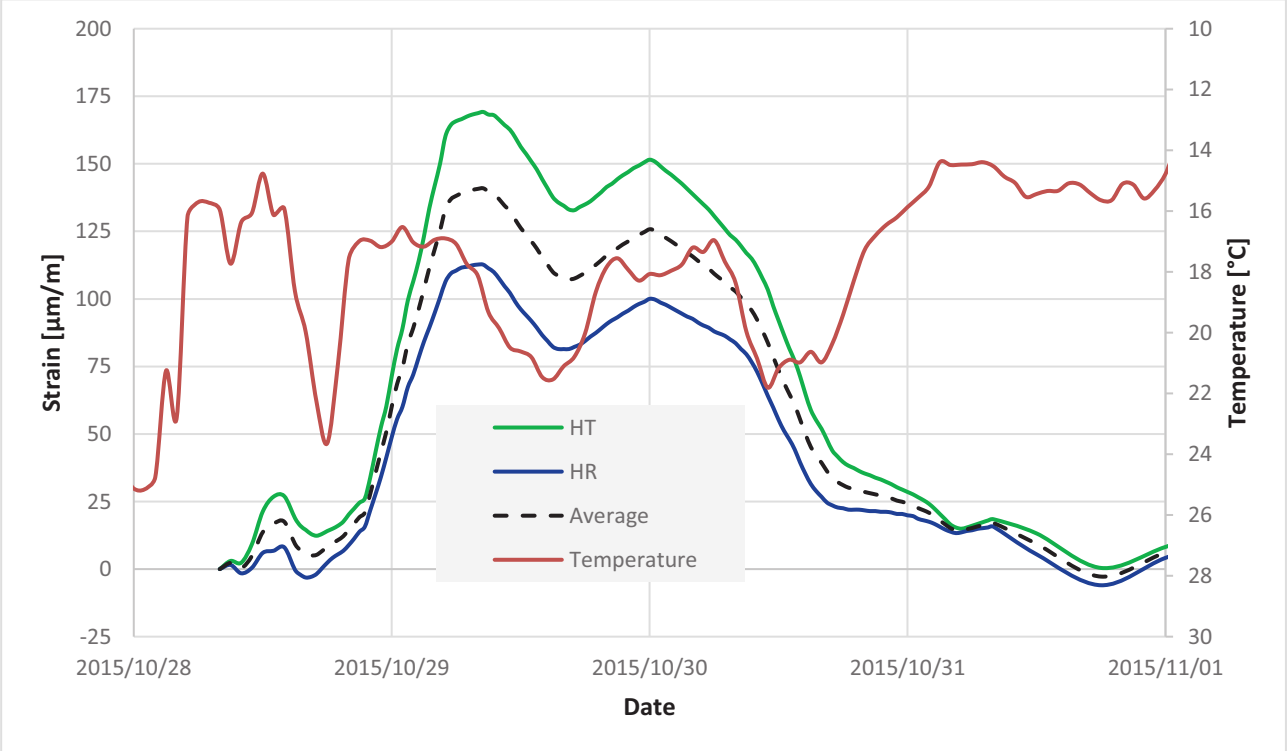

Figure 59: Unit 2 3rd ILRT Data – Strain and Temperature

The average strain is again considered at peak pressure during the ILRTs. This is a reasonable assumption as the cyclic behaviour of the temperature difference is then negated.

The average strains during peak pressure for each unit, as well as the calculated E_{Mod} is provided in Table 16 below:

Table 16: Calculated Concrete EMod from 3rd ILRTs – Domes

Unit	Average ε [µm/m]	Result ε [µm/m]	% Diff	E_{mod} [GPa]
Unit 1	171.89	171.83	0.035%	22.6
Unit 2	123.81	123.92	0.089%	33.4

The E_{Mod} values of the concrete as calculated in Table and Table 16 can be used to more accurately perform the TLAA following the calibration using the data from the 3rd ILRTs. The TLAA calculations can be re-performed for the dome using the most conservative result from Table 16, i.e., 33.4 GPa (for Unit 2). This is, however, only applicable to the LOCA pressure and not the E_{Mod} associated with long-term loads, including the prestress, shrinkage and creep loads. In §7, it is mentioned that a calculated E_{Mod} for the concrete can be calculated to be 19 GPa, compared to the 15 GPa conservatively used in the TLAA.

By reperforming the TLAA with the aforementioned E_{Mod} values, the resultant stress is -0.66 MPa and -0.38 MPa at 40 and 60 years respectively as shown in Table 17 and Table 18 .

Table 17: Dome - Measured Strain at 40 years

Redacted - PAIA section 36(1)(b); PAIA section 37(1)(a)

Total Stresses	Begin of Lifetime		End of Lifetime		LOCA end of Life	
	σ_h	σ_v	σ_h	σ_v	σ_h	σ_v
Materials	[MN/m²]	[MN/m²]	[MN/m²]	[MN/m²]	[MN/m²]	[MN/m²]
Concrete	-8.41	-8.41	-5.84	-5.84	**-0.66**	**-0.66**
Liner	-103.25	-103.25	-204.11	-204.11	-167.97	-167.97
Rebars	-70.80	-70.80	-139.96	-139.96	-115.18	-115.18
Tendons	**1 194.0**	**1 194.0**	**1 097.3**	**1 097.3**	**1 120.8**	**1 120.8**

Table 18: Dome - Extrapolated Strain at 60 Years

Redacted - PAIA section 36(1)(b); PAIA section 37(1)(a)

Total Stresses	Begin of Lifetime		End of Lifetime		LOCA end of Life	
	σ_h	σ_v	σ_h	σ_v	σ_h	σ_v
Materials	[MN/m²]	[MN/m²]	[MN/m²]	[MN/m²]	[MN/m²]	[MN/m²]
Concrete	-8.48	-8.48	-5.56	-5.56	**-0.38**	**-0.38**
Liner	-104.16	-104.16	-216.61	-216.61	-180.46	-180.46
Rebars	-71.42	-71.42	-148.53	-148.53	-123.75	-123.75
Tendons	**1 204.5**	**1 204.5**	**1 089.7**	**1 089.7**	**1 113.3**	**1 113.3**

The TLAA and the associated safety margins in the Unit 2 dome's TLAA with a refined estimate of the concrete's E_{Mod} is presented graphically in Figure 60.

The above calculations show that the assumptions made in §7 were conservative and, although it indicated that both Units are qualified for an additional 20 years of operation, the margin indicated during the analysis was deemed small. With the refined E_{Mod} values, the analysis indicates that there is sufficient safety margin and that the concrete does not go into any tension during a LOCA pressure up to (and beyond) 60 years of operation.

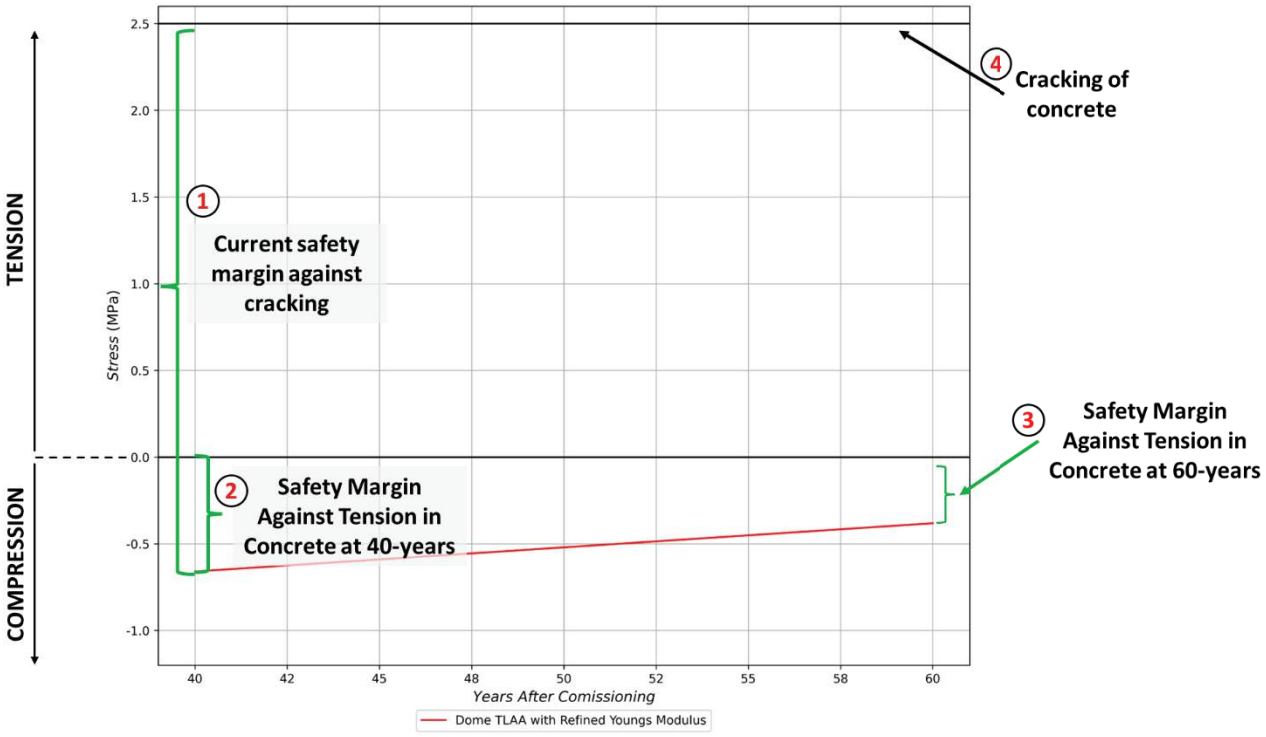

Figure 60: Unit 2 Dome TLAA Safety Margin

9. TLAA with In-Situ Concrete Material Properties

This section provides a refinement of the TLAA calculations presented in §7. It incorporates the material properties obtained from the testing of concrete cores extracted from the Unit 1 and Unit 2 containment buildings. The purpose of this exercise was to confirm the validity of material properties used in the original TLAA calculations and compare mechanical properties of concrete of unit 1 with that of unit 2, and to improve the overall confidence in the TLAA outcomes and conclusions.

Furthermore, this section clarifies the conclusion arrived at by the NNR that the TLAA 301 is fully validated for unit 1 for the proposed 20 years and for unit 2 for 8 years based on information obtained from Figure 4 in reference [39], at the time. Based on the refined TLAA calculations presented in this section (§9), the design margins for both containment buildings are demonstrated to be adequate for safe operation for an additional 20 years and beyond.

The original concrete parameters were compared with the test results, and the updated calculations demonstrate an improved margin to the original design assumptions. In addition, the material test reports [37] and [38] conclude that although the concrete in unit 2 has a lower compressive strength than unit 1, the two units have comparable behaviour in terms of stiffness, Poisson's ratio and tensile strength. This improves the accuracy of the TLAA and reinforces that the outcomes in §7 were conservative.

9.1 Test Methodology

The test program included measurements of key mechanical properties such as compressive strength, static and dynamic modulus of elasticity, Indirect tensile strength and Poisson's ratio. Full details of the testing methodology and results are documented in References [37] and [38].

A total of 20 core samples were obtained from the cylindrical walls and domes of Unit 1 and Unit 2 containment buildings. The cores were grouped into four categories representing the domes and walls of Unit 1 and Unit 2, respectively. Core extraction from the cylindrical walls was performed horizontally, i.e., perpendicular to the direction of casting, while samples from the domes were extracted vertically, i.e., parallel to the casting direction.

Given the dense reinforcement and presence of embedded post-tensioning tendons in the containment structures, core samples with dimensions of 80 mm in diameter and 100 mm in length were extracted. Six from each dome and four from each cylindrical wall. These samples were used for compressive strength, static and dynamic modulus of elasticity and Indirect tensile strength tests. Three 45mm by 100mm core samples (one from unit 1 and two from unit 2) were used for Poisson's ratio test (Refer to the chain of custody record for concrete samples: QP-26-1).

The compression test was performed using local South African standard SANS 5865 while the balance of the tests was performed using international American code ASTM C469/CC469M. SANS 5865 recommends 100 mm diameter core samples but permits the use of samples with diameters exceeding 65 mm for compression test, provided the length-to-diameter ratio exceeds 0.85. The calculated length to diameter ratio of various samples obtained for compression test exceed the ratio of 0.85, as required by SANS 5865.

For the remainder of the tests, ASTM C469/C469M was applied which refers to C42/C42M for the determination of preferred sample size. C42/42M states "core diameters less than 94mm are not prohibited and if core diameter is less than 94mm report reason". Furthermore, C42/C42 requires samples for static Young's modulus and Poisson's ratio testing to have length to diameter ratio of 1.5. However, due to excessive congestion of steel reinforcement in the Koeberg containment structures and the presence of embedded tendons located at approximately 110mm within the concrete section, the requirement of length to diameter ratio of 1.5 could not be achieved for the static Young's modulus samples. The steel reinforcement congestion and embedded tendons constraints do not allow for easy coring of a 100mm diameter core which will require to core to depths of 180 mm to 200 mm deep to get a final length of 150 mm which will in turn satisfy the L/D ratio of 1.5.

Recognizing this limitation, the application of correction factors to the core sample lengths was evaluated in accordance with ASTM C469/C469M. While these correction factors were applied, it was observed that their influence marginally reduced the variability of the results but did not alter the overall trends in the measured static modulus values. It was therefore concluded that the impact of the correction factors is negligible and that the measured values, as obtained, remain valid and representative of the material properties.

The samples used for determination of Poisson's ratio were cored at a later stage after initial samples identified for this test were found to have anomalies. The samples used for this test were small in diameter size (45mm diameter and 90mm in length) compared to the samples used for static Young's modulus of elasticity. However, the samples complied with the dimensional requirements as well as the criteria of length to diameter ratio of 1.5. The diameter of 45mm for the Poisson's ration samples is allowed as per the provisions in clauses in 7.1.1 and 7.1.2 of ASTM C469/C469. Clause 7.1.1 states core specimens shall be at least 94mm or at least two times the nominal maximum size of the coarse aggregate, whichever is larger. In this case, as per the original construction information, the nominal maximum size of coarse aggregate is 19mm which equates to 36mm when multiplied by 2 as required by this clause. However, the larger value between 94mm and 36mm is 94mm which makes clause 7.1.2 more suitable for our scenario. Clause 7.1.2 simply states "core diameters of less than 94mm are not prohibited, if used provide a reason". The reason is as stated in the preceding paragraph. It is on this basis that core samples used for Poisson ratio tests meet all the requirements prescribed in ASTM C469/C469M and C42/42M respectively.

The test method for calculating dynamic modulus of elasticity followed the American Standard Test Method (ASTM) C597-22 for Ultrasonic Pulse Velocity Through Concrete. As noted in [37], the dynamic modulus of elasticity value obtained from this method is "*applicable to assess the uniformity and relative quality of concrete, to indicate the presence of voids and cracks, and to evaluate the effectiveness of crack repairs. It is also applicable to indicate changes in the properties of concrete, and in the survey of structures, to estimate the severity of deterioration or cracking. If used to monitor changes in condition over time, test locations are to be marked on the structure to ensure that tests are repeated at the same positions*" Furthermore, "*The results obtained by the use of this test method are not to be considered as a means of measuring strength nor as an adequate test for establishing compliance of the modulus of elasticity of field concrete with that assumed in the design*."

9.2 Results of In-situ Concrete Tests

Compressive strength results revealed that Unit 1 exhibits higher values compared to Unit 2; however, both units conform to the expected performance criteria for 40 MPa concrete. Additionally, the stiffness of concrete in the cylindrical walls was observed to be lower than that of the domes, yet still within the long-term stiffness values assumed. The reduced stiffness in the wall elements is likely due to the coring direction relative to the principal loading axis, as well as the effects of sustained long-term loads introduced by post-tensioning.

For both units the static modulus of elasticity measured for the dome concrete was comparable to what would be assumed as the original characteristic E-value for design purposes indicating the slow rate of ageing of the in-situ concrete. Furthermore, the Poisson's ratio of the concrete from Unit 1 and Unit 2 is similar and in the region of 0.23 to 0.25, which is typical for concrete. Overall, it can be concluded that the mechanical properties of concrete from both unit 1 and unit 2 containment building are comparable.

The results obtained from the in-situ core sample testing indicate mechanical properties that are more favourable than the conservative assumptions initially adopted in the TLAA calculations. All measured values remain within the original design margins, thereby validating the structural integrity and mechanical performance of the containment buildings for continued long-term operation.

9.3 Material Properties

Similar to §7.3, the material properties are used for the bi-axial equilibrium analysis. The material properties used for the analysis in this section are [37] [38]:

Table 19: In-situ Concrete Material Properties Used in TLAA

Material	Young's Modulus [GPa]			Poisson's ratio	$A_{Horizontal}$ [mm²/m]	$A_{Vertical}$ [mm²/m]	Dome [mm²/m]
		Walls	Dome				
Concrete	Static	24	28.2	0.23	900,000	900,000	800,000
	Dynamic	40	40				
Liner	210			0.28	7,000	6,800	9,000
Reinforcement	200			N/A	1,610	2,790	7,060
Tendons	190			N/A	9,900	4,910	6,830

The concrete Young's modulus (E_{Mod}) is considered a time dependant parameter and reduces with time. The original design documents used 15 GPa as the long-term E_{Mod}. 15 GPa is conservative and estimating the long-term E_{mod} using modern codes such as the French RCC-CW code, the E_{mod} for the concrete may be in the region of 19 GPa. Regardless, the original design values of 15 GPa is used in the analysis in §7.5 and §7.6.

In this section, the TLAA is reperformed using the in-situ concrete material properties. Long-term static E_{Mod} of 24 GPa for the walls and 28.2 GPa for the dome and Poisson ratio 0.23. The in-situ dynamic E_{Mod} was also determined in the tests. The TLAA in §7 uses 40 GPa as the dynamic E_{Mod}. In this section, the use of the dynamic E_{Mod} of 40 GPa is retained due to reasons provided in §8.1.

9.4 Cylindrical Wall Analysis

The assumptions in 7.4 remain valid for the following calculations.

9.4.1 Cylindrical Wall – Predicted Strain at 40 years

Redacted - PAIA section 36(1)(b); PAIA section 37(1)(a)

Total Stresses	Begin of Lifetime		End of Lifetime		LOCA end of Life	
	σ_h	σ_v	σ_h	σ_v	σ_h	σ_v
Materials	[MN/m²]	[MN/m²]	[MN/m²]	[MN/m²]	[MN/m²]	[MN/m²]
Concrete	-12.74	-7.44	-11.87	-6.75	**-4.37**	**-2.90**
Liner	-116.73	-72.10	-140.64	-90.93	-99.58	-68.26
Rebars	-91.95	-37.53	-109.69	-49.10	-76.63	-38.46
Tendons	1256.00	1431.00	1196.14	1338.02	1227.55	1348.12

9.4.2 Cylindrical Wall – Measured Strain at 40 Years

Redacted - PAIA section 36(1)(b); PAIA section 37(1)(a)

Total Stresses	Begin of Lifetime		End of Lifetime		LOCA end of Life	
	σ_h	σ_v	σ_h	σ_v	σ_h	σ_v
Materials	[MN/m²]	[MN/m²]	[MN/m²]	[MN/m²]	[MN/m²]	[MN/m²]
Concrete	-12.74	-7.43	-10.23	-5.55	**-2.74**	**-1.70**
Liner	-116.73	-72.09	-240.05	-182.73	-198.99	-160.07
Rebars	-91.94	-37.53	-179.89	-110.02	-146.83	-99.39
Tendons	**1256.00**	**1431.00**	**1129.45**	**1280.14**	**1160.86**	**1290.24**

9.4.3 Cylindrical Wall – Extrapolated Strain at 60 Years

Redacted - PAIA section 36(1)(b); PAIA section 37(1)(a)

Total Stresses	Begin of Lifetime		End of Lifetime		LOCA end of Life	
	σ_h	σ_v	σ_h	σ_v	σ_h	σ_v
Materials	[MN/m²]	[MN/m²]	[MN/m²]	[MN/m²]	[MN/m²]	[MN/m²]
Concrete	-12.74	-7.43	-9.97	-5.38	**-2.47**	**-1.53**
Liner	-116.73	-72.09	-256.03	-196.01	-214.97	-173.35
Rebars	-91.94	-37.53	-191.56	-118.41	-158.50	-107.77
Tendons	**1256.00**	**1431.00**	**1118.36**	**1272.17**	**1149.77**	**1282.27**

Table 20: Summary of the walls TLAA results with in-situ material properties

Final Stress		Begin of Lifetime		End of Lifetime		LOCA end of Life	
Material	Analysis	σ_h	σ_v	σ_h	σ_v	σ_h	σ_v
		MPa	MPa	MPa	MPa	MPa	MPa
Concrete	40a P	-12.7	-7.44	-11.87	-6.75	-4.37	-2.90
	40a M	-12.7	-7.44	-10.23	-5.55	-2.74	-1.70
	60a	-12.7	-7.43	-9.97	-5.38	-2.47	-1.53
Liner	40a P	-116.7	-72.10	-140.64	-90.93	-99.58	-68.26
	40a M	-116.7	-72.10	-240.07	-182.74	-199.01	-160.07
	60a	-116.7	-72.09	-256.03	-196.03	-214.97	-173.37
Rebars	40a P	-91.9	-37.53	-109.69	-49.10	-76.63	-38.46
	40a M	-91.9	-37.53	-179.91	-110.02	-146.85	-99.38
	60a	-91.9	-37.53	-191.56	-118.42	-158.50	-107.79
Tendons	40a P	1256.0	1431.00	1196.14	1338.02	1227.55	1348.12
	40a M	1256.0	1431.00	1129.43	1280.14	1160.84	1290.25
	60a	1256.0	1431.00	1118.36	1272.16	1149.77	1282.26

9.5 Dome Analysis

9.5.1 Dome – Predicted Strain at 40 Years

Redacted - PAIA section 36(1)(b); PAIA section 37(1)(a)

Total Stresses	Begin of Lifetime		End of Lifetime		LOCA end of Life	
	σ_h	σ_v	σ_h	σ_v	σ_h	σ_v
Materials	[MN/m²]	[MN/m²]	[MN/m²]	[MN/m²]	[MN/m²]	[MN/m²]
Concrete	-8.96	-8.96	-7.85	-7.85	**-2.53**	**-2.53**
Liner	-71.35	-71.35	-108.31	-108.31	-78.45	-78.45
Rebars	-48.93	-48.93	-74.27	-74.27	-53.80	-53.80
Tendons	**1 194.0**	**1 194.0**	**1 138.9**	**1 138.9**	**1 158.4**	**1 158.4**

9.5.2 Dome - Measured Strain at 40 Years

Redacted - PAIA section 36(1)(b); PAIA section 37(1)(a)

Total Stresses	Begin of Lifetime		End of Lifetime		LOCA end of Life	
	σ_h	σ_v	σ_h	σ_v	σ_h	σ_v
Materials	[MN/m²]	[MN/m²]	[MN/m²]	[MN/m²]	[MN/m²]	[MN/m²]
Concrete	-8.96	-8.96	-6.17	-6.17	**-0.86**	**-0.86**
Liner	-71.35	-71.35	-181.60	-181.60	-151.75	-151.75
Rebars	-48.93	-48.93	-124.53	-124.53	-104.06	-104.06
Tendons	**1 194.0**	**1 194.0**	**1 091.2**	**1 091.2**	**1 110.6**	**1 110.6**

9.5.3 Dome – Extrapolated Strain at 60Years

Redacted - PAIA section 36(1)(b); PAIA section 37(1)(a)

Total Stresses	Begin of Lifetime		End of Lifetime		LOCA end of Life	
	σ_h	σ_v	σ_h	σ_v	σ_h	σ_v
Materials	[MN/m²]	[MN/m²]	[MN/m²]	[MN/m²]	[MN/m²]	[MN/m²]
Concrete	-9.04	-9.04	-5.87	-5.87	**-0.55**	**-0.55**
Liner	-71.98	-71.98	-195.11	-195.11	-165.25	-165.25
Rebars	-49.36	-49.36	-133.79	-133.79	-113.32	-113.32
Tendons	**1 204.5**	**1 204.5**	**1 082.8**	**1 082.8**	**1 102.2**	**1 102.2**

Table 21: Summary of the dome TLAA results with in-situ material properties

Total Stresses		Begin of Lifetime		End of Lifetime		LOCA end of Life	
Material	Analysis	σ_h	σ_v	σ_h	σ_v	σ_h	σ_v
		MPa	MPa	MPa	MPa	MPa	MPa
Concrete	40a P	-8.96	-8.96	-7.85	-7.85	-2.53	-2.53
	40a M	-8.96	-8.96	-6.17	-6.17	-0.86	-0.86
	60a	-9.04	-9.04	-5.87	-5.87	-0.55	-0.55
Liner	40a P	-71.35	-71.35	-108.31	-108.31	-78.45	-78.45
	40a M	-71.35	-71.35	-181.60	-181.60	-151.75	-151.75
	60a	-71.98	-71.98	-195.11	-195.11	-165.26	-165.26
Rebars	40a P	-48.93	-48.93	-74.27	-74.27	-53.80	-53.80
	40a M	-48.93	-48.93	-124.53	-124.53	-104.06	-104.06
	60a	-49.36	-49.36	-133.79	-133.79	-113.32	-113.32
Tendons	40a P	1194.00	1194.00	1138.93	1138.93	1158.37	1158.37
	40a M	1194.00	1194.00	1091.18	1091.18	1110.63	1110.63
	60a	1204.50	1204.50	1082.79	1082.79	1102.24	1102.24

9.6 Results discussion

The results of the TLAA comparing the initial concrete material properties with the in-situ concrete properties are as follows:

Table 22: Comparison of TLAA results

Location & Time		Compression Stress [MPa] using initial concrete properties		Compression Stress [MPa] using in-situ concrete properties	
		Horizontal	Vertical	Horizontal	Vertical
Cylindrical Walls (P)	40 years	-3.85	-2.56	-4.37	-2.9
Cylindrical Walls (M)	40 years	-2.35	-1.44	-2.74	-1.70
Cylindrical Walls	60 years	-2.10	-1.29	-2.47	-1.53
Dome (P)	40 years	-1.77		-2.53	
Dome (M)	40 years	-0.31		-0.86	
Dome	60 years	-0.05		-0.55	

The in-situ concrete material properties are greater than the initial concrete material properties used in § 7.3. The in-situ values show that the assumptions made during the TLAA were conservative and, although it indicated that both Units are qualified for an additional 20 years of operation, the resultant safety margin during the analysis was initially deemed small. With the refined E_{Mod} and Poisson ratio values, the analysis currently indicates that there is greater margin and confirms that the concrete does not go into any tension during a LOCA pressure up to (and beyond) 60 years of operation.

Figure 61 shows a graphical summary of the TLAA results when using the in-situ concrete material properties. Compared to Figure 46, it is evident that the margin has increased between the Dome stresses and the Tension-Compression Transition.

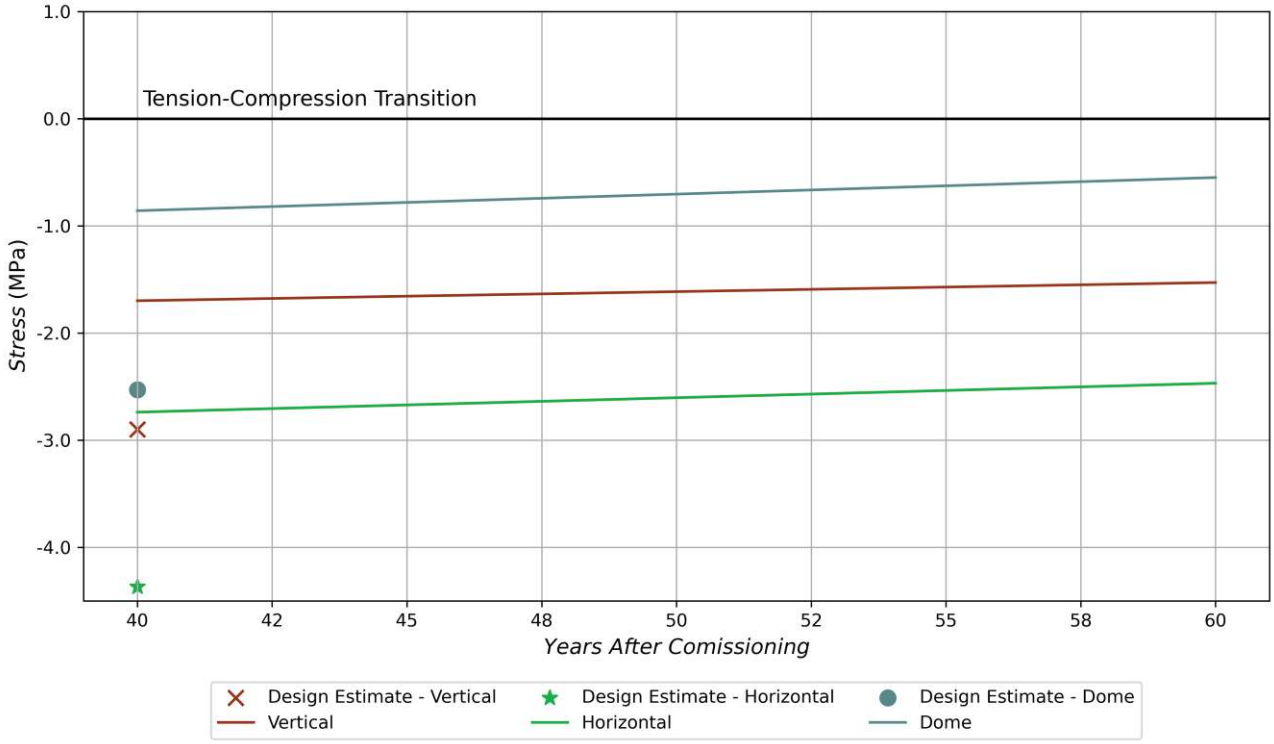

Figure 61: Graphical Summary of TLAA results using in-situ material properties

Furthermore, the analysis was re-performed for both Units and a range of strain data values were used to indicate the upper and lower limit range for the data used. This is provided in Figure 62. The analysis is similar to that which is depicted in Figure 46.

From this analysis, it is concluded that even with more conservative estimates applied to achieve a “Worst-Case”, the design limit is not exceeded. There is a 0.3 MPa margin between the “Worst-Case” for the dome and the Tension-Compression Transition threshold.

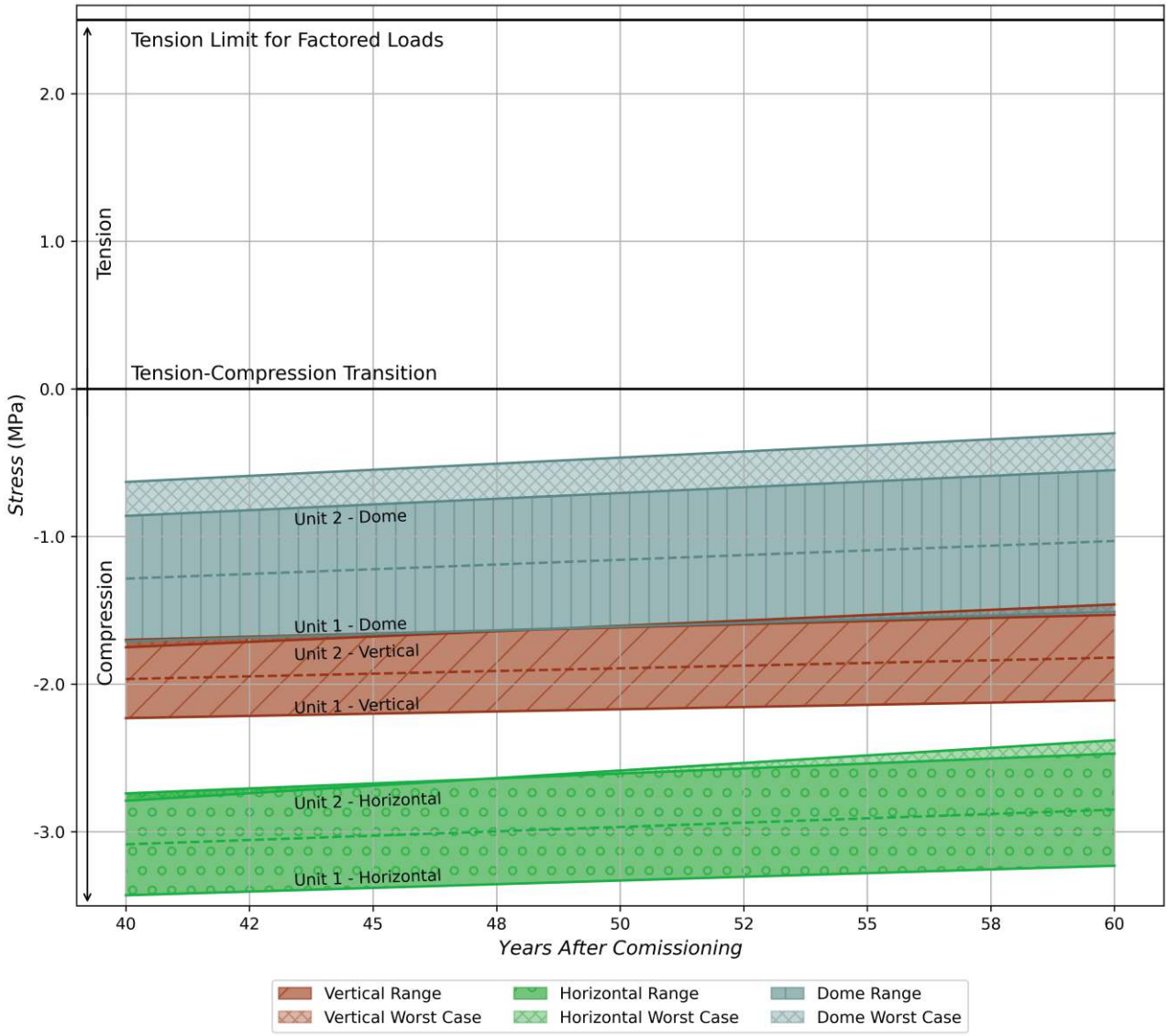

Figure 62: Graphical Summary of TLAA Results for All Sections with in-situ Material Properties

9.6.1 TLAA with most conservative Emod value

The TLAA was reperformed using the most conservative Emod values obtained from the material properties tests of 21.1 GPa for the walls and 22.6 GPa for the domes. This was done to demonstrate and ensure that even with the lowest and most conservative of the in-situ Emod values, there remains sufficient design margin between the 'Worst-Case' and Tension-Compression transition. The use of the most conservative Emod values marginally decreased the design margin, compared to when the average Emod was used. The graphical summary in Figure 62 is recreated in Figure 63 to show the impact of using the most conservative Emod values. It is important to note that there remains sufficient margin, even with the 'Worst-Case', up to and beyond 60 years. There is a 0.16 MPa margin between the "Worst-Case" for the dome and the Tension-Compression transition threshold.

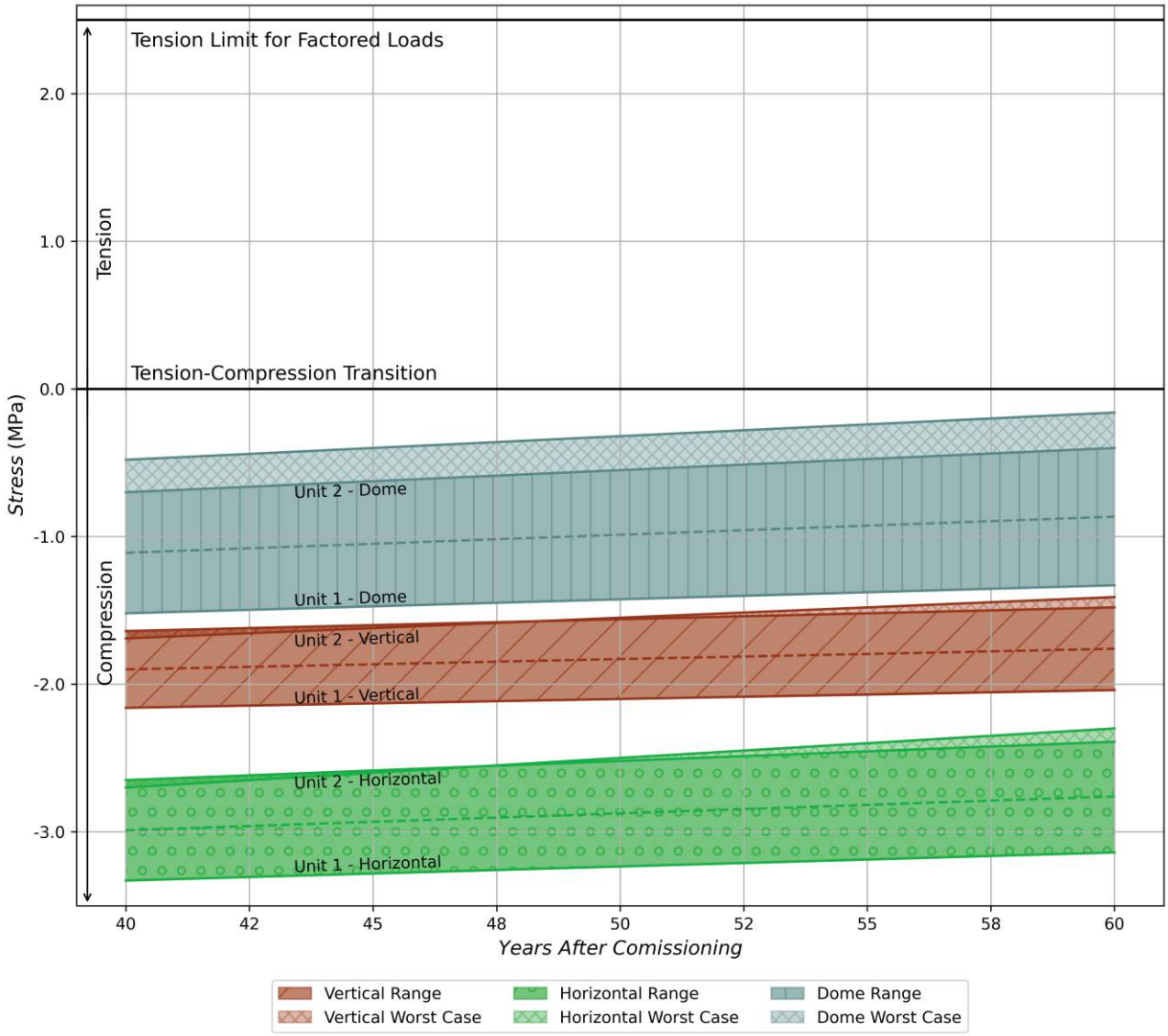

Figure 63: Graphical Summary of TLAA results with most conservative Emod

In summary, the application of both conservative and average in-situ measured values in the revised TLAA assessments remains consistent with the original TLAA calculations and assumptions. The results reaffirm the structural integrity and confirm that the containment buildings maintain sufficient design safety margins to accommodate a further 20 years of service life.

10. EDF Delayed Strain

To further support the TLAA, Eskom requested that EDF to provide Eskom with the range of their containment structures' monitoring data that are similar to Koeberg containment structures. The delayed strain data from the EDF fleet was overlayed with the data of Koeberg as presented in §7.

Eskom only requested the highest and lowest strains for comparative reasons and did not request each individual plants data. The results are provided below:

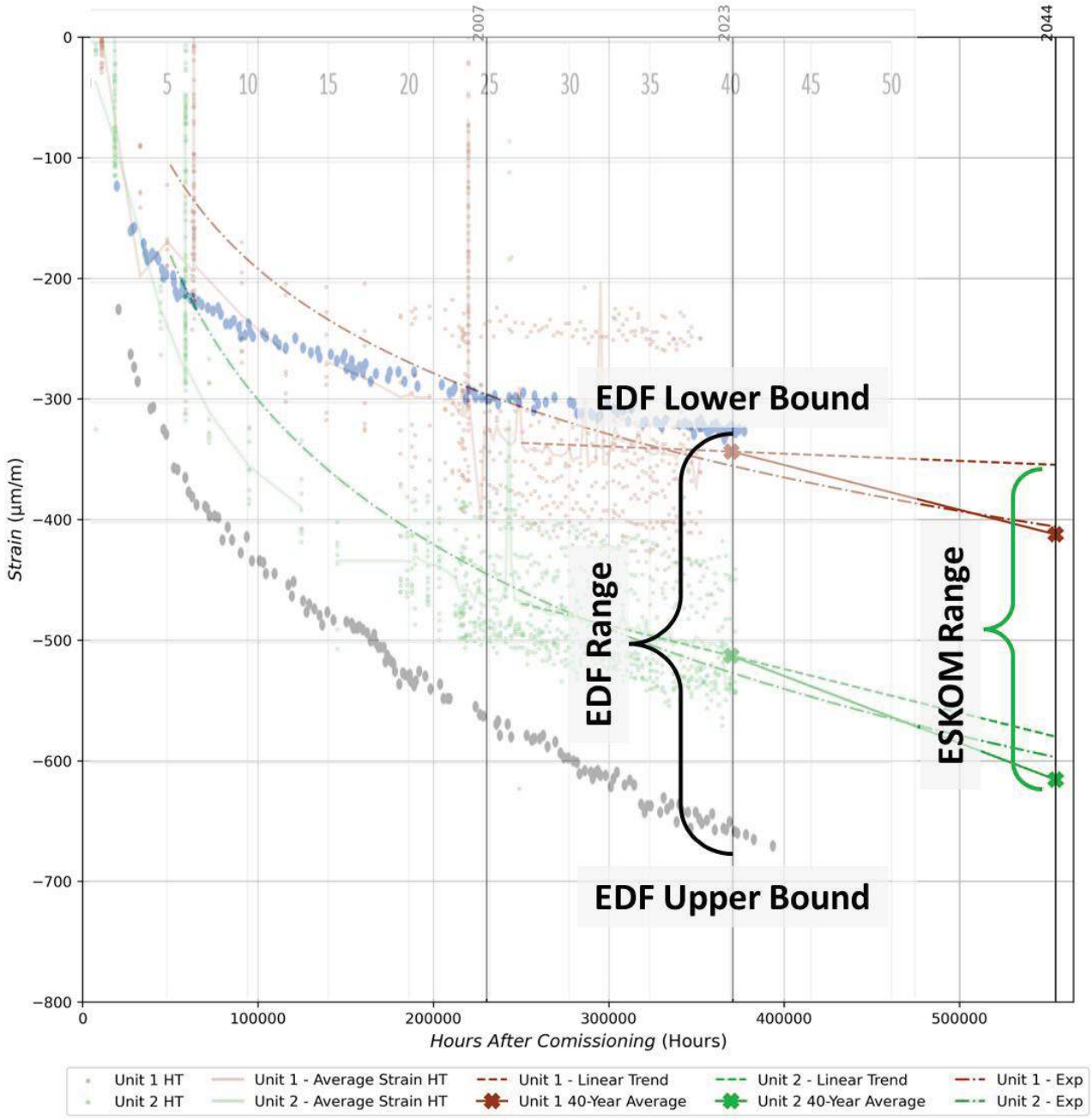

Figure 64: Eskom and EDF Fleet Horizontal Delayed Strain Data

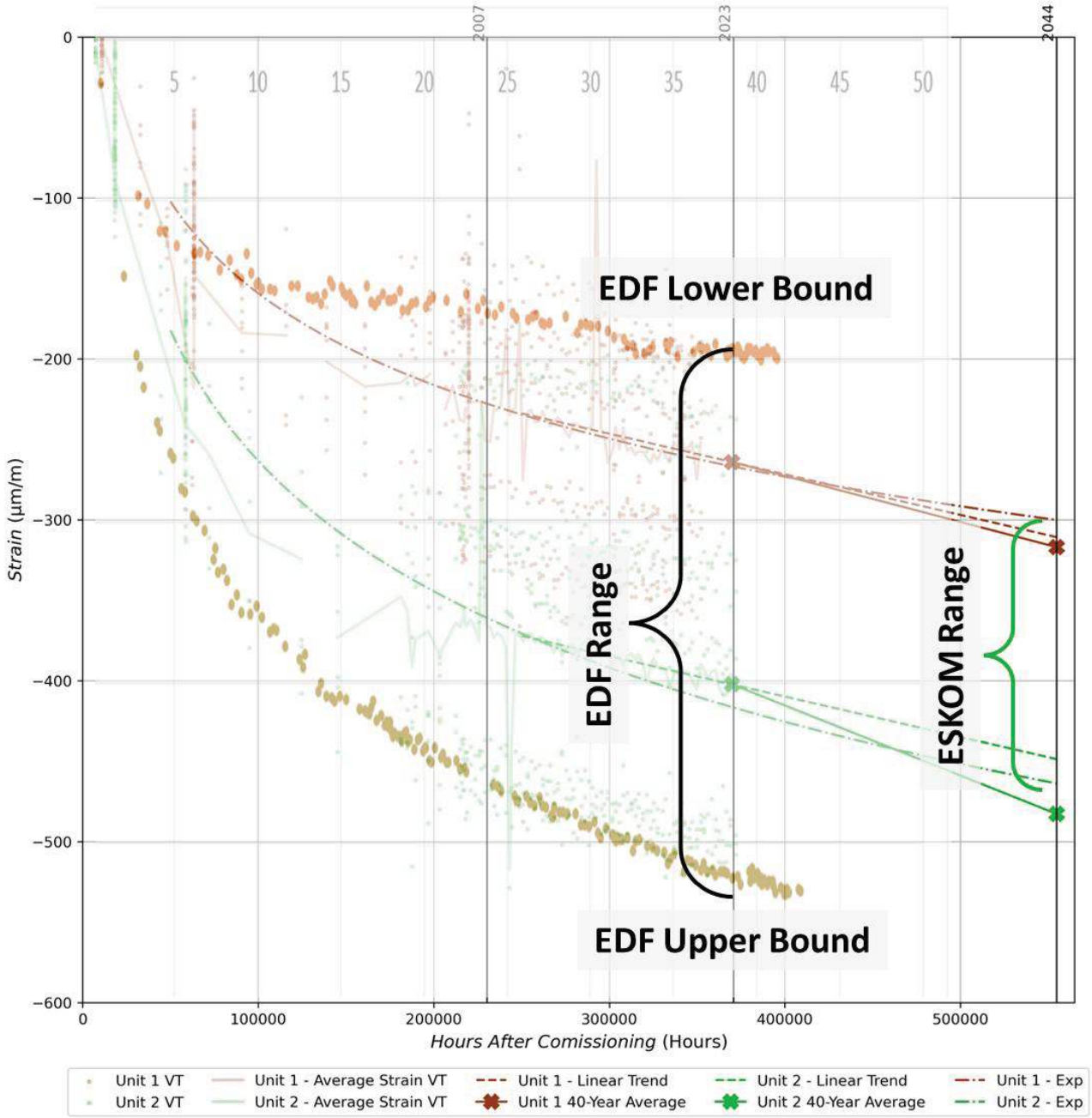

Figure 65: Eskom and EDF Fleet Vertical Delayed Strain Data

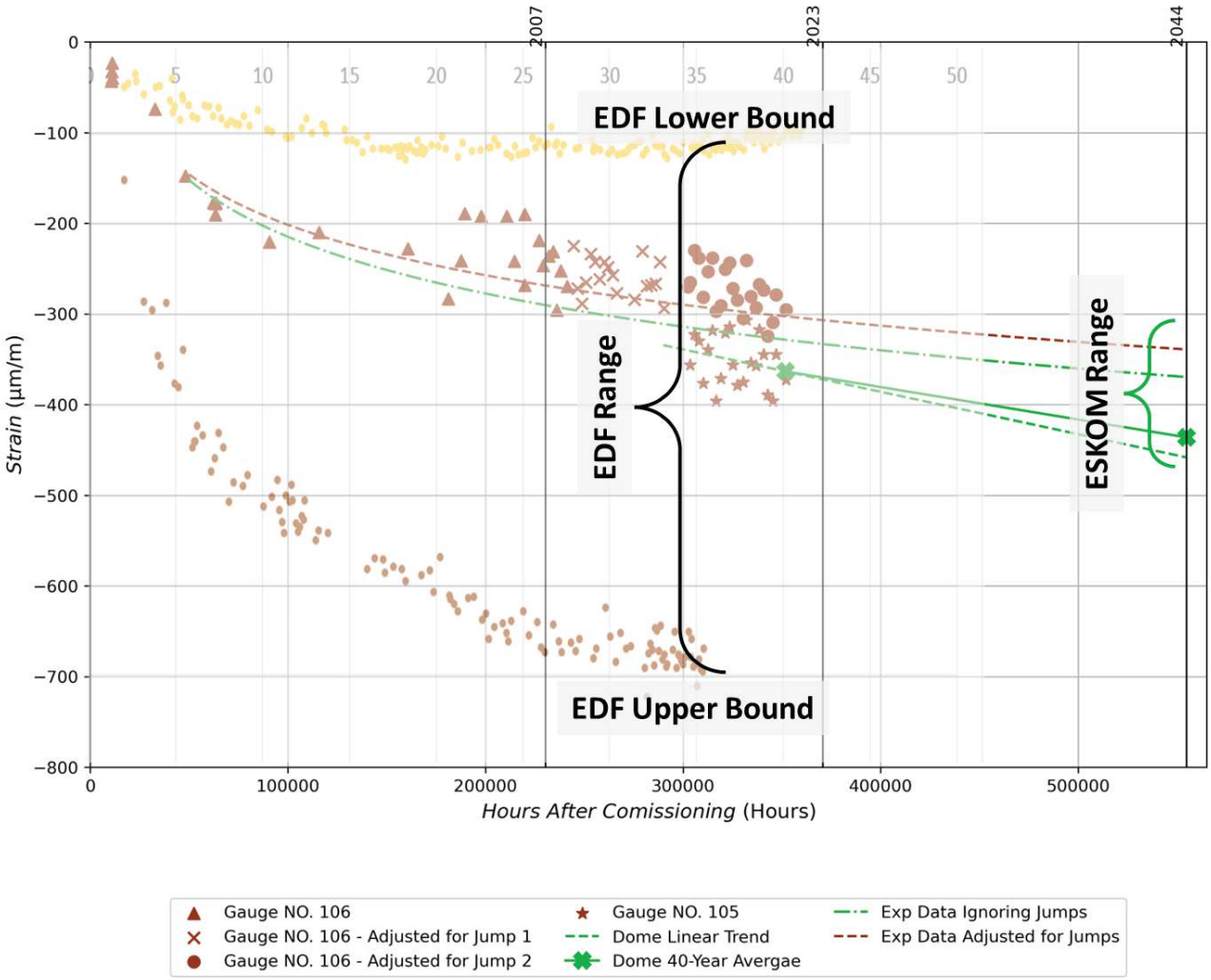

Figure 66: Eskom and EDF Fleet Dome Delayed Strain Data

The data provides confidence in the Koeberg results and indicates that the EDF fleet and Koeberg behaves consistently over time and no concerns about the structural integrity or durability of the Koeberg containment buildings are highlighted by the delayed strain data.

11. Durability

Koeberg is located in a marine environment adjacent to the cold Benguela current of the Atlantic Ocean, roughly 40km north of Cape Town, South Africa. The local environmental conditions at Koeberg (humidity, proximity to the sea, temperature, precipitation patterns, dominant wind etc.) contribute to the highly corrosive conditions and cause severe degradation of the exposed surfaces of the structures at Koeberg. The corrosion mechanism is mainly due to electro-chemical reactions induced by airborne chloride ions.

11.1 Delamination

11.1.1 Causes

Since circa 2000 the reinforced concrete structures at Koeberg have shown signs of degradation. After several studies and investigations, it was identified that chloride induced corrosion is the cause of the delamination.

Chloride ingress attacks the outermost layer of reinforcement and corrodes the steel. The corrosion product has a smaller density compared to steel (i.e., a greater volume for a similar mass) which induces tension forces on the concrete. The concrete, which is weak in tension, then fails and delaminates from the in-situ concrete. The delamination can increase laterally and eventually may spall (fall off the structure). An illustration of the cross section of the containment structures is provided below for a visual context of the delamination and the relative position to the embedded components:

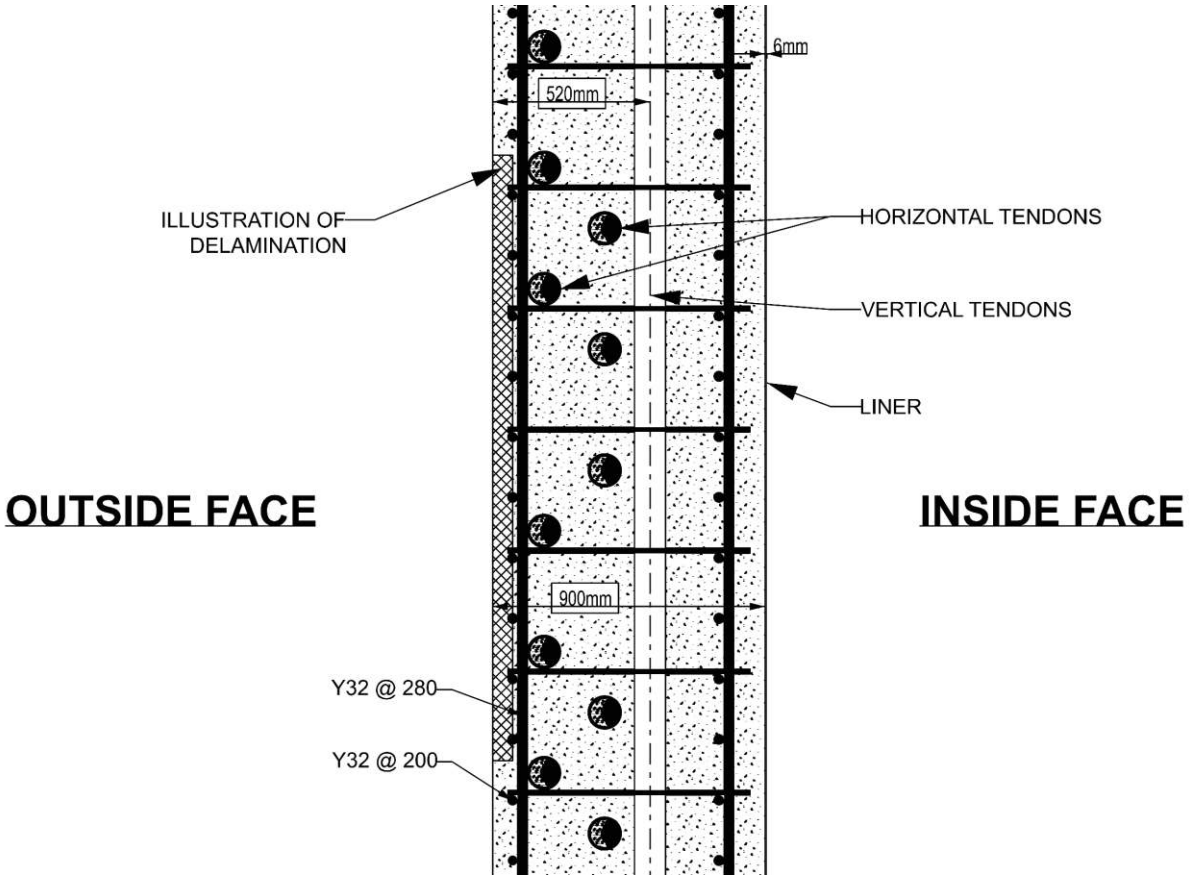

Figure 67: Section of Containment Wall

Note the two layers of horizonal post-tensioning, where the outer layer is closer to the external surface compared to the internal layer and the vertical which is deeper.

The containment structures were subsequently coated (circa 2000) to prevent further chloride ingress; however, the coating has failed. In 2015 a refurbishment project was initiated which repaired each area (or patch) of delamination. These patch repairs considered all the delamination identified at the time and repaired all of it. The delamination repaired circa 2017 is indicated in Figure 68 for Unit 2, while Unit 1 is in a similar condition. The delaminated area constituted 11.54% of the structure's surface. Full concrete repairs of the delaminated areas is planned for quarter 4 of 2025 followed by installation of ICCP on the domes and walls of the containment structures. It should be noted that concrete repairs and implementation of ICCP are ageing management actions aimed at ensuring continued durability of the containment structures during the period of LTO.

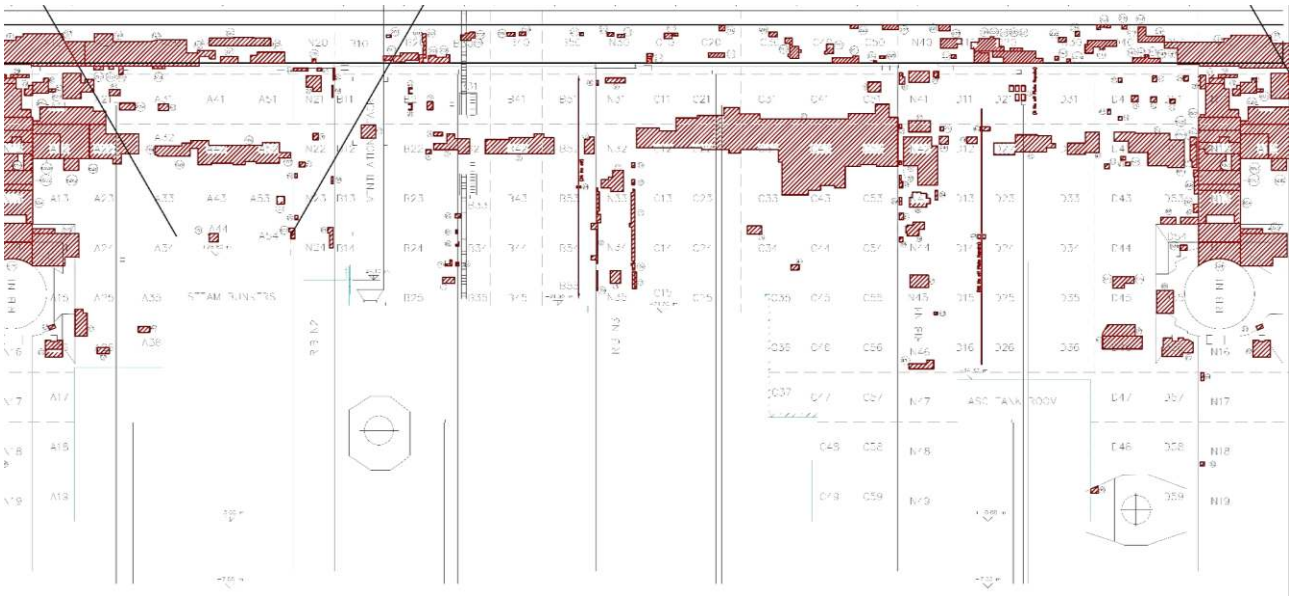

Figure 68: Delamination on 2HRX circa 2017

11.1.2 Consequence

Several investigations were performed to determine the effect of the delamination on the containment structures. The most comprehensive study, which included earthquake, LOCA and ILRT loads, concluded that the surface delamination has minimal impact on the structural performance of the containment structure and that the performance is largely governed by the post tensioning forces [19]. Another study which investigated the effect of the delamination [10] concluded the same, although this study mainly considered LOCA conditions and the effect of delamination on the compressive stress of the concrete, as well as the effect of the loss of a vertical tendon.

It was concluded in the studies that the tendons are the main components of the containment structures and as long as the tendons are protected and integrity is ensured, surface delamination will not affect the safe performance of the containment structures.

From a TLAA re-analysis perspective, the calculations can be repeated with a reduced concrete section. However, that would be counterintuitive, because the compressive stress in the concrete increases with a decreasing cross section (i.e., the concrete goes more into compression) which works in the favour of the compressive requirement for the TLAA for the re-analysis and the sections analysed. Therefore, the calculations are not repeated.

The effect on the reduction on the concrete cross-sectional area results in an increase in the concrete stress (i.e., more compressive) is not considered a concern as the concrete compressive strength is much higher compared to the tensile strength.

It is furthermore important to note that once the concrete has delaminated, compressive stress cannot be regained in the patch repaired. The stress has already redistributed to the remainder of the concrete section and the new patch only protects the steel components from further degradation.

12. Further Considerations

As chloride ingress continuous to occur, delamination will also be expected to continue. Corrosion of the steel reinforcement is continuous until such time that the chemical reaction is arrested either through concrete repairs (where the delamination has already occurred) or the corrosion is arrested by some other means (such as cathodic protection,i.e. ICCP). This issue is expected to be addressed through concrete repairs in the fourth quarter of 2025, followed by the application of a long-term, sustainable corrosion solution in the form of ICCP. Eskom has already advanced the design and secured funding for this initiative.

A patch repair considers the local effects of repaired area. It has been seen that delamination is likely to develop immediately adjacent to the repaired patch due to *incipient anode or ring anode effect* as illustrated in Figure 69. The ring anode effect is where the patching of concrete creates a new anodic area, which is more susceptible to corrosion. Patch repairs effectively address the immediate area of concern, while the ICCP ensures long term durability of the entire structure.

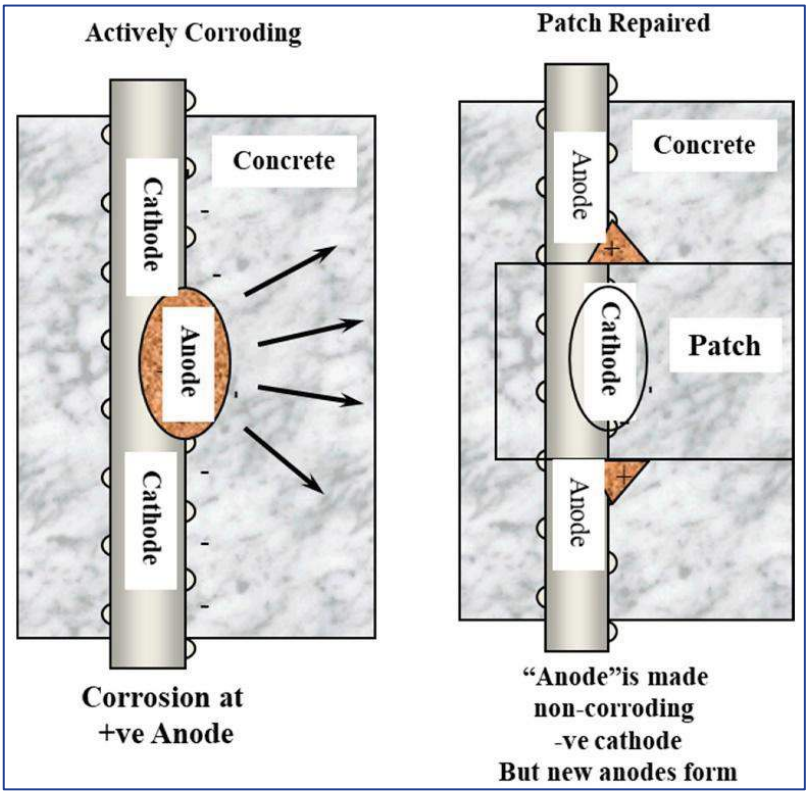

Figure 69: The incipient anode or ring anode effect, where patching creates new anodic corrosion sites around the repair. Ref [12]

12.1 Condition of Tendon Ducts

During the patch repair activities of the reinforced concrete on the containment structures, several tendon ducts were exposed as a result of the intrusive nature of the work to and to investigate the condition of the tendon ducts [20].

The tendon ducts were mostly in a good condition with no to very limited surface corrosion (which was considered to be the original condition when the duct was cast into the concrete [20]) as shown in Figure 70.

Figure 70: Exposed Tendon Duct

Cases of corrosion were identified and it was concluded during investigation [20] that the corroded part of this tendon duct is located in an area where a horizontal and vertical cold joint in the concrete occurred (note the chicken wire mesh used in the cold joint of Figure 71).

Figure 71: Corroded Duct (Cold Joint)

A similar case was identified where a construction joint was identified – see Figure 72.

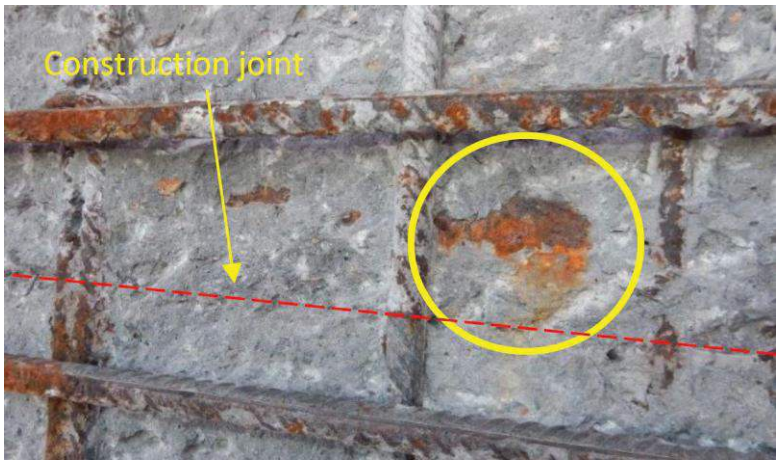

Figure 72: Corroded Duct (Construction Joint)

After further investigation and cleaning of the duct, it was observed that through wall corrosion had occurred in small areas of duct, exposing the grout inside the duct. A sample of concrete directly in contact with the corroded duct was tested and chloride content of 0.35% was measured. In contrast, the chloride content of the grout inside the duct was measured to be 0.06% [20]. For reference, the threshold for corrosion is 0.4% and the 'critical threshold' is 0.8% [17].

The durability of the tendons has therefore not been challenged, even though some investigations have discovered corroded ducts. Further investigation into the durability of the tendons by the responsible engineer did not highlight any concerns, and the identified duct was postulated to be corroded due to its location, relative to a porous construction joint.

12.2 Dome Cracks

12.2.1 Identification

During the ISI routine civil inspections, circumferential dome cracking ("the dome crack") on both Unit 1 and 2 was identified (circa 2010 and 2011 respectively). The dome crack is along the entire circumference of the dome (± 110m) and is located on ± 17.3m radius from the containment centre, as shown in Figure 73, a photo of the crack is also shown in Figure 74.

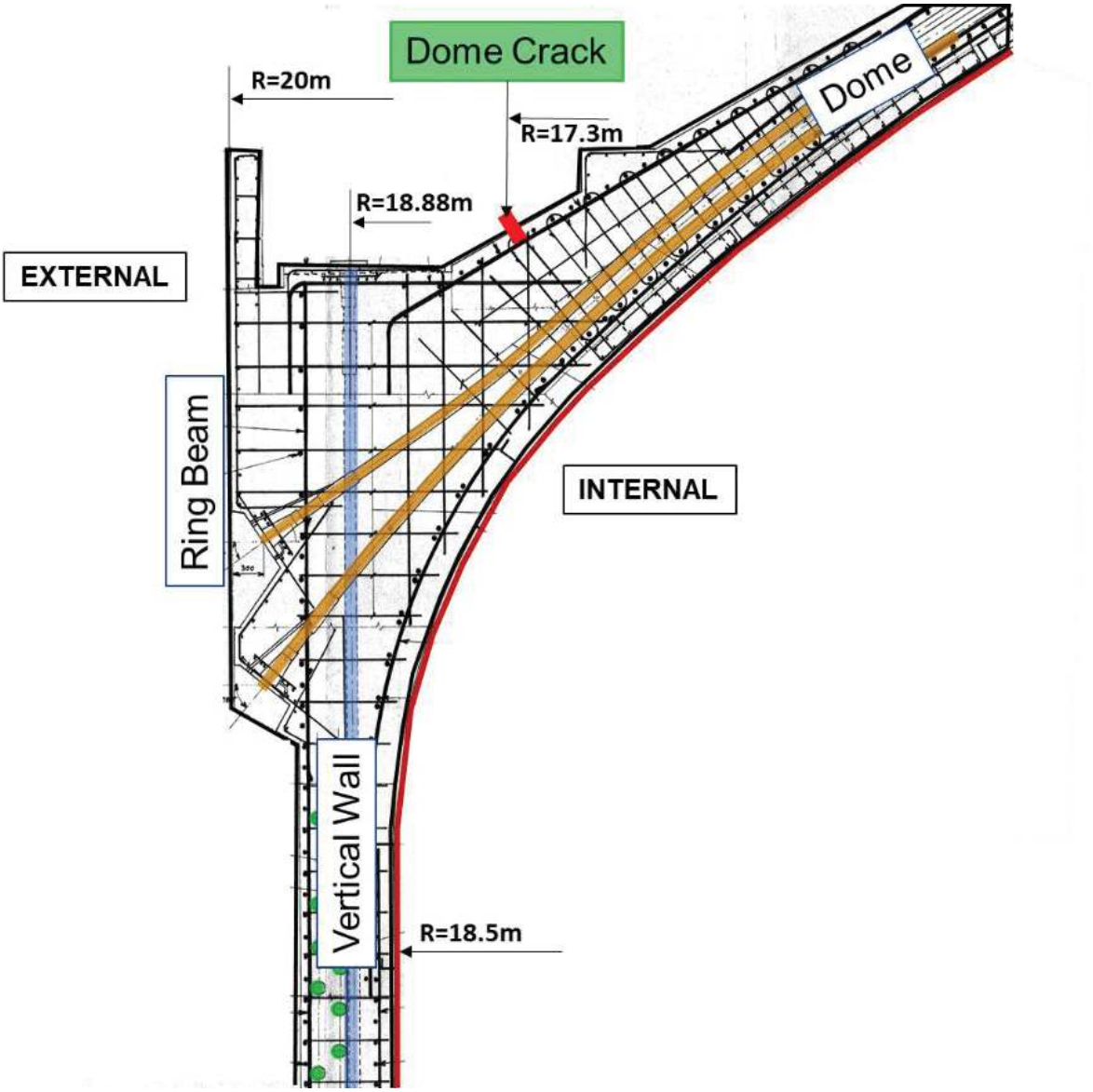

Figure 73: Circumferential Dome Crack

Figure 74: Crack on Domes

12.2.2 Investigation

The dome crack was investigated and measured when it was identified. The measured crack thickness was <0.3mm in width.

Eskom engaged EdF regarding the dome cracks and during March 2014, a team of EdF experts visited Koeberg and conducted an inspection (amongst other activities) of the containment dome. They confirmed to Eskom that the dome crack has also been identified on other similar containment structures. The EdF experts recommended that the cracks be sealed to prevent corrosion of the steel elements inside the concrete. Eskom therefore decided that the cracks will be sealed as part of the containment refurbishment project in 2015.

Prior to the crack sealing, both containment buildings underwent ILRT testing. During the testing and the external monitoring of the containment structures, crack monitoring devices were placed over the dome cracks to monitor the behaviour of the cracks during the ILRT pressurisation. The crack monitoring result is plotted during the pressurization of the ILRT, and the result is presented in Figure 75.

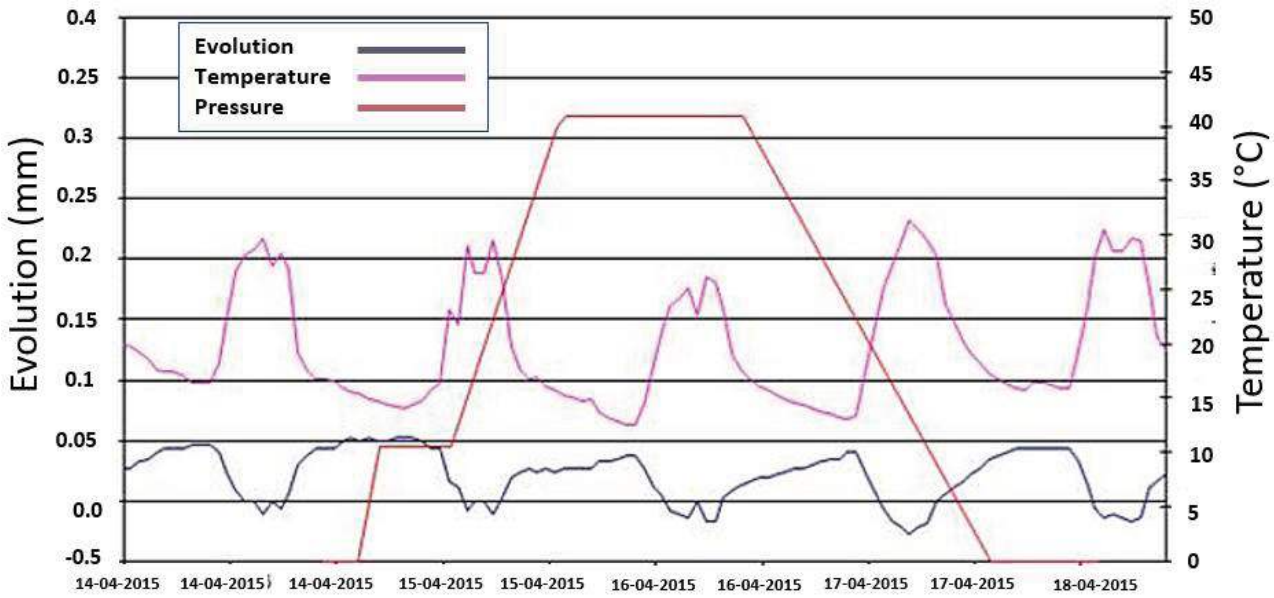

Figure 75: Crack Monitoring During ILRT 121

The result of the crack monitoring indicated that, with an increase in internal pressure, the dome crack did not have a corresponding widening, confirming non-structural. The crack movement, which was observed, correlates inversely proportional to temperature (an increase in temperature leads to a decrease in crack width), indicating that the crack is temperature related.

12.2.3 Repair

After the ILRT tests and as part of the patch repair project, the dome cracks were sealed on both dome structures in accordance with the crack repair specification developed for the dome (reference [10]). A photo of the crack post-repair is provided in Figure 76 (June 2018).

Figure 76: Repaired Crack

12.2.4 Condition Assessment

During Outage 126 on Unit 1, an inspection was performed on the dome of the containment structure (October 2023). The repair of the dome crack has performed well with minor degradation of the coating, as illustrated in Figure 77.

Figure 77: Condition Assessment of Repaired 1 HRX Dome Crack

There is minor delamination, which is adjacent to the crack in some areas, as indicated in Figure 78.

Figure 78: Delamination on Dome, adjacent to dome crack

The delamination adjacent to the crack is most likely due to chloride ingress which occurred naturally in the reinforced concrete or through the crack, prior to the crack being sealed. Regardless, this is to be expected and not a cause for concern and shall be repaired as part of normal maintenance.

12.3 Planned Test – Integrated Leak Rate Test

As part of the Koeberg in-service inspection programme, Eskom performs integrated Leak Rate Tests (ILRT) on the containment structures every 10 years (the previous was performed in 2015). During the ILRT, the internal pressure on the containment structures is increased to 400 kPa to mimic LOCA conditions. The ILRT is being performed in the current outage (Outage 127, in 2025) and Outage 227 for Unit 2.

The primary objective of the ILRT is intended to identify leakage from containment (verification that the leak-tight liner and apertures remain within acceptable leakage rates, based on code requirements). Secondly, it intends to place the containment in a design basis pressurised condition to verify the concrete support structure' behaviour. This aspect does not have clear acceptance criteria and is dependent on comparison of relative containment expansion movement with previous tests and ILRTs of the EDF fleet to indicate overall acceptable behaviour (largely based on Engineering judgement).

12.4 Planned Modification – ICCP and Further Patch Repairs

In 2014-2015 Eskom appointed an expert panel [21] to investigate the degradation of the containment structures and to propose a solution to prolong the useable life of the structures. The expert panel concluded that: "The only available repair method identified which can meet the defined performance criteria for the containment structures is cathodic protection using impressed current." Accordingly, a modification entitled Impressed Current Cathodic Protection System on Unit 1 And Unit 2 Containment Buildings at Koeberg Nuclear Power Station was initiated to install a duly designed Impressed Current Cathodic Protection (ICCP) system on both containment buildings. The ICCP modification is currently in the design phase and the detailed design has been submitted to the NNR for their acceptance.

The following important notes are worth highlighting with respect to ICCP:

1. Design and implementation of a CP system for such important structures should only be undertaken by internationally qualified companies."
2. The ICCP modification is a complex project with numerous variables that may influence the performance of the ICCP on the structures, and the effectiveness of the modification to prevent further reinforcement corrosion. For example, one such variable is the concrete resistivity. A study performed as part of the ICCP investigations indicated that the resistivity of the concrete varies significantly across the structure, due to several reasons, including the difference in the age of the concrete and the age of the patch repairs
3. ICCP is currently envisaged to be installed with a mortar overlay of ±30mm to enclose the cathode (in this case, Titanium mesh) on the containment structure surface.
3. An Integrated Leak Rate Test (ILRT) is scheduled for the planned outages X27 for 2025 on Unit 1 and 2026 on Unit 2. This ILRT requires that the concrete surface be inspected during the pressurisation tests. Accordingly, the ICCP only be installed post the ILRT.
4. The first phase of the ICCP involves repairing the current delaminated concrete followed by installation of the ICCP system.

Importantly, the ICCP and patch repairs do not influence the TLAA and does not change the conclusion of the re-analysis, if the assumptions listed in § 7.4 holds.

12.5 Potential Negative Consequences of ICCP

ICCP will not address the loss of pre-stress forces but will protect the embedded steel components from corrosion during the period of LTO. ICCP is not required as part of the containment re-analysis. The re-assessment is however based on the assumption that the cables do not degrade due to corrosion, and it is assumed that the cables will not corrode.

A potential negative consequence of ICCP is hydrogen embrittlement of the post-tensioning tendons. Hydrogen embrittlement will adequately be addressed through a competent design which considers the limits of voltage applied to the containment structures to ensure hydrogen embrittlement is not a possibility. This is addressed through the design of the ICCP. It therefore has no influence on the TLAA.

ICCP will only address the potential of corrosion of the tendons and act as corrosion protection, therefore preventing their potential degradation due to chloride induced corrosion.

12.6 Planned Modification – Additional Monitoring Devices

The increasing number of non-functioning monitoring devices is a concern. It is clear from the strain data, for example, that the Unit 2 Dome does not have sufficient monitoring equipment. Accordingly, a modification (Upgrade/replacement of the Defective Containment Monitoring Equipment) was approved for initiation by Eskom. This modification is planned for implementation in X29 to supplement and eventually supersede the current containment online monitoring equipment.

As an interim bridging strategy, Eskom is currently installing additional modern online monitoring equipment in the form of externally mounted Vibrating Wire Strain Gauges (VWSGs) and Optical Fibres on the domes and walls of the containment buildings prior to X27 ILRTs outages, in efforts to supplement the existing EAU system and to improve the quality of the monitoring data. The information obtained from the bridging strategy shall be used as an input data into the feasibility studies.

Furthermore, the following requirements are prescribed to a modification (which is currently in pre-feasibility stage) by the Responsible Engineer:

- **For each Dome –** 10 strain gauges shall be installed with associated thermocouples (if required by the type of strain gauge installed. The strain gauges shall be placed on the axis of the invar wire and pendulum stations, midway between the dome apex and circumference. This shall account for four locations with two strain gauges each: radial and tangential, accounting for eight gauges. The remaining two gauges shall be placed as close as practical to the dome's apex.
- It is recommended that crack monitoring devices be installed at (minimum) four locations around the dome circumferential crack.
- **For each cylindrical wall –** An additional 24 strain gauges shall be installed across the external façade of both containment structures. Two strain gauges shall be placed at 12 locations, corresponding to the anchor points of the pendulums: longitudinal and tangential, respectively.

It is noted that retrofitting monitoring devices pose complex challenges, and it might be difficult to measure the actual strain of the old concrete, as is the intent of adding new strain gauges. It is impossible to measure the current strain of the concrete with new devices, and the installation date will essentially be a new datum, which can supplement monitoring in the future.

Therefore, the feasibility study, which will form the basis of the modification referred to earlier, is recommended to investigate the practicality of installing external monitoring devices and the possibility of utilising new technologies such as fibre optic sensors.

13. Conclusion

The IAEA SALTO process required the revalidation of the containment structures in accordance with established standards and principles to demonstrate that it is safe for continued operation for an additional 20 years. The revalidation used the embedded strain gauges and confirmed that the containment buildings met the safety criteria for 60 years of operation.

A comparison with the EDF fleet of containment buildings showed that the Koeberg and the EDF fleet are comparable behave consistently over time and there are no concerns about the integrity of the Koeberg containment buildings.

To further substantiate the assumptions and refine the calculations, cross-validation using strain values obtained from the 3rd ILRT (2015) was performed. The revalidation confirmed the initial conclusion that the containment buildings are safe for an additional 20 years, and the results demonstrated that the initial analysis was conservative, as the updated analysis showed an increased design safety margin exists.

In addition, to further demonstrate the robustness of the calculations, in-situ containment concrete samples were taken to determine the material properties used in the calculations. The results of the in-situ testing confirmed that the original assumed concrete material property values were conservative. It also confirmed that the concrete material properties were consistent between Unit 1 and Unit 2. Furthermore, the material test results were used to refine the revalidation calculations, which resulted in a higher design safety margin.

Therefore, the re-analysis verifies that the containment structures meet the safety criteria and will remain in compression for the full period of LTO including during the unlikely event of a LOCA.

An in-service inspection, maintenance and monitoring programme for the containment buildings is implemented to ensure that the containment buildings remain in good condition and potential deterioration is detected for recovery actions in a timely manner. Refurbishment of the online containment monitoring system have been completed in 2023 and 2024 to support the monitoring and inspection programme.

Repairs to address concrete spalling continue and installation of the ICCP system as the long-term sustainable ageing management solution for the containment structures will follow during the planned period of LTO. An advanced online monitoring system, i.e., optical fibre and vibrating wire strain gauges are currently being installed on the containment building to enhance the monitoring capability.

14. Acceptance

This document has been seen and accepted by:

Name	Designation
A Maumela	System Engineer
B Oaker	Engineering Consultant
DT Malale	LTO Project Engineering Manager

15. Revisions

Date	Rev.	Compiler	Remarks
July 2025	4	N Behardien	Additional section incorporated to assess the impact of revised TLAA calculations on the overall safety margin using the most conservative values from the measured in-situ data. Inclusion of additional Dynamometer data from 2023 to 2025, post-calibration.
June 2025	3	N Behardien	Inclusion of: • Information on additional material testing. • A comprehensive review to ensure accuracy and to clarify Section 7, TLAA 301, while confirming that the remaining chapters serve to support this section.
May 2025	2	N Behardien	Addition of 3 sections: 8. TLAA with in-situ Concrete Material Properties 9. TLAA with 3rd ILRT's data 10. EDF Delayed Strain Update 'Next Review Date' after x27 Outage
June 2024	1b	SJ Venter	Inclusion of 'Next Review Date' after Outage 127 ILRT Expanded on objective of ILRT
March 2024	1a	SJ Venter	Minor Update per NNR comments, letter k29772N: • Addition of Appendix B and Appendix C • Additions and changes to the Symbols Table • Addition of "SIT" to Abbreviations
November 2023	1	SJ Venter	First Compilation

16. Development Team

- N/A

17. Acknowledgements

Emuel Venter Previous Responsible Engineer and initial compiler of the document (331-691 Rev1b).

Emeritus Professor JA Wium for his contribution and review of the document (331-691 Rev.1).

Appendix A – Full List of all Installed Strain Gauges

Unit	Name	Orientation	Plan	Level (m)	Axis (Gr)
1	No. 1	HR	B3	-9.48	0
1	No. 2	HT	B3	-9.48	0
1	No. 3	HR	C3	-7.5	0
1	No. 4	HT	C3	-7.5	0
1	No. 5	HR	E3	-5	0
1	No. 6	HT	E3	-5	0
1	No. 7	VT	F3 E	-4.25	0
1	No. 8	HT	F3 E	-4.25	0
1	No. 9	VT	F7 E	-4.25	0
1	No. 10	HT	F7 E	-4.25	0
1	No. 11	VT	H3 I	-0.25	300
1	No. 12	HT	H3 I	-0.25	300
1	No. 13	VT	H7 E	-0.25	300
1	No. 14	HT	H7 E	-0.25	300
1	No. 15	HR	B4	-9.48	100
1	No. 16	HT	B4	-9.48	100
1	No. 17	HR	C4	-7.5	100
1	No. 18	HT	C4	-7.5	100
1	No. 19	HR	E4	-5	100
1	No. 20	HT	E4	-5	100
1	No. 21	VT	F8 E	-4.25	100
1	No. 22	HT	F8 E	-4.25	100

Unit	Name	Orientation	Plan	Level (m)	Axis (Gr)
1	No. 23	VT	H4 I	-0.25	100
1	No. 24	HT	H4 I	-0.25	100
1	No. 25	VT	H8 E	-0.25	100
1	No. 26	HT	H8 E	-0.25	100
1	No. 27	HR	B1	-9.5	200
1	No. 28	HT	B1	-9.5	200
1	No. 29	HR	C1	-7.5	200
1	No. 30	HT	C1	-7.5	200
1	No. 31	HR	E1	-5	200
1	No. 32	HT	E1	-5	200
1	No. 33	HR	B5	-9.5	Centre
1	No. 34	HT	B5	-9.5	Centre
1	No. 35	HR	C5	-7.5	Centre
1	No. 36	HT	C5	-7.5	Centre
1	No. 37	HR	E5	-3.85	Centre
1	No. 38	HT	E5	-3.85	Centre
1	No. 39	VT	F1 E	-4.25	200
1	No. 40	HT	F1 E	-4.25	200
1	No. 41	VT	F5 E	-4.25	200
1	No. 42	HT	F5 E	-4.25	200
1	No. 43	VT	H1 I	-0.25	200
1	No. 44	HT	H1 I	-0.25	200

Unit	Name	Orientation	Plan	Level (m)	Axis (Gr)
1	No. 45	VT	H5 E	-0.25	200
1	No. 46	HT	H5 E	-0.25	200
1	No. 47	HR	B2	-9.48	300
1	No. 48	HT	B2	-9.48	300
1	No. 49	HR	C2	-7.5	300
1	No. 50	HT	C2	-7.5	300
1	No. 51	HR	E2	-5	300
1	No. 52	HT	E2	-5	300
1	No. 53	VT	F2 E	-4.25	300
1	No. 54	HT	F2 E	-4.25	300
1	No. 55	VT	F6 E	-4.25	300
1	No. 56	HT	F6 E	-4.25	300
1	No. 57	VT	H2 I	-0.25	300
1	No. 58	HT	H2 I	-0.25	300
1	No. 59	VT	H6 E	-0.25	270
1	No. 60	HT	H6 E	-0.25	270
1	No. 61	HT	I3 I	22.89	41
1	No. 62	VT	I3 I	22.89	41
1	No. 63	HT	I7 E	22.89	41
1	No. 64	VT	I7 E	22.89	41
1	No. 65	HT	I4 I	22.89	141
1	No. 66	VT	I4 I	22.89	141
1	No. 67	HT	I8 E	22.89	141
1	No. 68	VT	I8 E	22.89	141
1	No. 69	HT	I1 I	22.89	241
1	No. 70	VT	I1 I	22.89	241
1	No. 71	HT	I5 E	22.89	241
1	No. 72	VT	I5 E	22.89	241
1	No. 73	HT	I2 I	22.89	341
1	No. 74	VT	I2 I	22.89	341
1	No. 75	HT	I6 E	22.89	341
1	No. 76	VT	I6 E	22.89	341
1	No. 77	VT	J4	45.6	239
1	No. 78	HT	J4	45.6	239
1	No. 79	VT	J3	45.6	239
1	No. 80	HT	J3	45.6	239
1	No. 81	VT	J2	45.6	272
1	No. 82	HT	J2	45.6	272
1	No. 83	VT	J1	45.6	272
1	No. 84	HT	J1	45.6	272
1	No. 85	HT	K4	48.8	239
1	No. 86	VT	K3	47.8	239

Unit	Name	Orientation	Plan	Level (m)	Axis (Gr)
1	No. 87	HT	K3	47.8	239
1	No. 88	HT	K2	48.8	272
1	No. 89	VT	K1	47.8	272
1	No. 90	HT	K1	47.8	272
1	No. 91	HR	N1	49.8	239
1	No. 92	HT	N1	49.8	239
1	No. 93	HR	N4	49.8	272
1	No. 94	HT	N4	49.8	272
1	No. 95	HR	N2	50	239
1	No. 96	HT	N2	50	239
1	No. 97	HR	N3	50.7	239
1	No. 98	HT	N3	50.7	239
1	No. 99	HR	N5	50	272
1	No. 100	HT	N5	50	272
1	No. 101	HR	N6	50.7	272
1	No. 102	HT	N6	50.7	272
1	No. 103	HT	J1*	56.58	340
1	No. 104	HR	J1*	56.58	340
1	No. 105	HT	J2*	56.58	340
1	No. 106	HR	J2*	56.58	340
2	No. 1	HT	J1 E	56	300
2	No. 2	HR	J1 E	56	300
2	No. 3	HT	J2 I	56	300
2	No. 4	HR	J2 I	56	300
2	No. 5	HT	I3	22.89	10
2	No. 6	VT	I3	22.89	10
2	No. 7	HT	I7	22.89	10
2	No. 8	VT	I7	22.89	10
2	No. 9	HT	I4	22.89	110
2	No. 10	VT	I4	22.89	110
2	No. 11	HT	I8	22.89	110
2	No. 12	VT	I8	22.89	110
2	No. 13	HT	I1	22.89	209
2	No. 14	VT	I1	22.89	209
2	No. 15	HT	I5	22.89	209
2	No. 16	VT	I5	22.89	209
2	No. 17	HT	I2	22.89	311
2	No. 18	VT	I2	22.89	311
2	No. 19	HT	I6	22.89	311
2	No. 20	VT	I6	22.89	311
2	No. 21	VT	G5 E	10.45	220
2	No. 22	VT	G6 I	10.45	220

Unit	Name	Orientation	Plan	Level (m)	Axis (Gr)
2	No. 23	VT	G7 E	11.08	227
2	No. 24	HT	G7 E	11.08	227
2	No. 25	HT	G8 I	11.08	227
2	No. 26	VT	G8 I	11.08	227
2	No. 27	HT	G9 E	12.95	227
2	No. 28	VT	G9 E	12.95	227
2	No. 29	HT	G10 I	12.95	227
2	No. 30	VT	G10 I	12.95	227
2	No. 31	HT	G1 E	9.14	215
2	No. 32	VT	G1 E	9.14	215
2	No. 33	HT	G2 I	9.14	215
2	No. 34	VT	G2 I	9.14	215
2	No. 35	HT	G3 E	9.14	210
2	No. 36	VT	G3 E	9.14	210
2	No. 37	HT	G4 I	9.14	210
2	No. 38	VT	G4 I	9.14	210
2	No. 39	HT	D5 E	12.45	378
2	No. 40	HT	D6 I	12.45	378
2	No. 41	HT	D7 E	3.05	377
2	No. 42	VT	D7 E	3.05	377

Unit	Name	Orientation	Plan	Level (m)	Axis (Gr)
2	No. 43	HT	D8 I	3.05	377
2	No. 44	VT	D8 I	3.05	377
2	No. 45	HT	D9 E	4.25	377
2	No. 46	VT	D9 E	4.25	377
2	No. 47	HT	D10 I	4.25	377
2	No. 48	VT	D10 I	4.25	377
2	No. 49	HT	D1 E	1.15	380
2	No. 50	VT	D1 E	1.15	380
2	No. 51	HT	D2 I	1.15	380
2	No. 52	VT	D2 I	1.15	380
2	No. 53	HT	D3 E	1.15	389
2	No. 54	VT	D3 E	1.15	389
2	No. 55	HT	D4 I	1.15	389
2	No. 56	VT	D4 I	1.15	389
2	No. 57	HR	B1	-9.5	Centre
2	No. 58	HT	B1	-9.5	Centre
2	No. 59	HR	C1	-7.5	Centre
2	No. 60	HT	C1	-7.5	Centre
2	No. 61	HR	E1	-4.25	Centre
2	No. 62	HT	E1	-4.25	Centre

Appendix B – Containment On-line Monitoring (Invar and Pendulum Wires)

As an appendix to the TLAA the Containment On-line Monitoring of the Invar and Pendulum Wires is discussed in more detail, and for completeness of the TLAA, appended to the report.

B.1 Invar Wire Monitoring

B.1.1 Available Data

The invar wire monitoring data recommenced in 2009Q2, although four of the eight invar wires did not provide readings. From 2009Q3 to 2011Q2, seven of the eight invar wires were producing readings after intervention (only IV4 on unit 2 provided could not be read) and during 2011Q3 and Q4 IV3 on unit 1 also failed. During 2012Q1 all the devices were reinstated and were monitored, although soon after in 2012Q2 IV1 on unit 1 and IV3 on unit 2 failed. This condition prevailed until 2014Q2 when all the instrumentation were reinstated. During 2015Q1 all the unit 1 instrumentation were refurbished and during 2015Q3 unit 2 was refurbished. Thereafter, the invar wires have consistently been monitored.

It is important to note that the issue with the invar wires is the loss of the datum or reference from commissioning. The ‘acceptance criteria’ has been at the discretion of the Responsible Engineer who has not highlighted deviations. Any concerns with respect to the invar wire data has been either the lack of data prior to 2009 or could be attributed to local failure or degradation of the invar wire devices, wires, brackets, PVC ducts, etc.

The available, raw data (at the time of compiling the response) from the Invar Wire monitoring is provided below in Figure B 1 for illustration (refer to the official inspection reports for a comprehensive summary of the respective periodical readings).

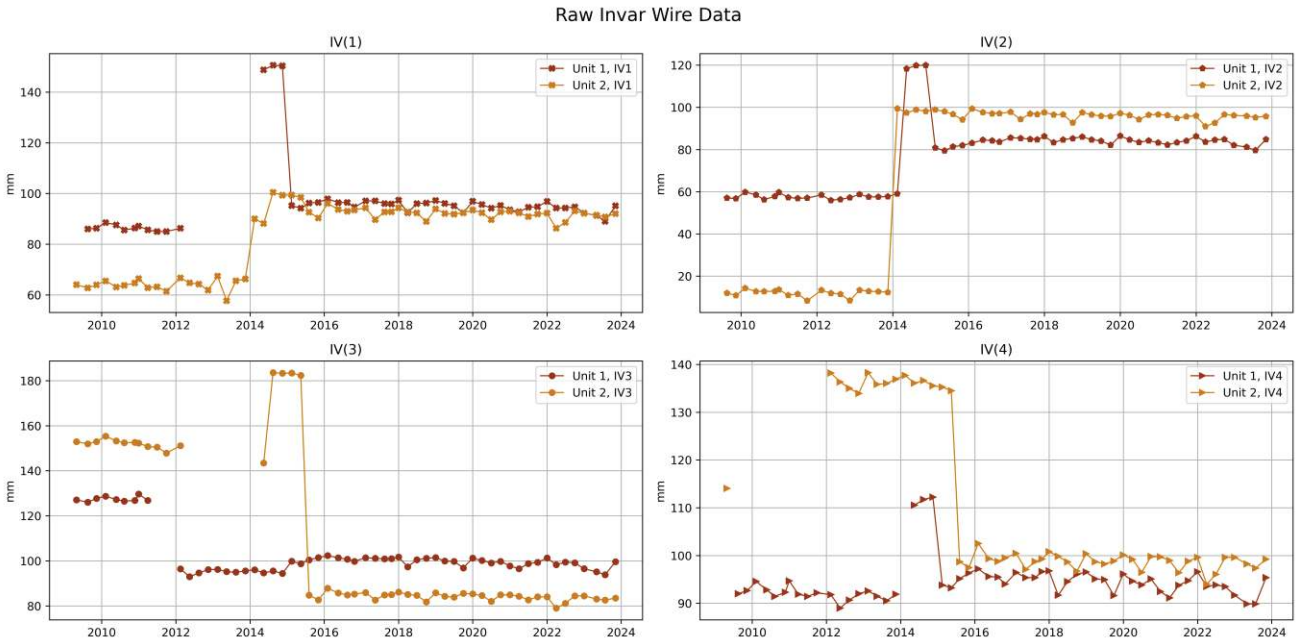

Figure B 1: Available Invar Wire data from 2009Q2

To analyse the data holistically, the data may be adjusted to the average for the period where readings were available. E.g., consider IV(2) unit 1. From circa 2009-2014 the average is ≈ 60mm, for 2014, average ≈ 120 and from 2015 onward the average is ≈ 80. For each of these periods, the corresponding readings are reduced by the specific average. The result is provided below:

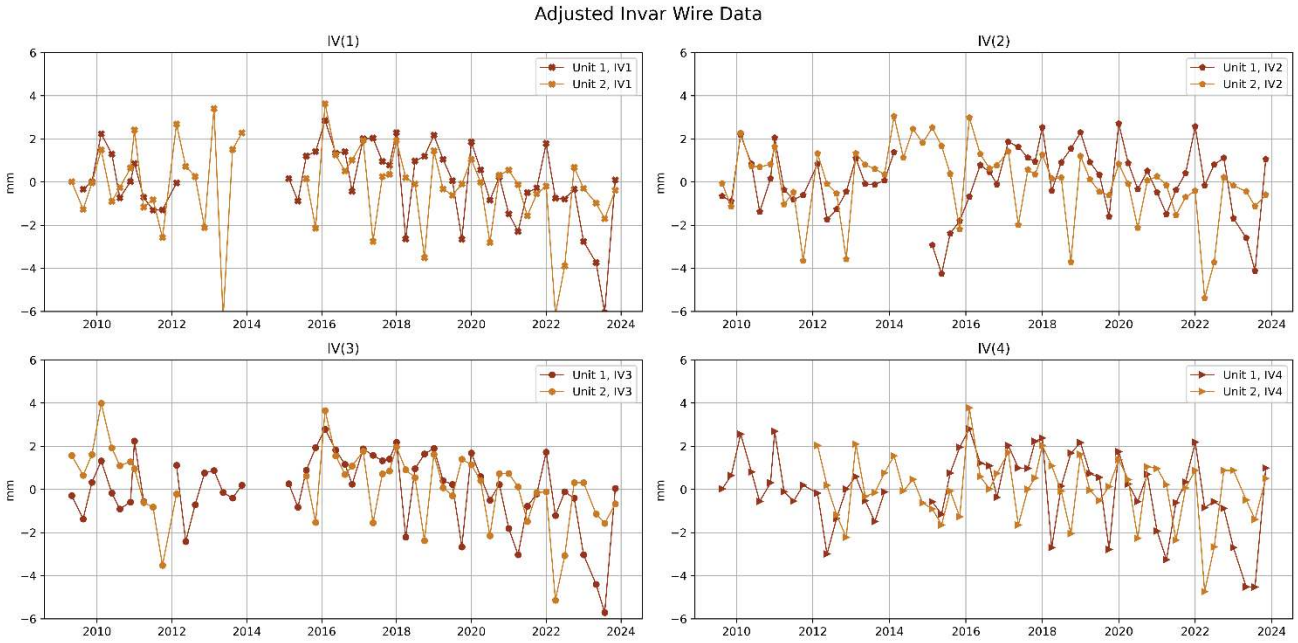

Figure B 2: Adjusted Invar Wire Data

B.1.2 Fibre Optic measurements

From 2015Q3 to 2017Q3 Eskom, in partnership with EPRI, installed a fibre optic cable system on the 2HRX structure. The initial intent of the fibre optic monitoring system was to determine the effectiveness of the monitoring during the 2HRX ILRT which was performed in November 2015, and the fibre optic cable was installed adjacent to the invar wire P4.

The result of the monitoring results from the fibre optic measurements from installation until after the ILRT is provided below:

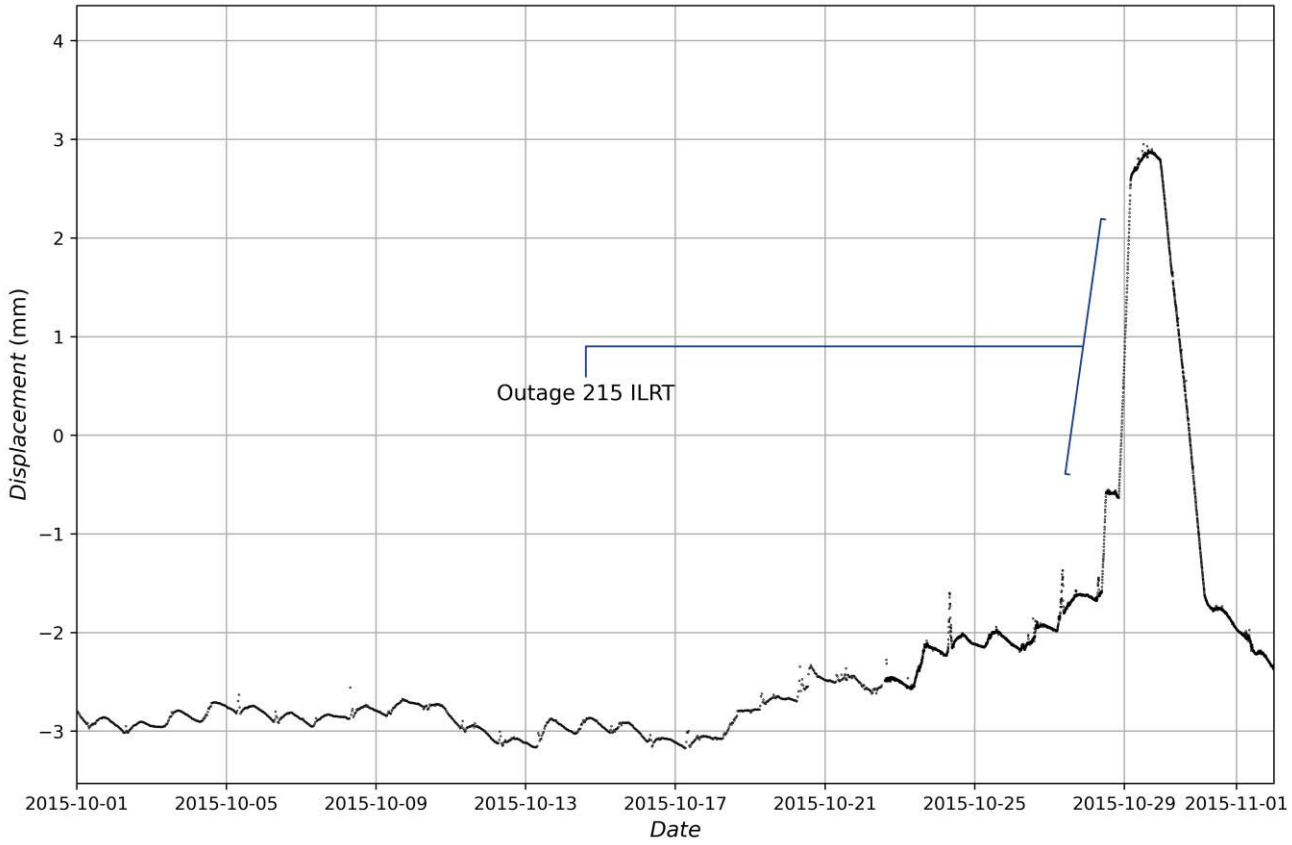

Figure B 3: Fibre Optic Results from 2HRX ILRT, 2015

All the data from the fibre optic can be shown, and compared to the Invar Wire IV4, as shown in Figure B 3. On the figure below, summer and winter peaks are indicated as well as times where the fibre optic unit was not measuring any data. The invar and fibre optic instrumentation do not share a datum, and therefore the data is adjusted vertically, but not manipulated, to show the correspondence in the shape of the respective instrumentation.

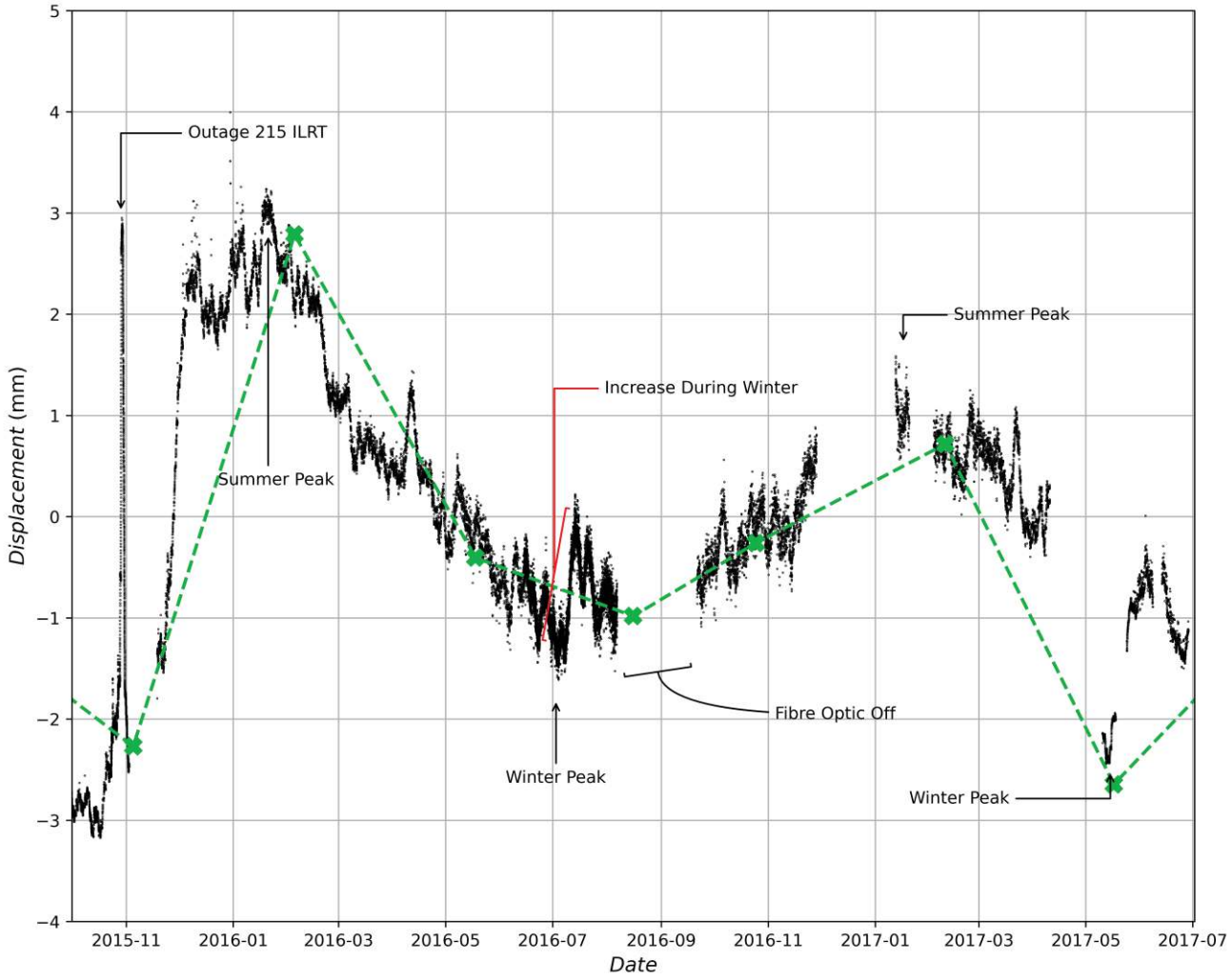

Figure B 4: Fibre Optic and Unit 2 IV4 Data

The Fibre Optic data and the Invar Wire data corresponded well. The increased frequency of the fibre optic measuring device also provided a much better overview of the behaviour of the structure, albeit at a single area. For example, the day-to-day temperature effects of on the structure is clearly observable:

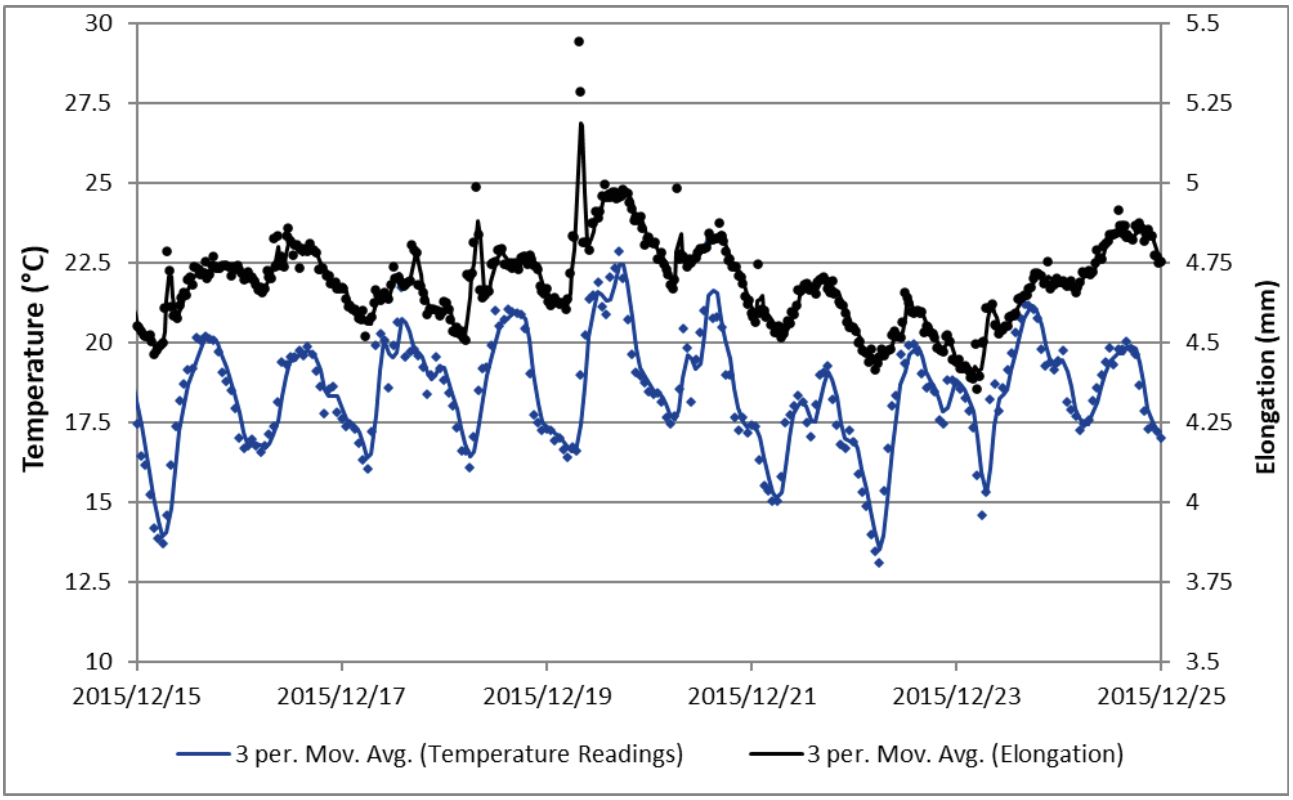

Figure B 5: Fibre Optic and Temperature Readings

Changes in elongation of more than **0.25 mm** can be observed in Figure B 5 in a single day which correlates very well with the change in temperature measurements.

From Figure B 4 the difference between the 2016 (January) summer peak and the 2017 winter measurement is ≈ **6 mm**.

During the winter of 2016, there was also an increase in almost **1.5 mm** over a short period. This illustrates the variability which can be expected in the measurements due to environmental influences, specifically with a quarterly measurement frequency.

B.1.3 Analysis of Invar Wire Measurements

The adjusted data (as discussed in § *B.1.1* Available Data) can be considered overtime and a linear regression of the data performed to develop long-term estimates for the change in the vertical elongation of the containment structures. This is provided in Figure B 6.

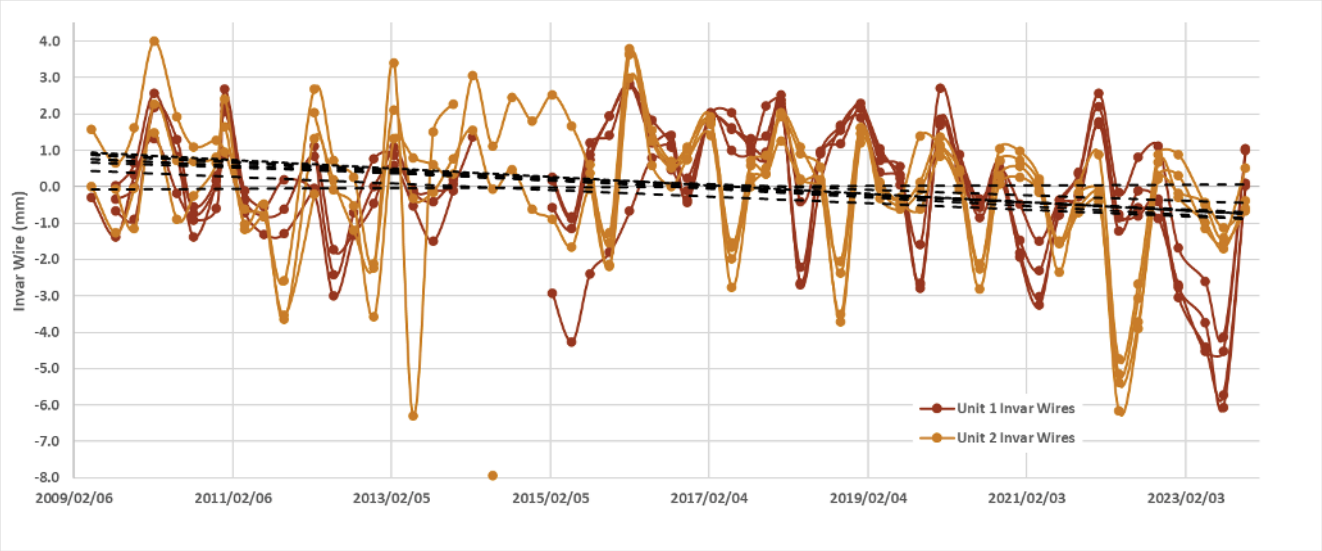

Figure B 6: Linear Regression of All Invar Wire Readings

The slope of the linear regression lines varies as summarized below:

Table B 1: Linear Regression Analysis of Invar Wire Data

Instrument	Unit 1 (mm/y)	R^2	Unit 2 (mm/y)	R^2
IV1	-0.116	0.083	-0.091	0.041
IV2	0.009	0.001	-0.118	0.085
IV3	-0.102	0.067	-0.112	0.059
IV4	-0.101	0.062	-0.076	0.031
Average	**-0.071**	**0.038**	**-0.094**	**0.059**

It can be seen from Table B 1 (by inspection of the coefficient of determination, R^2) that the data does not have a good fit ($R^2 = 1$ means a perfect fit of the data) this may be to a large extent due to the seasonal variation as identified in Figure B 4 – Figure B 6. As with the thermocouples, the seasonal variation cancels out.

Regardless, the slopes of the linear regression lines may be used to estimate the long-term change in elongation of the containment structures.

The strain is estimated from the reference date of 2009Q2 based on the formula for strain due to change in height, i.e.:

$$\Delta\varepsilon = \frac{\Delta_L}{L_0}$$

Where: $\Delta\varepsilon$ = Change in Strain due to a change in Length

Δ_L = Change in Length (Invar Wire Readings based on the change in slope)

L_0 = Original Length (Assumed to be 49.07m)

Table B 2: Unit 1 Strain Estimates

Instrument	Slope (mm/y)	Δε (2009-2023) µm/m	Δε (2023-2044) µm/m
IV1	-0.116	-34.25	**-48.70**
IV2	0.009	2.77	3.94
IV3	-0.102	-30.23	-42.97
IV4	-0.101	-29.79	-42.35
Average	**-0.071**	-21.07	-29.96

Table B 3: Unit 2 Strain Estimates

Instrument	Slope (mm/y)	Δε (2009-2023) µm/m	Δε (2023-2044) µm/m
IV1	-0.091	-26.91	-38.26
IV2	-0.118	-35.09	**-49.89**
e	-0.112	-33.25	-47.28
IV4	-0.076	-22.56	-32.08
Average	**-0.071**	-27.78	-39.49

The maximum estimated long-term additional strain expected on the containment structures is **-49.89 µm/m**. This change in strain corresponds well to the change in strain expected from the exponentially extrapolated strain as indicated in Table 7 (-416.90 µm/m at 40-years and -463.36 µm/m → **Δε = -46.46 µm/m**).

It can therefore be concluded that the vertical invar wires may be used for the validation of the TLAA, although due to the uncertainties regarding the long-term measurement data from 1984-2009 the use of the invar wire data should be approached with caution.

B.2 Pendulum Monitoring

The pendulum monitoring is simpler than the invar wire measurements in the case of breakage of a wire, as long as the connection point remains unchanged. Considering that the pendulums hang and the horizontal coordinates of bottom of the pendulum is measured, and not the vertical, the length of the cable is less important. Therefore, when remeasuring of the containment on-line monitoring continued in 2009Q2, the measurements were simply taken, and no adjustments are made in this report for the pendulums.

It is noted that the pendulum readings cannot directly be correlated to strain measurements, as the strain gauges in the concrete read tangential strain (tension or compression) while the pendulums measure movement Furthermore, there is also no acceptance criteria for the pendulums. Accordingly, the results are not interpreted, only presented for completeness.

B.2.1 Monitoring Results

The results of the pendulum monitoring were processed, and the ‘X’ and the ‘Y’ coordinates of the measurements were determined. Therefore, presenting the pendulum results requires 3-D interpretation of the results. To this extent, colours are introduced in the presentation of the data providing a scale for the date, while the XY data is plotted in a 2D cartesian plane.

Incorporated in the results is an indicative circle (radius of 4mm) to provide perspective to the reader.

The results for all the monitoring since 2009 are presented below:

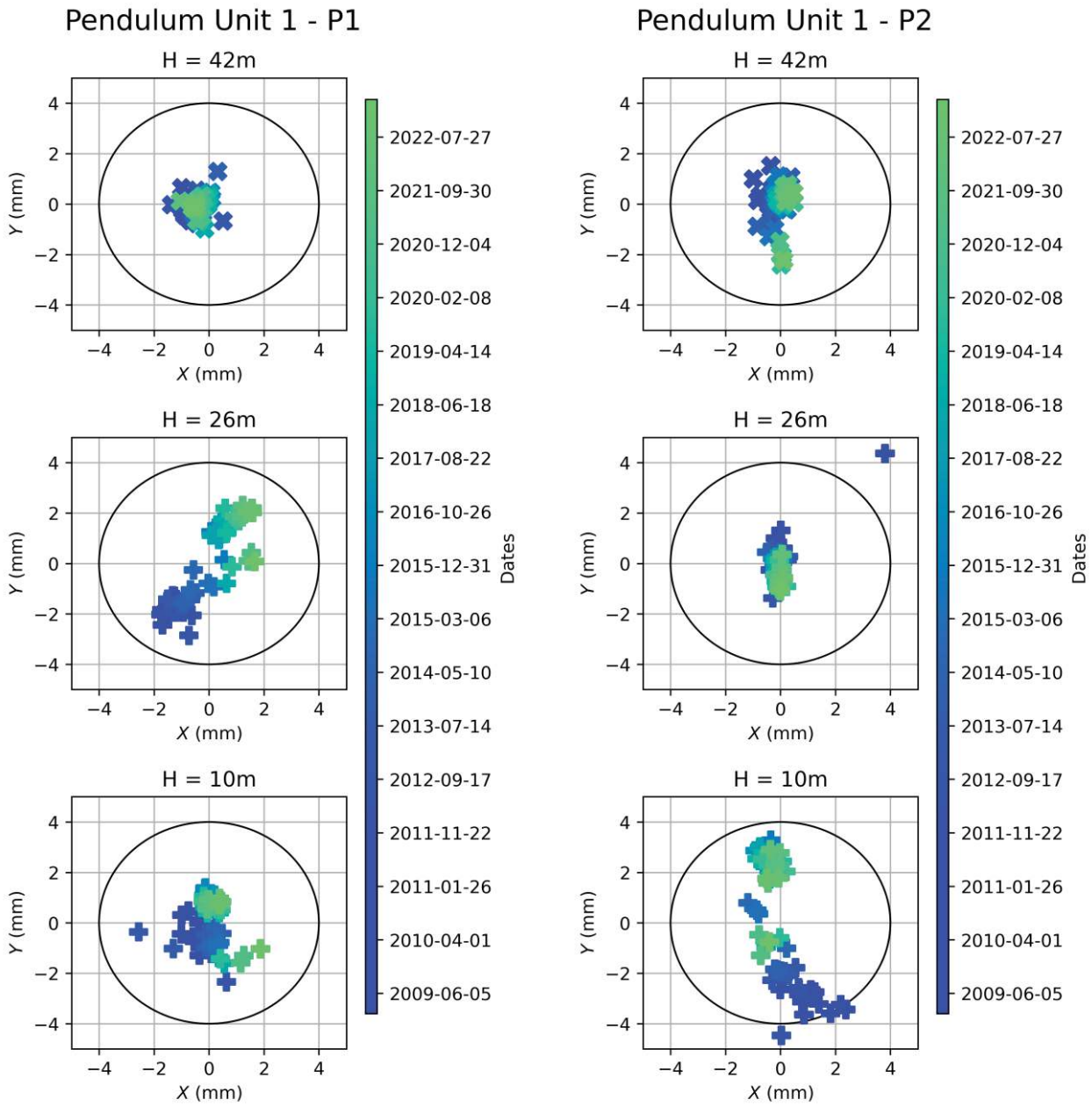

Figure B 7: Pendulum Cartesian Results, Unit 1 P1 & P2

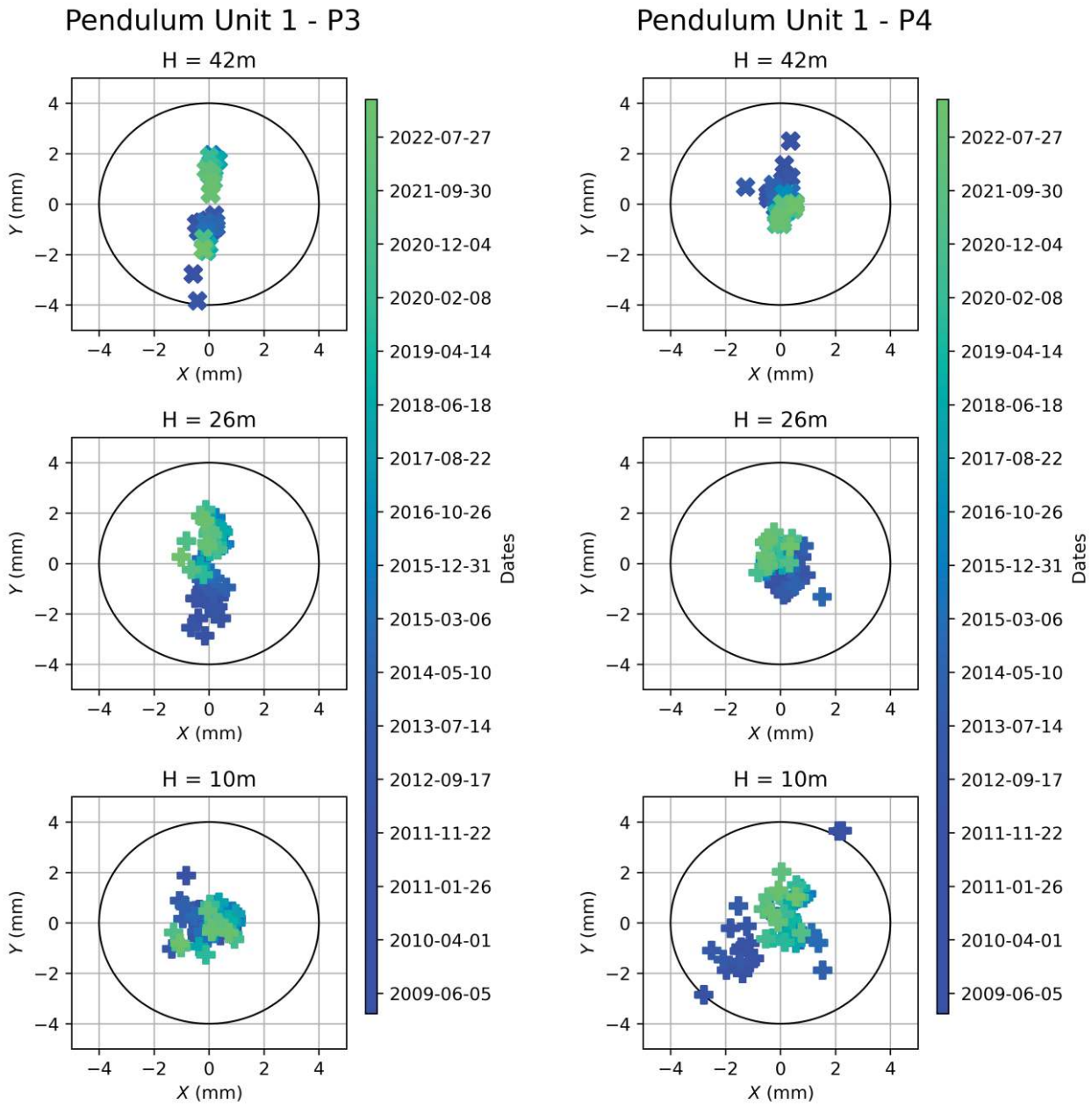

Figure B 8: Pendulum Cartesian Results, Unit 1 P3 & P4

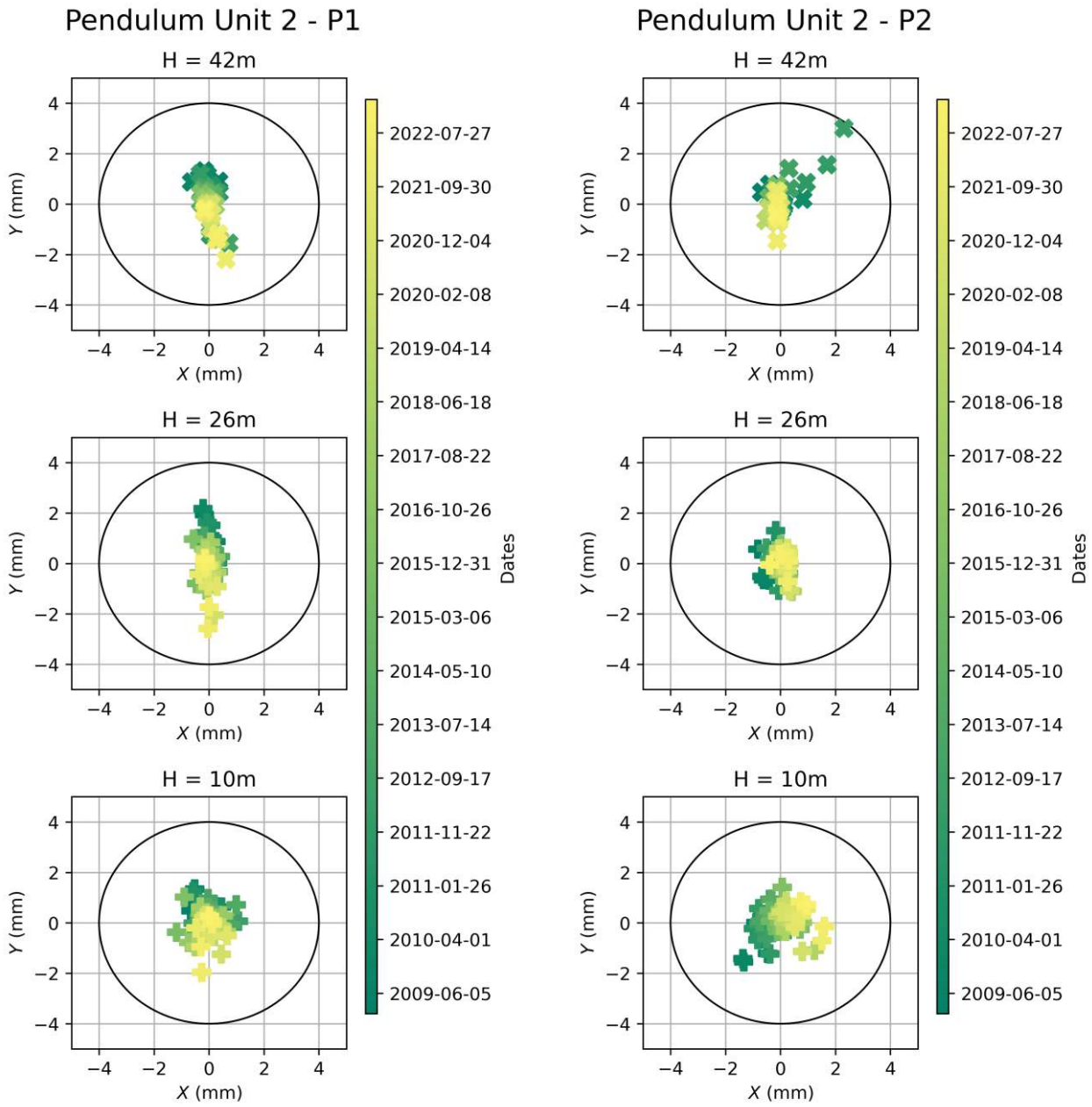

Figure B 9: Pendulum Cartesian Results, Unit 2 P1 & P2

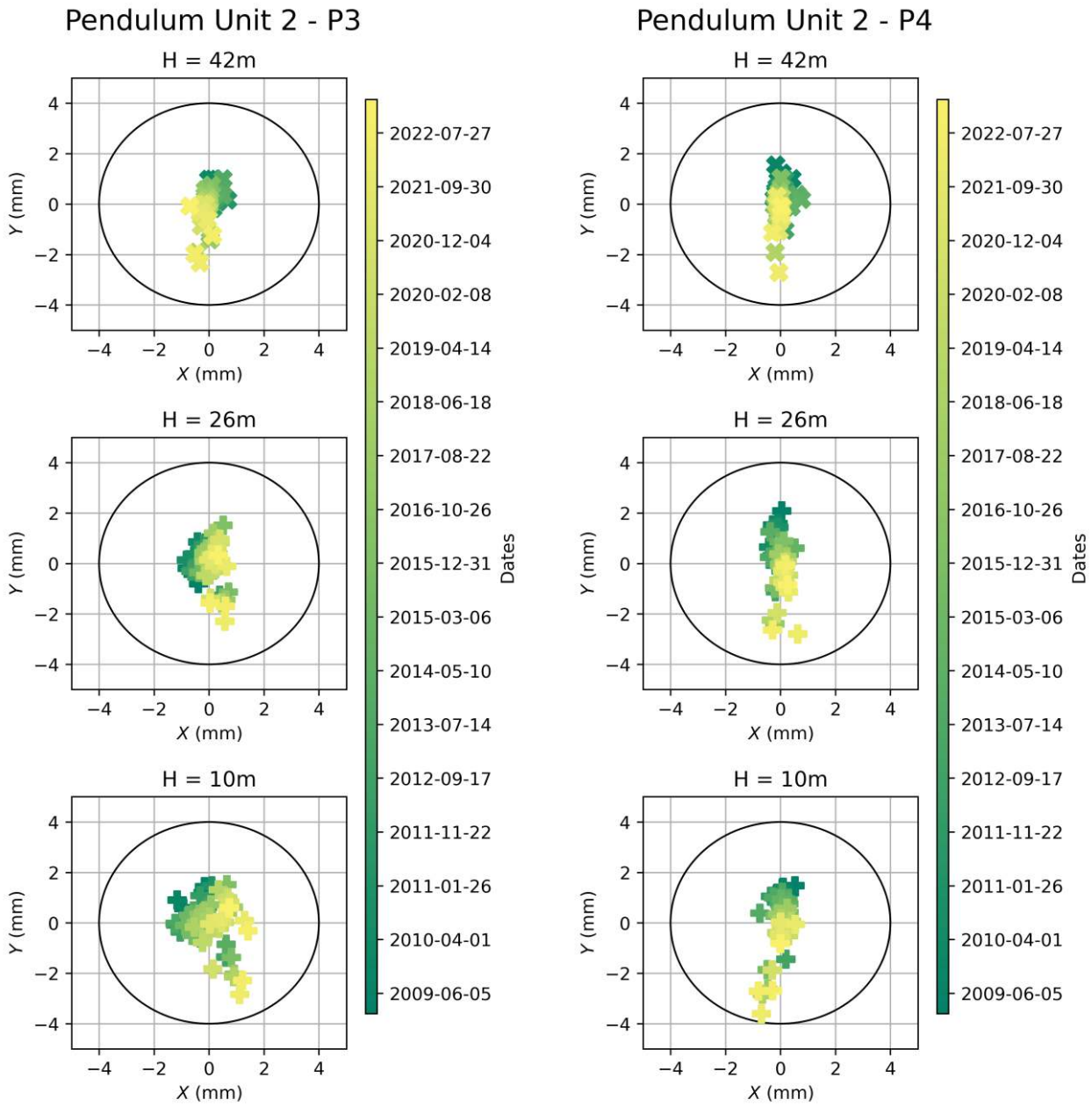

Figure B 10: Pendulum Cartesian Results, Unit 2 P3 & P4

The results above were limited to 5mm on either side to provide a clear view of the results, although there are some outlier data beyond these bounds. To this extent, the figure below was produced to indicate all the results, for both units, to provide an indication of the extent of the outliers:

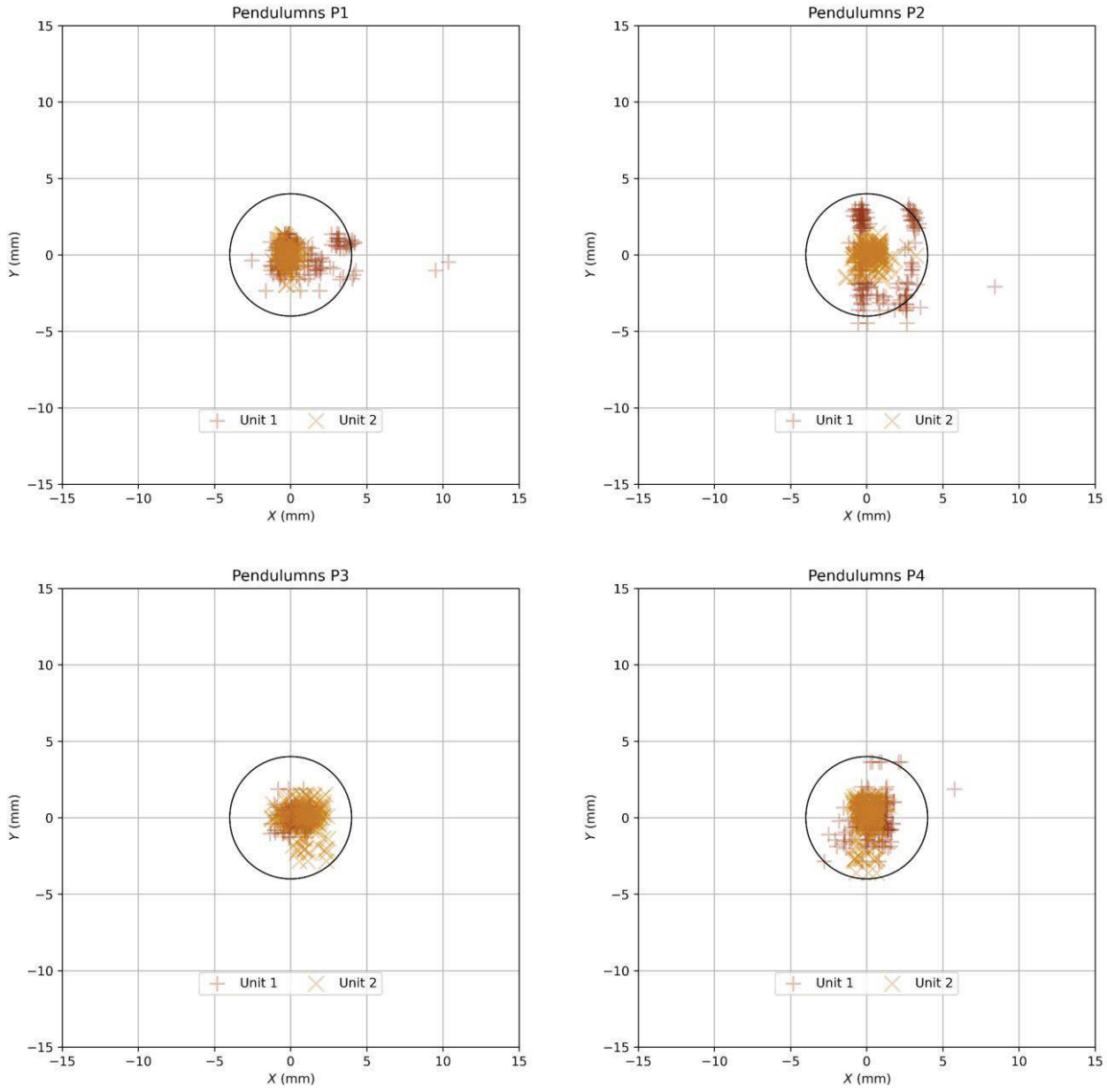

Figure B 11: All Pendulum Cartesian Results with Outliers

An alternative method to interpret the results is to consider the change in the radius, Δr, and the angle of the pendulum from the centre.

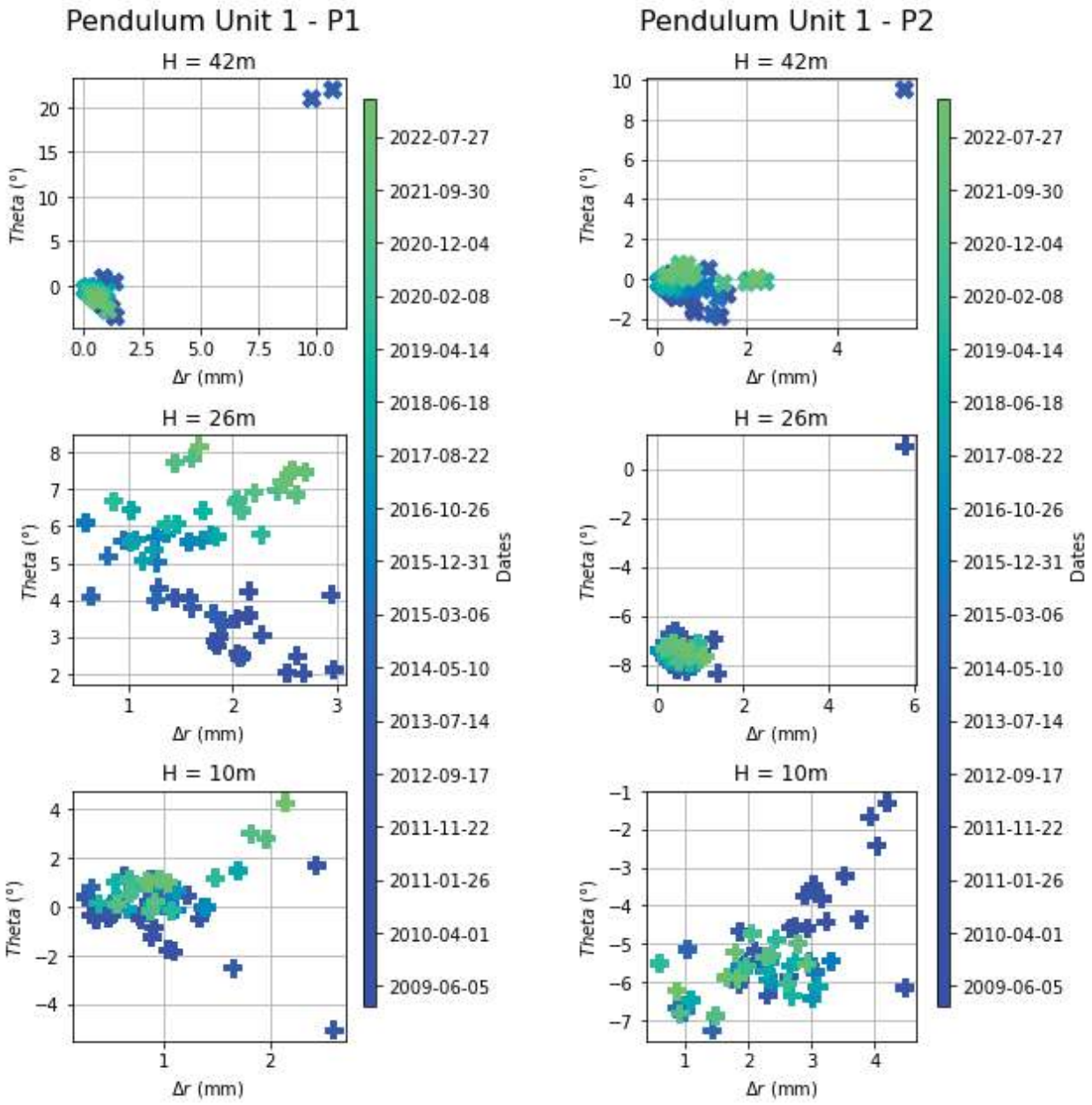

Figure B 12: Pendulum Polar Results, Unit 1 P1 & P2

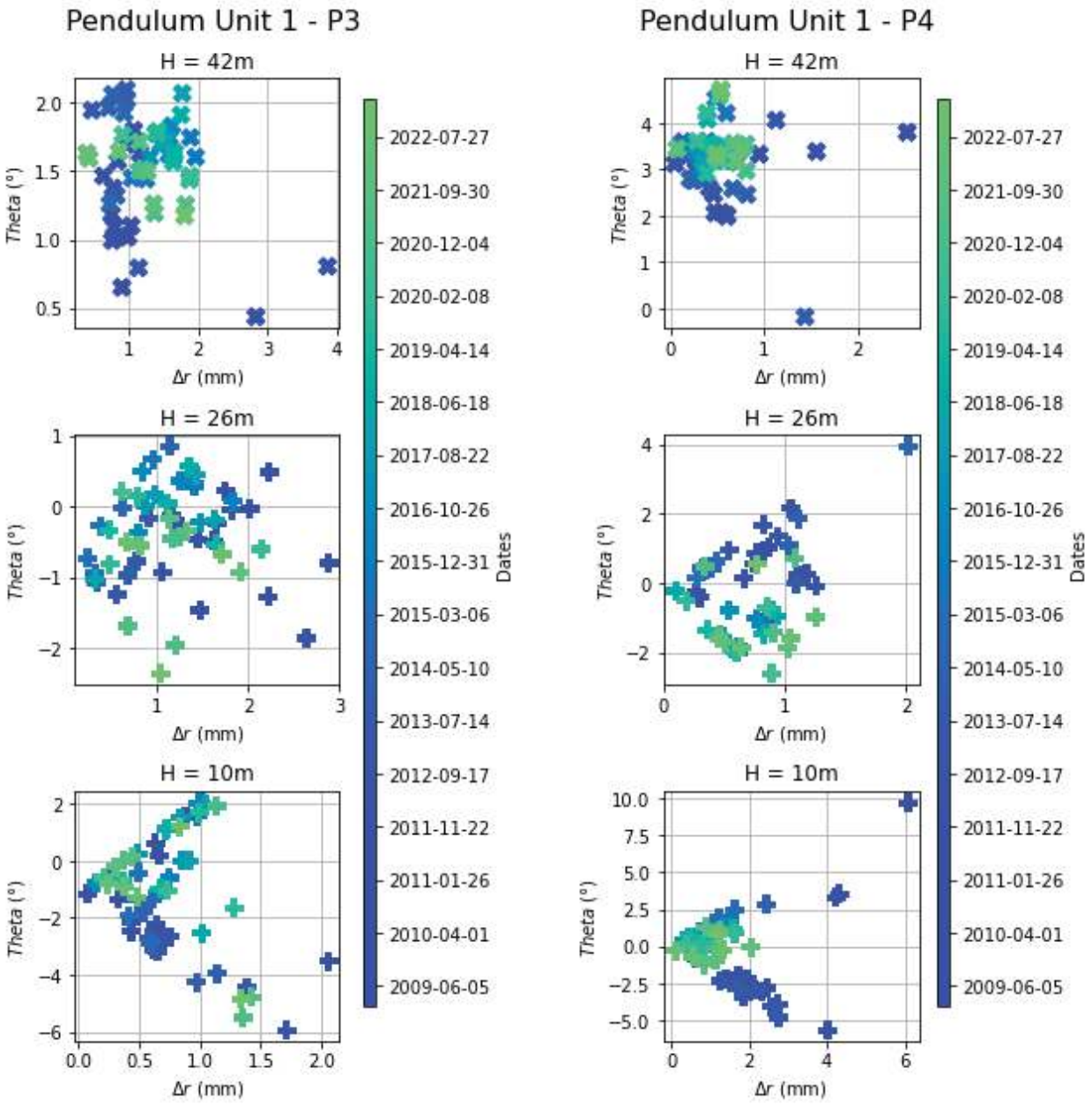

Figure B 13: Pendulum Polar Results, Unit 1 P3 & P4

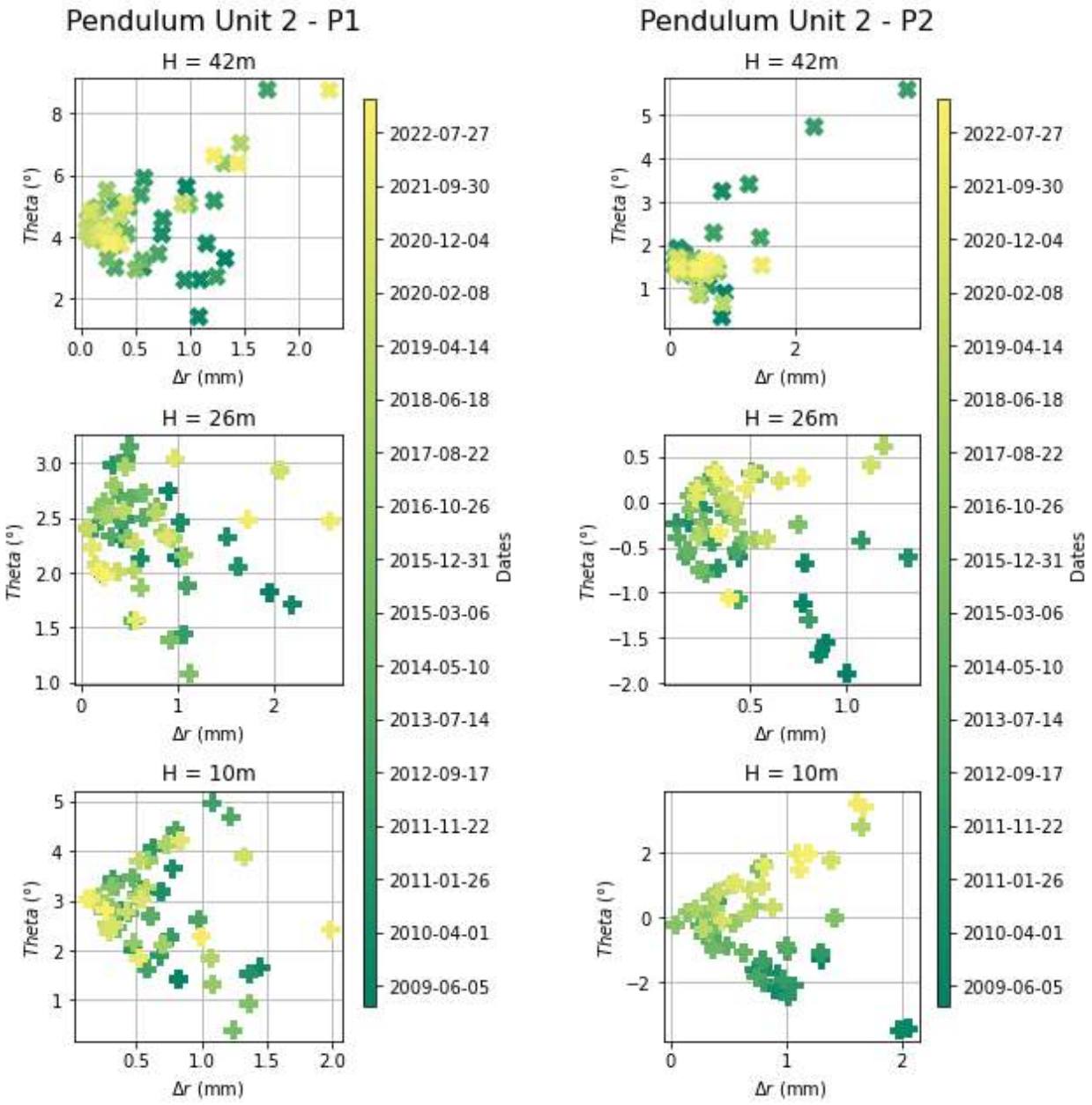

Figure B 14: Pendulum Polar Results, Unit 2 P1 & P2

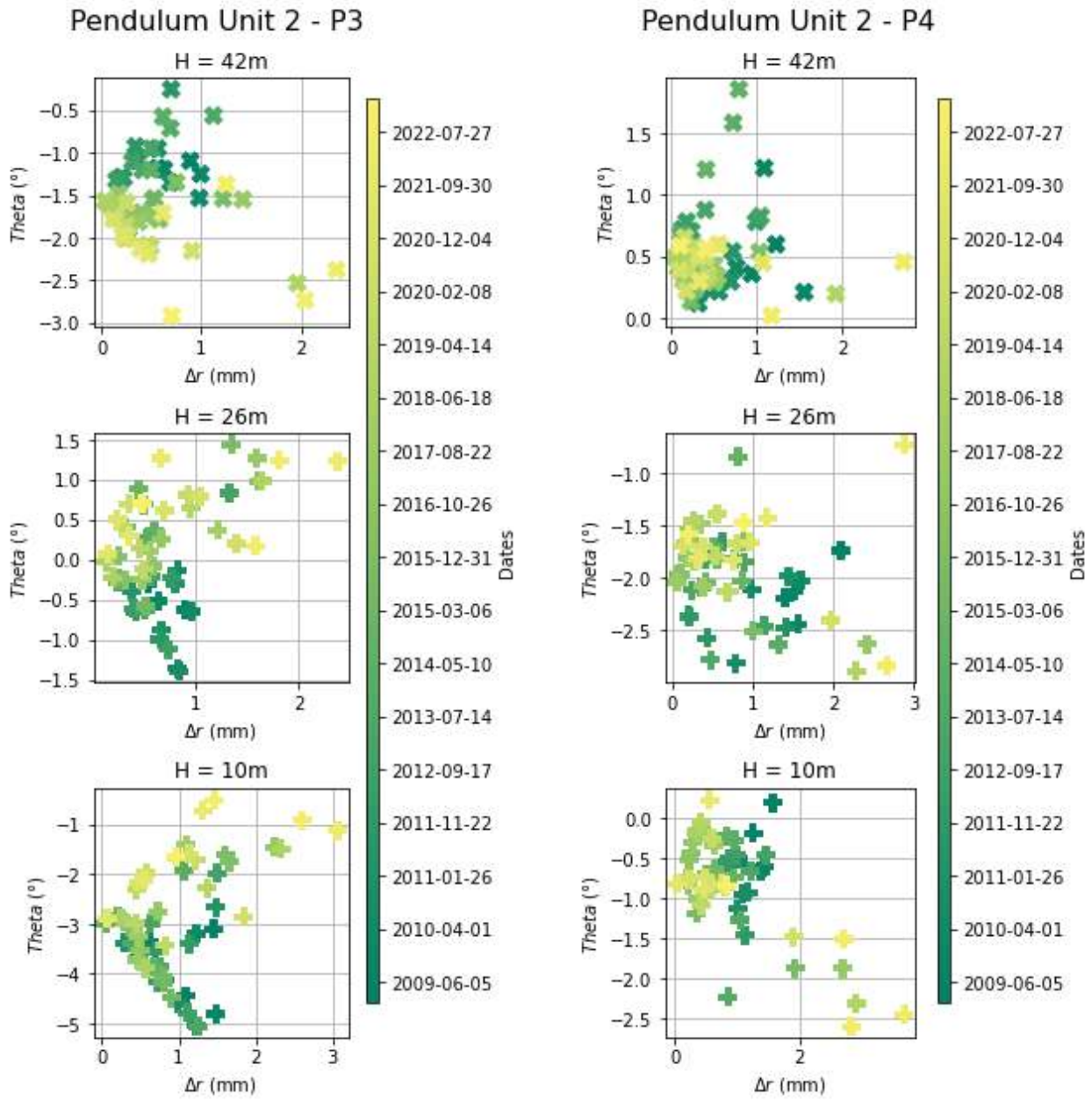

Figure B 15: Pendulum Polar Results, Unit 2 P3 & P4

Appendix C– All Tendon Design Prediction Curves